ESAIM: M2AN 52 (2018) 659–702
https://doi.org/10.1051/m2an/2018019

ESAIM: Mathematical Modelling and Numerical Analysis
www.esaim-m2an.org

MULTIPLE TRACES FORMULATION AND SEMI-IMPLICIT SCHEME FOR MODELLING BIOLOGICAL CELLS UNDER ELECTRICAL STIMULATION[☆]

Fernando Henríquez[1] and Carlos Jerez-Hanckes[2,*]

Abstract. We model the electrical behavior of several biological cells under external stimuli by extending and computationally improving the multiple traces formulation introduced in Henríquez *et al.* [*Numer. Math.* **136** (2016) 101–145]. Therein, the electric potential and current for a single cell are retrieved through the coupling of boundary integral operators and non-linear ordinary differential systems of equations. Yet, the low-order discretization scheme presented becomes impractical when accounting for interactions among multiple cells. In this note, we consider multi-cellular systems and show existence and uniqueness of the resulting non-linear evolution problem in finite time. Our main tools are analytic semigroup theory along with mapping properties of boundary integral operators in Sobolev spaces. Thanks to the smoothness of cellular shapes, solutions are highly regular at a given time. Hence, spectral spatial discretization can be employed, thereby largely reducing the number of unknowns. Time-space coupling is achieved *via* a semi-implicit time-stepping scheme shown to be stable and second order convergent. Numerical results in two dimensions validate our claims and match observed biological behavior for the Hodgkin–Huxley dynamical model.

Mathematics Subject Classification. 65M38, 65M12, 65R20

Received May 10, 2017. Accepted March 9, 2018.

1. Introduction

Research and development in biomedical engineering as well as in biological sciences have greatly benefited from our ever-increasing ability to simulate complex cellular processes [32, 33, 41]. As computational resources and algorithmic efficiency improves, more realistic mathematical models can be used to better understand and enhance techniques such as localization and stimulation of peripheral nerves for anesthesia [9, 10, 48], cardiac defibrillation [54, 59], gene transfection [15, 45], membrane electro-permeabilization [57], and electro-chemotherapy of tumors [22, 53]. Yet, the intertwinement of multi-scale time-space phenomena, such as that which occurs when stimulating tissues containing several cells, remains a major challenge to the applied and computational mathematics community.

[☆] This work was partially funded by Fondecyt Regular 1171491, Conicyt Anillo ACT1417, Chile CORFO Engineering 2030 program through grant OPEN-UC 201603 and ETH Zürich through Grant ETH4417-1.

Keywords and phrases: Multiple traces formulation, semi-implicit time stepping, biological cells, exponential convergence

[1] Seminar for Applied Mathematics, ETH Zürich, CH-8092 Zürich, Switzerland.
[2] School of Engineering, Pontificia Universidad Católica de Chile, Santiago, Chile.

[*] Corresponding author: cjerez@ing.puc.cl

Cellular electrical behavior is dictated by the movement of ions through channels across the cell membrane. These channels are in turn composed of a large number of gates opening and closing randomly. Ion conduction occurs when all channel gates are open, an event whose probability depends on the voltage jump at the membrane. Several phenomenological descriptions of such random process have been offered [35]. The pioneering work of Hodgkin and Huxley [31] stands out as being the first model capable of describing axon electrical activity and will constitute our model of choice without loss of generality. In order to obtain voltage differences between intra- and extra-cellular domains, Maxwell equations are employed. As bioelectric signals are significantly slower than electromagnetic ones, a quasi-static regime can be assumed that leads to the solving of Laplace equations in each subdomain. Hence, one seeks to couple a dynamic model taking place on cellular membranes with a static volumic one. The former is described by non-linear ordinary differential equations (ODEs) while the latter by partial differential equations. In the case of multiple cells, non-local electrostatic interactions need also to be duly accounted for.

Homogenization models present an alternative to simplify the above coupling [1–4]. Here, the underlying idea hinges on reducing the heterogenous domain into an homogenous or effective medium. Hence, the methods rely on requiring a very large numbers of cells with respect to the physical scales of the quantities of interest simulated. Since we seek to understand the interactions among a large but finite number of closely interacting or *packed* cells, we opt for a different approach to homogenization though we cannot over stress the usefulness of such models in many biological simulations [21]. Among numerical methods able to model actual cellular structure, we mention the work of Poignard and co-workers [28, 34, 38] as well as the references therein. The so-called Voronoi Interface Method introduced there is based on a Cartesian grid and achieves second-order convergence constituting a volume-based alternative to the approach here considered.

In [29], we modeled the electrical activity of one biological cell under external stimuli by coupling the local *Multiple Traces Formulation* (MTF) [16, 17, 30] with ionic dynamics at the membrane. Although the MTF was introduced to model heterogenous penetrable structures as in composite materials, it lends itself to solve scattering by multiple disjoint homogenous bodies. The gist of the MTF is to consider as unknowns Dirichlet and Neumann traces on either side of the cellular membrane. These traces must satisfy two requirements: Calderón identities per subdomain and transmission conditions. Hence, the volume problem is condensed to one posed over the cell boundary. To numerically couple it with our nonlinear dynamical model, in [29] we adopted a *time-stepping semi-implicit* Galerkin scheme for spatial low-order basis functions, with proven stability independent of space discretization and second order convergence. Our approach showed a considerable reduction of degrees of freedom when compared to previous methods as well as good agreement with experimental data. However, the method scales poorly in number of cells, with quickly increasing number of degrees of freedom and conditioning numbers. Extending our previous work to address packed cells constitutes the main goal of the present work. It should be mentioned that other single or multiple trace approaches could have been taken [13, 16, 17, 49, 62]. For instance, we could have chosen the Laplacian version of the Poggio–Miller–Chang–Harrington–Wu–Tsai (PMCHWT) as it requires half the number of unknowns of the local MTF. Still, we have chosen to extend the strategy [29] to focus on multiple scatterers and further work is required to determine the most suitable boundary integral formulation for the problem at hand.

As a first challenge, we are required to show that the resulting multi-cellular dynamic MTF system is well posed on the continuous level. Due to our boundary reduction, we must perform the analysis of Dirichlet-to-Neumann operators relating transmembrane voltages to currents given by the Hodgkin–Huxley model. For this, we heavily rely on: (i) the mapping properties of boundary integral operators in fractional Sobolev spaces [18]; (ii) analytic group theory [40, 43, 47], and (iii) linearity of the underlying system. The latter will allow us to define a suitable splitting of the sources of transmembrane currents on a given cell and analyze them individually. This result is valid for a finite number of cells in two and three dimensions. In the case of single-cell electro-permeabilization, Kavian *et al.* [34] obtain well-posedness using Dirichlet-to-Neumann maps but in a bounded domain, somehow constituting a more restricted version of our results.

Computationally, one possible way to reduce the number of spatial unknowns relies on the observation that cellular shapes are smooth. Indeed, cells seek to maximize their area-to-volume ratio as a means to pass nutrients efficiently, which explains small cellular sizes and differentiable surfaces. Consequently, electric potentials

will portray high regularity as long as the external stimulus is also sufficiently regular and that cells are not touching each other. This scenario entails the possibility of replacing low-order basis by spectral ones – Fourier polynomials in two dimensions or spherical harmonics in 3D – eventually yielding exponential convergence rates, and consequently, greatly reducing the number of unknowns (*cf.* [11, 27, 37], [7], Sect. 6.5 or [51]). Still, cross interactions among cells potentials can foil computational performance regardless of the discretization basis employed.

Several schemes have been proposed to tackle multiple interactions [6, 8, 23, 24, 42]. The book by Martin [42] provides an extensive review of the main techniques in the subject. In [6], the two-dimensional time-harmonic acoustic multiple scattering problem at high-frequencies is solved by using series expansion. The method described hinges on the boundary decomposition technique introduced by Balabane [8] while the resolution and preconditioning of the underlying linear system is improved through the identification of particular matrix structures. In [23–25] the authors tackle Helmholtz and Maxwell multiple scattering problems by proposing different boundary integral equations, usually coupled with other techniques such as Balabane's boundary decomposition method [8] or the T-matrix method [61]. However, and to our knowledge, coupling such methods with nonlinear time dependent models as the one taking place in packed cells stimulation has not been yet performed. We believe the present work will open the path for such implementations though we will not tackle this here. Moreover, our approach could be extended to describe cardiac electrophysiology when adequately adapting non-linear models constructed *via* asymptotic expansions such as the ones given in [14, 20].

This article is arranged as follows. In Section 2, we introduce necessary notation and tools to state the mathematical model problem for the interaction of multiple biological cells. Section 3 introduces boundary integral operators along with their main properties. In Section 4, the MTF is employed to recast the original volume problem as a problem solely posed on the cellular membranes. Existence and uniqueness of the boundary integral problem is presented in Section 5. The main tool in this case is analytic semigroup theory. Our numerical discretization scheme is described in Section 6, with stability and convergence analyses carried out in Sections 6.4 and 6.6, respectively. In Section 7, we show and discuss numerical results in the light of previous theoretical and experimental insights, to then conclude in Section 8.

2. Preliminaries and volume model problem

2.1. Notation

Following [29], we set some of the recurring notation used throughout, with exceptions duly indicated. Let $D \subseteq \mathbb{R}^d$, with $d = 1, 2, 3$, be open. We denote by $\mathcal{C}^k(D)$ the space of k-times differentiable continuous functions over D with $k \in \mathbb{N}_0$. Also, let $L^p(D)$ be the standard equivalence class of functions with bounded L^p-norm over D. For $s \in \mathbb{R}$, $H^s(D)$ denotes standard Sobolev spaces with $H^0(D) \equiv L^2(D)$ ([44], Chap. 3). For $s \geq 0$, we write $H^s_{\mathrm{loc}}(D)$ for the local Sobolev space of distributions whose restriction to every compact set $K \Subset D$ lies in $H^s(K)$. Similarly, we introduce the notation $H^s_{\mathrm{comp}}(D)$ for the space of compactly supported $H^s(D)$-functions in D, for $s \in \mathbb{R}$. We will also use the notation $H^1_{\mathrm{loc}}(\Delta, D)$ for functions $u \in H^1_{\mathrm{loc}}(D)$ with $\Delta u \in L^2_{\mathrm{comp}}(D)$, for a domain D not necessarily bounded. We consider as well the space:

$$H^1_{\mathrm{loc}}(\Delta, \mathbb{R}^d \backslash \partial D) := \{u \in L^2(\mathbb{R}^d) : \ u|_D \in H^1_{\mathrm{loc}}(\Delta, D) \text{ and } \ u|_{D^c} \in H^1_{\mathrm{loc}}(\Delta, D^c)\}.$$

For a Banach space V, $k \in \mathbb{N}_0$, functional spaces $\mathcal{C}^k([0,T]; V)$ denote k-times continuous functions in t with bounded V-norm for all $t \in [0,T]$. An equivalent definition holds for $L^p([0,T]; V)$ spaces with $p \in [1, \infty]$. $\mathcal{S}'(\mathbb{R}^d)$ denotes the Schwartz functional space of tempered distributions over $\mathbb{R}^d$. For Banach spaces X and Y, we also introduce the space of bounded linear mappings $\mathcal{L}(X, Y)$ from X into Y.

Duality products are denoted by angular brackets, $\langle \cdot, \cdot \rangle$, while inner products by round brackets, $(\cdot, \cdot)$, both with subscripts accounting for the domain of definition. Dual adjoint operators are denoted by prime superscripts, *e.g.*, A'. Norms and semi-norms are written as $\|\cdot\|$, $|\cdot|$, respectively, with subscripts indicating the

associated functional space. We use $\|\cdot\|_2$ to denote the Euclidean norm in $\mathbb{R}^d$. Furthermore, time derivatives and vectors are denoted by the symbol ∂_t and by bold symbols, respectively.

2.2. Problem geometry

Set $J \in \mathbb{N}$. Let $\Omega_j \Subset \mathbb{R}^d$ with $d = 2, 3$ and $j = 1, \ldots, J$, be bounded Lipschitz – eventually smooth – subdomains, each one with a connected boundary $\Gamma_j := \partial\Omega_j$ and complement $\Omega_j^c := \mathbb{R}^d \setminus \overline{\Omega}_j$. We assume that the set of subdomains is pairwise or mutually disjoint, *i.e.* $\overline{\Omega}_j \cap \overline{\Omega}_k = \emptyset$ whenever $j \neq k$, for $j, k = 1, \ldots, J$. The exterior domain to all subdomains, Ω_0, and its boundary, Γ_0, are defined as

$$\Omega_0 := \mathbb{R}^d \setminus \bigcup_{j=1}^{J} \overline{\Omega}_j \quad \text{and} \quad \Gamma_0 := \bigcup_{j=1}^{J} \Gamma_j. \tag{2.1}$$

2.3. Trace operators and multiple trace spaces

Let us denote by $\boldsymbol{\nu}_j$ the outward unitary normal vector to the boundary Γ_j, for $j = 1, \ldots, J$. Let γ^j be the interior trace operator acting continuously from $H^s_{\mathrm{loc}}(\Omega_j)$ into $H^{s-\frac{1}{2}}(\Gamma_j)$, for $\frac{1}{2} < s < \frac{3}{2}$ if Ω_j is Lipschitz, and if it is a $\mathcal{C}^k$-domain, for $\frac{1}{2} < s < k$ ([52], Thms. 2.6.8 and 2.6.9). For $u \in H^1_{\mathrm{loc}}(\Delta, \Omega_j)$, we introduce *interior* Dirichlet and Neumann traces:

$$\gamma^j_{\mathrm{D}} u := \gamma^j u \quad \text{and} \quad \gamma^j_{\mathrm{N}} u := \gamma^j \left(\boldsymbol{\nu}_j \cdot \nabla u\right), \tag{2.2}$$

respectively. Analogously, we define *exterior* traces:

$$\gamma^{j,c}_{\mathrm{D}} u := \gamma^{j,c} u \quad \text{and} \quad \gamma^{j,c}_{\mathrm{N}} u := \gamma^{j,c} \left(\boldsymbol{\nu}_j \cdot \nabla u\right), \tag{2.3}$$

where $\gamma^{j,c}$ is the exterior trace operator mapping $H^s_{\mathrm{loc}}(\Omega_0)$ into $H^{s-\frac{1}{2}}(\Gamma_j)$ with conditions on s as those stated for interior traces. For a given subdomain boundary $\partial\Omega_j$, we set the product trace spaces per subdomain:

$$\mathbf{V}^s_j := H^{\frac{1}{2}+s}(\partial\Omega_j) \times H^{-\frac{1}{2}+s}(\partial\Omega_j),$$

with $|s| \leq \frac{1}{2}$ for a bounded Lipschitz domain Ω_j or $s \in \mathbb{R}$ if Ω_j is bounded and $\mathcal{C}^\infty$. We identify $\mathbf{V}_j \equiv \mathbf{V}^0_j$. Also, for any $\boldsymbol{\varphi}$, $\boldsymbol{\xi}$ in $\mathbf{V}^s_j$, we define the *cross* or $\times$-duality product over Γ_j as (*cf.* [30], Sect. 2.2.1):

$$\langle \boldsymbol{\varphi}, \boldsymbol{\xi} \rangle_{\times,j} := \langle \varphi_{\mathrm{D}}, \xi_{\mathrm{N}} \rangle_j + \langle \varphi_{\mathrm{N}}, \xi_{\mathrm{D}} \rangle_j . \tag{2.4}$$

Given an operator $\mathsf{B} : \mathbf{V}_k \to \mathbf{V}_j$, we can write

$$\mathsf{B} = \begin{pmatrix} \mathsf{B}_{\mathrm{DD}} & \mathsf{B}_{\mathrm{DN}} \\ \mathsf{B}_{\mathrm{ND}} & \mathsf{B}_{\mathrm{NN}} \end{pmatrix},$$

with obvious mapping properties, and obtain its $\times$-*dual adjoint* $\mathsf{B}^\dagger : \mathbf{V}_j \to \mathbf{V}_k$ as

$$\mathsf{B}^\dagger = \begin{pmatrix} \mathsf{B}'_{\mathrm{NN}} & \mathsf{B}'_{\mathrm{DN}} \\ \mathsf{B}'_{\mathrm{ND}} & \mathsf{B}'_{\mathrm{DD}} \end{pmatrix}, \tag{2.5}$$

since, for any $\boldsymbol{\lambda} \in \mathbf{V}_k$ and $\boldsymbol{\varphi} \in \mathbf{V}_j$, it holds

$$\begin{aligned}\langle \mathsf{B}\boldsymbol{\lambda}, \boldsymbol{\varphi}\rangle_{\times,j} &= \langle \mathsf{B}_{\mathrm{DD}}\lambda_{\mathrm{D}}, \varphi_{\mathrm{N}}\rangle_j + \langle \mathsf{B}_{\mathrm{DN}}\lambda_{\mathrm{N}}, \varphi_{\mathrm{N}}\rangle_j + \langle \mathsf{B}_{\mathrm{ND}}\lambda_{\mathrm{D}}, \varphi_{\mathrm{D}}\rangle_j + \langle \mathsf{B}_{\mathrm{NN}}\lambda_{\mathrm{N}}, \varphi_{\mathrm{D}}\rangle_j \\ &= \langle \lambda_{\mathrm{D}}, \mathsf{B}'_{\mathrm{DD}}\varphi_{\mathrm{N}}\rangle_k + \langle \lambda_{\mathrm{N}}, \mathsf{B}'_{\mathrm{DN}}\varphi_{\mathrm{N}}\rangle_k + \langle \lambda_{\mathrm{D}}, \mathsf{B}'_{\mathrm{ND}}\varphi_{\mathrm{D}}\rangle_k + \langle \lambda_{\mathrm{N}}, \mathsf{B}'_{\mathrm{NN}}\varphi_{\mathrm{D}}\rangle_k \\ &= \left\langle \boldsymbol{\lambda}, \mathsf{B}^{\dagger}\boldsymbol{\varphi}\right\rangle_{\times,k}.\end{aligned}$$

For shorthand, let us introduce the trace operators:

$$\boldsymbol{\gamma}^j u := \begin{pmatrix}\gamma_{\mathrm{D}}^j u \\ \gamma_{\mathrm{N}}^j u\end{pmatrix} : H^1_{\mathrm{loc}}(\Delta, \Omega_j) \to \mathbf{V}_j, \qquad \boldsymbol{\gamma}^{j,c} u := \begin{pmatrix}\gamma_{\mathrm{D}}^{j,c} u \\ \gamma_{\mathrm{N}}^{j,c} u\end{pmatrix} : H^1_{\mathrm{loc}}(\Delta, \Omega_j^c) \to \mathbf{V}_j. \tag{2.6}$$

Moreover, we define trace *jump* and *average* operators across Γ_j as follows: for $u \in H^1_{\mathrm{loc}}(\Delta, \Omega_j \cup \Omega_j^c)$, then

$$[\boldsymbol{\gamma} u]_j = \boldsymbol{\gamma}^{j,c} u - \boldsymbol{\gamma}^j u, \qquad \{\boldsymbol{\gamma} u\}_j = \frac{1}{2}\left(\boldsymbol{\gamma}^j u + \boldsymbol{\gamma}^{j,c} u\right), \tag{2.7}$$

respectively. Finally, we introduce the space $\mathbf{V}_j^{(2)} := \mathbf{V}_j \times \mathbf{V}_j$ as well as the *multiple traces space* $\mathbb{V}_J$ as the Cartesian product of interior and exterior trace spaces per subdomain boundary Γ_j:

$$\mathbb{V}_J := \prod_{j=1}^{J} \mathbf{V}_j^{(2)}.$$

These spaces[1] will be used in the MTF formulation of Section 3. For all Cartesian product spaces, inner and duality products as well as norms are sums of individual components with cross duality pairings. For example, for any $\boldsymbol{\lambda}_j^{(2)} = (\boldsymbol{\lambda}_j^c, \boldsymbol{\lambda}_j)^\top$ and $\boldsymbol{\varphi}_j^{(2)} = (\boldsymbol{\varphi}_j^c, \boldsymbol{\varphi}_j)^\top$ in $\mathbf{V}_j^{(2)}$, their dual product is defined as

$$\left\langle \boldsymbol{\lambda}_j^{(2)}, \boldsymbol{\varphi}_j^{(2)}\right\rangle_{\times,j} := \left\langle \boldsymbol{\lambda}_j^c, \boldsymbol{\varphi}_j^c\right\rangle_{\times,j} + \left\langle \boldsymbol{\lambda}_j, \boldsymbol{\varphi}_j\right\rangle_{\times,j}, \tag{2.8}$$

with norm

$$\begin{aligned}\left\|\boldsymbol{\varphi}_j^{(2)}\right\|_{\mathbf{V}_j^{(2)}} &:= \left\|\boldsymbol{\varphi}_j^c\right\|_{\mathbf{V}_j} + \left\|\boldsymbol{\varphi}_j\right\|_{\mathbf{V}_j} \\ &= \left\|\varphi_{\mathrm{D},j}^c\right\|_{H^{\frac{1}{2}}(\Gamma_j)} + \left\|\varphi_{\mathrm{N},j}^c\right\|_{H^{-\frac{1}{2}}(\Gamma_j)} + \left\|\varphi_{\mathrm{D},j}\right\|_{H^{\frac{1}{2}}(\Gamma_j)} + \left\|\varphi_{\mathrm{N},j}\right\|_{H^{-\frac{1}{2}}(\Gamma_j)}.\end{aligned} \tag{2.9}$$

For $s \in \mathbb{R}$, let us also define

$$\mathbb{H}_J^s := H^s(\Gamma_1) \times \cdots \times H^s(\Gamma_J). \tag{2.10}$$

The dual space of $\mathbb{H}_J^s$ is $\mathbb{H}_J^{-s}$ with duality pairing given as follows. Let $\boldsymbol{u} = (u_1, u_2, \ldots, u_J) \in \mathbb{H}_J^s$ and $\boldsymbol{w} = (w_1, w_2, \ldots, w_J) \in \mathbb{H}_J^{-s}$, then the duality pairing is

$$\langle \boldsymbol{u}, \boldsymbol{w}\rangle_{\Gamma_0} = \sum_{j=1}^{J} \langle u_j, w_j\rangle_j, \tag{2.11}$$

[1]Here, exterior traces are ordered differently from the multiple traces space provided in [16, 17, 30] wherein all exterior traces are placed consecutively.

where $\langle\cdot,\cdot\rangle_j$ is the standard pairing over Γ_j, for $j = 1,\dots,J$. We set

$$\mathbb{L}^2_J \equiv \mathbb{H}^0_J = L^2(\Gamma_1) \times \cdots \times L^2(\Gamma_J). \tag{2.12}$$

2.4. Continuous volume problem

In what follows, we extend the continuous model presented in ([29], Sect. 2) from a single cell to multiple ones. We assume the electric potential $u \in H^1_{\mathrm{loc}}(\Delta, \cup_{j=0}^J \Omega_j)$ to satisfy electrostatic equations in each subdomain Ω_j, *i.e.* for each $j = 0,\dots,J$, if $u_j := u|_{\Omega_j}$, it must hold

$$-\operatorname{div}(\sigma_j \nabla u_j) = 0 \quad \text{in} \quad \Omega_j,$$

where $\sigma_j \in L^\infty(\Omega_j)$ denotes the subdomain electrical conductivity [39, 60]. We further assume the σ_j to be strictly positive constants for all $j = 0,\dots,J$.

We define the *transmembrane potential* v_j as the electric potential jump across the membrane Γ_j, from the inside to the outside, *i.e.* Ω_j to Ω_j^c. Furthermore, let us assume as given a potential field Φ_e, defined in Ω_0, such that $-\Delta\Phi_e = 0$ in Ω_0. This potential plays the role of an external source and in practice can be produced, for instance, by charged electrodes.

As in [29], we assume that the current membrane follows a time-dependent model. For $k = 1,\dots,J$, the current i_k flowing across the membrane Γ_k is described as the sum of capacitive and ionic currents:

$$i_k = c_{m,k}\partial_t v_k + i_{\mathrm{ion},k} \quad \text{on} \quad \Gamma_k, \tag{2.13}$$

where $c_{m,k}$ is the membrane capacitance per unit area and $i_{\mathrm{ion},k}$ stands for the ionic current of the kth cell. Mathematically, a rigorous description of the ionic term is rather challenging, and thus, several models have been set forth based on experimental observations. Without loss of generality, we choose the so-called Hodgkin–Huxley (HH) model [21, 31] for the formulation presented below as well as for our numerical experiments (*cf.* [29]).

For a cellular membrane Γ_k, the HH model describes the ionic current $i_{\mathrm{ion},k}$ as a function of the transmembrane voltage v_k and a vector gate variable g_k. In the following, we write $i_{\mathrm{ion},k}(v_k, g_k)$ to explicitly state such dependence. Each vector gate variable g_k satisfies a system of ODEs in time over Γ_k, written as

$$\partial_t g_k = \mathcal{HH}_k(v_k, g_k) \quad \text{on} \quad \Gamma_k, \tag{2.14}$$

along with adequate initial conditions.

The functions $i_{\mathrm{ion},k}(v_k, g_k)$, $\mathcal{HH}_k(v_k, g_k) : \mathbb{R}\times\mathbb{R} \to \mathbb{R}$ are analytic in both variables and one may extend their action to Sobolev spaces on the boundary Γ_k, for $k = 1,\dots,J$ (*cf.* Chap. 5 from [50] and Lem. 5.4 of [43]).

Remark 2.1. The HH model actually incorporates three gates variables to describe the ionic current. For the sake of simplicity, throughout this work it is assumed the existence of solely one gate variable per biological cell, namely g_k. However, it is important to point out that in the computations presented in Section 7 the full HH model is employed. Details of the HH model together with the explicit expressions for $\mathcal{HH}_k$ and $i_{\mathrm{ion},k}$, $k = 1,\dots,J$ may be found in Appendix A.

The coupling between the membrane model, namely (2.13) and (2.14), and the potential field u relies on the membrane current:

$$i_k = -\sigma_k \gamma_{\mathrm{N}}^k u_k = -\sigma_0 \gamma_{\mathrm{N}}^{k,c} u_0 - \sigma_0 \gamma_{\mathrm{N}}^{k,c} \Phi_e, \quad \text{on} \quad \Gamma_k, \tag{2.15}$$

for $k = 1,\dots,J$. We can now state the volume formulation of the problem considered here as a generalization of ([29], Problem 1), assuming $c_{m,k} \equiv c_m$ to simplify the ensuing analysis.

Problem 2.2 (Continuous volume problem)**.** Set a final time $T \in \mathbb{R}_+$ and initial conditions $v_j(0) = v_j^0$, $g_j(0) = g_j^0$. We seek suitably defined functions u_0, u_j, v_j and g_j, for $j = 1, \ldots, J$, with support on Ω_0, Ω_j and Γ_j, respectively, such that, for all $t \in (0, T]$, it holds

$$
\begin{aligned}
-\Delta u_0 &= 0 && \text{in} \quad \Omega_0, && && (2.16a)\\
-\Delta u_j &= 0 && \text{in} \quad \Omega_j, && j = 1, \ldots, J, && (2.16b)\\
\gamma_{\mathrm{D}}^j u_j - \gamma_{\mathrm{D}}^{j,c} u_0 &= v_j + \gamma_{\mathrm{D}}^{j,c} \Phi_e && \text{on} \quad \Gamma_j, && j = 1, \ldots, J, && (2.16c)\\
\sigma_j \gamma_{\mathrm{N}}^j u_j - \sigma_0 \gamma_{\mathrm{N}}^{j,c} u_0 &= \sigma_0 \gamma_{\mathrm{N}}^{j,c} \Phi_e && \text{on} \quad \Gamma_j, && j = 1, \ldots, J, && (2.16d)\\
-\sigma_j \gamma_{\mathrm{N}}^j u_j &= c_m \partial_t v_j + i_{\mathrm{ion},j}(v_j, g_j) && \text{on} \quad \Gamma_j, && j = 1, \ldots, J, && (2.16e)\\
\partial_t g_j &= \mathcal{H}(v_j, g_j) && \text{on} \quad \Gamma_j, && j = 1, \ldots, J, && (2.16f)\\
u_0(\boldsymbol{x}) &= \mathcal{O}\left(\|\boldsymbol{x}\|_2^{-1} \right) && \text{as} \quad \|\boldsymbol{x}\|_2 \to \infty. && && (2.16g)
\end{aligned}
$$

Remark 2.3. Conditions at infinity of the type

$$
u_0(\boldsymbol{x}) = a + b \log \|\boldsymbol{x}\|_2 + \mathcal{O}\left(\|\boldsymbol{x}\|_2^{-1} \right) \quad \text{as} \quad \|\boldsymbol{x}\|_2 \to \infty, \tag{2.17}
$$

for some constants a and b, are usually considered in the treatment of the exterior Laplace problem in $\mathbb{R}^2$, instead of (2.16g) (*cf.* [19]). However, the intrinsic nature of the biological phenomenon that we would like to model *via* Problem 2.2 dictates that the exterior potential has to be bounded and, furthermore, has to decay at infinity, as established in (2.16g). Since we would like u_0 to vanish at infinity, from now on we set $a = 0$ in (2.17).

Let us define,

$$
\mathscr{L}_j := \left\{ u \in H^1_{\mathrm{loc}}\left(\Delta, \mathbb{R}^d \backslash \Gamma_j\right) : \ -\Delta u = 0 \text{ in } \mathbb{R}^d \backslash \Gamma_j \text{ satisfying (2.16g) if } d = 3 \text{ and (2.17) if } d = 2 \text{ with } a = 0 \right\}, \tag{2.18}
$$

for $j = 0, \cdots, J$. Besides, let us consider the following auxiliary problem:

Problem 2.4. Find $u_0 \in H^1_{\mathrm{loc}}(\Omega_0)$ and $u_j \in H^1(\Omega_j)$, for $j = 1, \ldots, J$, such that

$$
\begin{aligned}
-\Delta u_0 &= 0 && \text{in} \quad \Omega_0, && && (2.19a)\\
-\Delta u_j &= 0 && \text{in} \quad \Omega_j, && j = 1, \ldots, J, && (2.19b)\\
\gamma_{\mathrm{D}}^j u_j - \gamma_{\mathrm{D}}^{j,c} u_0 &= 0 && \text{on} \quad \Gamma_j, && j = 1, \ldots, J, && (2.19c)\\
\sigma_j \gamma_{\mathrm{N}}^j u_j - \sigma_0 \gamma_{\mathrm{N}}^{j,c} u_0 &= 0 && \text{on} \quad \Gamma_j, && j = 1, \ldots, J, && (2.19d)\\
u_0(\boldsymbol{x}) &= \mathcal{O}\left(\|\boldsymbol{x}\|_2^{-1} \right) && \text{as} \quad \|\boldsymbol{x}\|_2 \to \infty. && && (2.19e)
\end{aligned}
$$

Proposition 2.5. *Functions $u_0 \in H^1_{\mathrm{loc}}(\Omega_0)$ and $u_j \in H^1(\Omega_j)$, for $j = 1, \ldots, J$, satisfy Problem 2.4 if and only if $u_0 \equiv 0$ in Ω_0 and $u_j \equiv 0$ in Ω_j, for $j = 1, \ldots, J$.*

Proof. We take our cue from ([19], Prop. 4.7). Let $\varrho > 0$ be such that

$$
\bigcup_{j=1}^{J} \Omega_j \subset B_\varrho := \left\{ \boldsymbol{x} \in \mathbb{R}^d : \|\boldsymbol{x}\|_2 < \varrho \right\}. \tag{2.20}
$$

Assume that (2.19a)–(2.19e) hold. We apply Green's first identity over $\Omega_{0,\varrho} := \Omega_0 \cap B_\varrho$ and obtain

$$\sigma_0 \int_{\Omega_{0,\varrho}} |\nabla u_0|^2 \, \mathrm{d}\boldsymbol{x} = \sigma_0 \int_{\partial B_\varrho} u_0 \, (\boldsymbol{\nu}_\varrho \cdot \nabla u_0) \, ds_{\boldsymbol{x}} - \sigma_0 \sum_{j=1}^{J} \int_{\Gamma_j} u_0 \, (\boldsymbol{\nu}_j \cdot \nabla u_0) \, \mathrm{d}s_{\boldsymbol{x}}, \tag{2.21}$$

where $\boldsymbol{\nu}_\varrho$ is the outer normal vector to B_ϱ. Similarly, for $j = 1, \ldots, J$, we have

$$\sigma_j \int_{\Omega_j} |\nabla u_j|^2 \, \mathrm{d}\boldsymbol{x} = \sigma_j \int_{\Gamma_j} u_j \, (\boldsymbol{\nu}_j \cdot \nabla u_j) \, \mathrm{d}s_{\boldsymbol{x}}. \tag{2.22}$$

Thus,

$$\begin{aligned} \sigma_0 \int_{\Omega_{0,\varrho}} |\nabla u_0|^2 \, \mathrm{d}\boldsymbol{x} + \sum_{j=1}^{J} \sigma_j \int_{\Omega_j} |\nabla u_j|^2 \, \mathrm{d}\boldsymbol{x} &= \sigma_0 \int_{\partial B_\varrho} u_0 \, (\boldsymbol{\nu}_\rho \cdot \nabla u_0) \, \mathrm{d}s_{\boldsymbol{x}} \\ &\quad + \sum_{j=1}^{J} \int_{\Gamma_j} (\sigma_j \, u_j \, (\boldsymbol{\nu}_j \cdot \nabla u_j) - \sigma_0 \, u_0 \, (\boldsymbol{\nu}_j \cdot \nabla u_0)) \, \mathrm{d}s_{\boldsymbol{x}}. \end{aligned} \tag{2.23}$$

Using the transmission conditions (2.19c) and (2.19d) we obtain

$$\sigma_0 \int_{\Omega_{0,\varrho}} |\nabla u_0|^2 \, \mathrm{d}\boldsymbol{x} + \sum_{j=1}^{J} \sigma_j \int_{\Omega_j} |\nabla u_j|^2 \, \mathrm{d}\boldsymbol{x} = \sigma_0 \int_{\partial B_\varrho} u_0 \, (\boldsymbol{\nu}_\varrho \cdot \nabla u_0) \, \mathrm{d}s_{\boldsymbol{x}}. \tag{2.24}$$

The condition at infinity provided in (2.19e) allow us to conclude that $(\boldsymbol{\nu}_\varrho \cdot \nabla u_0) = \mathcal{O}(\varrho^{-2})$. Hence we have,

$$\int_{\partial B_\varrho} u_0 \, (\boldsymbol{\nu}_\varrho \cdot \nabla u_0) \, \mathrm{d}s_{\boldsymbol{x}} = \mathcal{O}(\varrho^{-1}). \tag{2.25}$$

The right-hand side in (2.24) tends to zero as $\varrho \to \infty$. Therefore, u_0 and u_j, for $j = 1, \ldots, J$ are constants over each domain. It follows from transmission and infinity conditions that $u_0 \equiv 0$ in Ω_0 and $u_j \equiv 0$ in Ω_j, for $j = 1, \ldots, J$. The converse claim is trivial. □

3. Multiple traces formulation

3.1. Boundary potentials and integral representation formula

For $d = 2, 3$, let $G(\boldsymbol{x}, \boldsymbol{y}) \in \mathcal{S}'(\mathbb{R}^d)$ be the fundamental solution to the Laplace operator in $\mathbb{R}^d$ (*cf.* [55], Chapter 5 or [52], Sect. 3.1), whose expression is

$$G(\boldsymbol{x}, \boldsymbol{y}) = \begin{cases} \frac{1}{2\pi} \log \|\boldsymbol{x} - \boldsymbol{y}\|_2^{-1} & \boldsymbol{x} \neq \boldsymbol{y} \in \mathbb{R}^2, \\ \frac{1}{4\pi} \|\boldsymbol{x} - \boldsymbol{y}\|_2^{-1} & \boldsymbol{x} \neq \boldsymbol{y} \in \mathbb{R}^3. \end{cases} \tag{3.1}$$

For $s \in \mathbb{R}$, we define the *Newton potential* $\mathcal{N} : H^s_{\text{comp}}(\mathbb{R}^d) \to H^{s+2}_{\text{loc}}(\mathbb{R}^d)$ ([52], Thm 3.1.2) informally as

$$(\mathcal{N}f)(\boldsymbol{x}) := \int_{\mathbb{R}^d} G(\boldsymbol{x},\boldsymbol{y}) f(\boldsymbol{y}) \mathrm{d}\boldsymbol{y}, \quad \forall\, \boldsymbol{x} \in \mathbb{R}^d, \tag{3.2}$$

with extension to Sobolev spaces based on density and duality arguments. Let us introduce the classic single and double layer potentials, $\mathcal{S}_j$ and $\mathcal{D}_j$, respectively, defined[2] over Γ_j as

$$\mathcal{S}_j := \mathcal{N} \circ \left(\gamma^j_{\mathrm{D}}\right)' \quad \text{and} \quad \mathcal{D}_j := \mathcal{N} \circ \left(\gamma^j_{\mathrm{N}}\right)', \qquad j = 1, \ldots, J. \tag{3.3}$$

Theorem 3.1 (Thms. 3.1.16 and 3.1.12 in [52], Lem. 3.5 in [19])**.** *For $j = 1, \ldots, J$, the potentials $\mathcal{S}_j : H^{-\frac{1}{2}}(\Gamma_j) \to H^1_{\text{loc}}\left(\mathbb{R}^d\right)$ and $\mathcal{D}_j : H^{\frac{1}{2}}(\Gamma_j) \to H^1_{\text{loc}}\left(\mathbb{R}^d \setminus \Gamma_j\right)$ are continuous. Moreover, for $u_j \in \mathscr{L}_j$, the integral representation formula:*

$$u_j = -\mathcal{S}_j\left(\left[\gamma_N u_j\right]_j\right) + \mathcal{D}_j\left(\left[\gamma_D u_j\right]_j\right) \quad \text{in} \quad \mathbb{R}^d \setminus \Gamma_j, \tag{3.4}$$

holds for all $j = 1, \ldots, J$. Besides, for $\psi_j \in H^{-\frac{1}{2}}(\Gamma_j)$ and $\phi_j \in H^{\frac{1}{2}}(\Gamma_j)$ we have that $\mathcal{S}_j(\psi_j) \in \mathscr{L}_j$ (with $b = \langle \psi_j, 1\rangle_{\Gamma_j}$ if $d = 2$) and $\mathcal{D}_j(\phi_j) \in \mathscr{L}_j$ (with $b = 0$ if $d = 2$).

Remark 3.2. For $d = 2$ and $j = 1, \ldots, J$, we observe that if $\left\langle \left[\gamma_{\mathrm{N}} u_j\right]_j, 1 \right\rangle_j = 0$, the integral representation formula (3.4) satisfies $u_j(\boldsymbol{x}) = \mathcal{O}\left(\|\boldsymbol{x}\|_2^{-1}\right)$ as $\|\boldsymbol{x}\|_2 \to \infty$. Furthermore, if $\psi_j \in H^{-\frac{1}{2}}(\Gamma_j)$ is such that $\langle \psi_j, 1\rangle_j = 0$, then $\mathcal{S}_j(\psi_j) = \mathcal{O}\left(\|\boldsymbol{x}\|_2^{-1}\right)$ as $\|\boldsymbol{x}\|_2 \to \infty$.

Remark 3.3. Functions satisfying (3.4) yield null trace jumps at subdomain boundaries Γ_k as long as $k \neq j$.

Theorem 3.4. *Let $u_0 \in \mathscr{L}_0$. If $d = 2$ we further assume that $\left\langle \left[\gamma_N u_0\right]_j, 1 \right\rangle_j = 0$, for $j = 1, \ldots, J$. Then, the following integral representation formula holds*

$$u_0 = \sum_{j=1}^{J} -\mathcal{S}_j\left(\left[\gamma_N u_0\right]_j\right) + \mathcal{D}_j\left(\left[\gamma_D u_0\right]_j\right) \quad \text{in} \quad \mathbb{R}^d \setminus \Gamma_0. \tag{3.5}$$

Proof. Choose $u_0 \in \mathscr{L}_0$. For $j = 1, \ldots, J$, we define a family of functions $u_j \in H^1_{\text{loc}}(\mathbb{R}^d \setminus \Gamma_j)$ solutions of problems:

$$-\Delta u_j = 0 \qquad \text{in} \quad \mathbb{R}^d \setminus \Gamma_j, \tag{3.6a}$$
$$[\gamma u_j]_j = [\gamma u_0]_j \qquad \text{on} \quad \Gamma_j, \tag{3.6b}$$
$$u_j(\boldsymbol{x}) = \mathcal{O}\left(\|\boldsymbol{x}\|_2^{-1}\right) \quad \text{as} \quad \|\boldsymbol{x}\|_2 \to \infty. \tag{3.6c}$$

For a given j, the above problem has a unique solution $u_j \in H^1_{\text{loc}}(\Delta, \mathbb{R}^d \setminus \overline{\Omega}_j)$ ([52], Thm 2.10.14). Set now

$$\hat{u}_0 := \sum_{j=1}^{J} u_j \quad \text{in} \quad \mathbb{R}^d \setminus \Gamma_0. \tag{3.7}$$

[2]Though one should use L^2-adjoints instead of dual adjoints as in the Helmholtz case, for Laplace operators both definitions are equivalent as the kernel is symmetric and inner and dual products are bilinear.

By Theorem 3.1 and considering Remark 3.2, we obtain

$$\hat{u}_0 = \sum_{j=1}^{J} -\mathcal{S}_j\left([\gamma_{\mathrm{N}} u_j]_j\right) + \mathcal{D}_j\left([\gamma_{\mathrm{D}} u_j]_j\right) \quad \text{in} \quad \mathbb{R}^d. \tag{3.8}$$

Clearly, $-\Delta\hat{u}_0 = 0$ in $\mathbb{R}^d\backslash\Gamma_0$ and by construction $\hat{u}_0 \in H^1_{\mathrm{loc}}\left(\Delta, \mathbb{R}^d\backslash\Gamma_0\right)$. By trace jump continuity across Γ_ℓ for u_j, with $\ell \neq j$, it holds

$$[\boldsymbol{\gamma}\hat{u}_0]_\ell = \sum_{j=1}^{J} [\boldsymbol{\gamma} u_j]_\ell = [\boldsymbol{\gamma} u_\ell]_\ell = [\boldsymbol{\gamma} u_0]_\ell\,. \tag{3.9}$$

Hence, $\bar{u}_0 := \hat{u}_0 - u_0$ satisfies $-\Delta\bar{u}_0 = 0$ in $\mathbb{R}^d\backslash\Gamma_0$ with zero jump conditions over Γ_0 and, furthermore, satisfies $\bar{u}_0(\boldsymbol{x}) = \mathcal{O}\left(\|\boldsymbol{x}\|_2^{-1}\right)$ as $\|\boldsymbol{x}\|_2 \to \infty$. By Proposition 2.5, we conclude that $\bar{u}_0 \equiv 0$, leading to $\hat{u}_0 \equiv u_0$. Thus, the integral representation formula (3.5) holds for u_0. □

For simplicity, given $\boldsymbol{\lambda}_j = (\lambda_{\mathrm{D}}^j, \lambda_{\mathrm{N}}^j)^\top \in \mathbf{V}_j$, we introduce the potential:

$$\Psi_j(\boldsymbol{\lambda}_j) := -\mathcal{S}_j\left(\lambda_{\mathrm{N}}^j\right) + \mathcal{D}_j\left(\lambda_{\mathrm{D}}^j\right) \quad \text{for } j = 1, \ldots, J. \tag{3.10}$$

3.2. Boundary integral operators

We introduce the standard Boundary Integral Operators (BIOs) over Γ_j [52]:

$$\mathsf{V}_j := \{\gamma_{\mathrm{D}} \circ \mathcal{S}_j\}_j : H^{-\frac{1}{2}}(\Gamma_j) \to H^{\frac{1}{2}}(\Gamma_j), \tag{3.11}$$

$$\mathsf{K}'_j := \{\gamma_{\mathrm{N}} \circ \mathcal{S}_j\}_j : H^{-\frac{1}{2}}(\Gamma_j) \to H^{-\frac{1}{2}}(\Gamma_j), \tag{3.12}$$

$$\mathsf{K}_j := \{\gamma_{\mathrm{D}} \circ \mathcal{D}_j\}_j : H^{\frac{1}{2}}(\Gamma_j) \to H^{\frac{1}{2}}(\Gamma_j), \tag{3.13}$$

$$\mathsf{W}_j := -\{\gamma_{\mathrm{N}} \circ \mathcal{D}_j\}_j : H^{\frac{1}{2}}(\Gamma_j) \to H^{-\frac{1}{2}}(\Gamma_j). \tag{3.14}$$

Theorem 3.5 ([55], Thm. 6.34)**.** *Let Γ_j be a bounded Lipschitz boundary in $\mathbb{R}^d$, $d = 2, 3$ for $j = 1, \ldots, J$ and $|s| \leq \frac{1}{2}$, the BIOs are linear and generate the following bounded mappings:*

$$\mathsf{V}_j : H^{-\frac{1}{2}+s}(\Gamma_j) \to H^{\frac{1}{2}+s}(\Gamma_j), \qquad \mathsf{K}_j : H^{\frac{1}{2}+s}(\Gamma_j) \to H^{\frac{1}{2}+s}(\Gamma_j),$$
$$\mathsf{K}'_j : H^{-\frac{1}{2}+s}(\Gamma_j) \to H^{-\frac{1}{2}+s}(\Gamma_j), \qquad \mathsf{W}_j : H^{\frac{1}{2}+s}(\Gamma_j) \to H^{-\frac{1}{2}+s}(\Gamma_j),$$

If Γ_j is a $\mathcal{C}^\infty$-boundary, the statement is valid for all $s \in \mathbb{R}$.

The traces of u_j, namely solutions of Problem 2.2, satisfy the following property:

$$\boldsymbol{\gamma}^j u_j = \begin{pmatrix} \gamma_{\mathrm{D}}^j u_j \\ \gamma_{\mathrm{N}}^j u_j \end{pmatrix} = \begin{pmatrix} \frac{1}{2}\mathsf{I} - \mathsf{K}_j & \mathsf{V}_j \\ \mathsf{W}_j & \frac{1}{2}\mathsf{I} + \mathsf{K}'_j \end{pmatrix} \begin{pmatrix} \gamma_{\mathrm{D}}^j u_j \\ \gamma_{\mathrm{N}}^j u_j \end{pmatrix} \text{ over } \Gamma_j, \quad j = 1, \ldots, J. \tag{3.15}$$

The block operator defined in (3.15), known as the *interior Calderón projector* and denoted by C_j, plays a key role in our boundary integral formulation. Consider the following decomposition:

$$\mathsf{C}_j := \frac{1}{2}\mathsf{I} + \mathsf{A}_j, \qquad \mathsf{A}_j := \begin{pmatrix} -\mathsf{K}_j & \mathsf{V}_j \\ \mathsf{W}_j & \mathsf{K}'_j \end{pmatrix}, \tag{3.16}$$

with $\mathsf{A}_j : \mathbf{V}_j^s \to \mathbf{V}_j^s$ continuously under the conditions given in Theorem 3.5. We also consider the *exterior* Calderón operator $\mathsf{C}_j^c := \frac{1}{2}\mathsf{I} - \mathsf{A}_j$.

Lemma 3.6 (Lem. 2 in [29]). *For each $j = 1, \ldots, J$, the operator $\mathsf{A}_j : \mathbf{V}_j \to \mathbf{V}_j$ is continuous and $\mathbf{V}_j$-coercive, i.e. it holds*

$$\langle \mathsf{A}_j \boldsymbol{\varphi}, \boldsymbol{\lambda} \rangle_{\times,j} \leq \alpha_j \, \|\boldsymbol{\varphi}\|_{\mathbf{V}_j} \, \|\boldsymbol{\lambda}\|_{\mathbf{V}_j}, \quad \forall\, \boldsymbol{\varphi}, \boldsymbol{\lambda} \in \mathbf{V}_j, \tag{3.17}$$

for a strictly positive constant α_j, and there exists a compact operator $\mathsf{T}_{\mathsf{A}_j} : \mathbf{V}_j \to \mathbf{V}_j$ and a positive constant μ_j such that

$$\langle \mathsf{A}_j \boldsymbol{\varphi}, \boldsymbol{\varphi} \rangle_{\times,j} + \langle \mathsf{T}_{\mathsf{A}_j} \boldsymbol{\varphi}, \boldsymbol{\varphi} \rangle_{\times,j} \geq \mu_j \, \|\boldsymbol{\varphi}\|^2_{\mathbf{V}_j}, \quad \forall\, \boldsymbol{\varphi} \in \mathbf{V}_j. \tag{3.18}$$

3.3. Multiple traces formulation

For every $k = 1, \ldots, J$, Theorem 3.1 allows the use of the following integral representation for $u_k \in \mathscr{L}_k$ satisfying the Laplace equation in Ω_k:

$$u_k = \mathcal{S}_k \left(\gamma_{\mathrm{N}}^k u_k\right) - \mathcal{D}_k \left(\gamma_{\mathrm{D}}^k u_k\right) \quad \text{in} \quad \Omega_k. \tag{3.19}$$

Furthermore, if $\widetilde{u}_k$ denotes the extension of u_k by zero over Ω_k^c, *i.e.* $\widetilde{u}_k|_{\Omega_k^c} \equiv 0$, then (3.19) also holds over $\mathbb{R}^d \setminus \Gamma_k$. Taking interior traces yields

$$\boldsymbol{\gamma}^k u_k = \mathsf{C}_k \, \boldsymbol{\gamma}^k u_k \quad \text{on} \quad \Gamma_k, \tag{3.20}$$

which is equivalent to

$$\frac{1}{2}\boldsymbol{\gamma}^k u_k = \mathsf{A}_k \, \boldsymbol{\gamma}^k u_k \quad \text{on} \quad \Gamma_k. \tag{3.21}$$

On the other hand, let $u_0 \in \mathscr{L}_0$ satisfy $-\Delta u_0 = 0$ in Ω_0, with a null extension over all Ω_k, written $\widetilde{u}_0$, *i.e.* $\widetilde{u}_0|_{\Omega_k} = 0$, for all $k = 1, \ldots, J$. Theorem 3.4 guarantees the representation:

$$u_0 = \sum_{j=1}^{J} -\mathcal{S}_j \left(\gamma_{\mathrm{N}}^{j,c} u_0\right) + \mathcal{D}_j \left(\gamma_{\mathrm{D}}^{j,c} u_0\right) \quad \text{in} \quad \mathbb{R}^d \setminus \Gamma_0. \tag{3.22}$$

Taking exterior traces $\boldsymbol{\gamma}^{k,c}$ on Γ_k, we obtain

$$\boldsymbol{\gamma}^{k,c} u_0 = \mathsf{C}_k^{\mathsf{c}} \, \boldsymbol{\gamma}^{k,c} u_0 + \sum_{\substack{j=1 \\ j \neq k}}^{J} \mathsf{T}_{k,j} \, \boldsymbol{\gamma}^{j,c} u_0 \quad \text{on} \quad \Gamma_k, \tag{3.23}$$

where

$$\mathsf{T}_{k,j} := \begin{pmatrix} \gamma_{\mathrm{D}}^{k,c} \circ \mathcal{D}_j & -\gamma_{\mathrm{D}}^{k,c} \circ \mathcal{S}_j \\ \gamma_{\mathrm{N}}^{k,c} \circ \mathcal{D}_j & -\gamma_{\mathrm{N}}^{k,c} \circ \mathcal{S}_j \end{pmatrix} : \mathbf{V}_j \to \mathbf{V}_k. \tag{3.24}$$

for $j, k = 1, \ldots, J$ such that $j \neq k$. Equation (3.23) may be written as follows

$$\frac{1}{2}\boldsymbol{\gamma}^{k,c} u_0 = -\mathsf{A}_j\, \boldsymbol{\gamma}^{k,c} u_0 + \sum_{\substack{j=1 \\ j\neq k}}^{J} \mathsf{T}_{k,j}\, \boldsymbol{\gamma}^{j,c} u_0 \quad \text{on} \quad \Gamma_k. \tag{3.25}$$

Let us set the excitation potential traces and transmembrane potential vectors:

$$\boldsymbol{\gamma}^{k,c}\Phi_e = (\gamma_{\mathrm{D}}^{k,c}\Phi_e, \gamma_{\mathrm{N}}^{k,c}\Phi_e)^\top \quad \text{and} \quad \mathcal{V}_k := (v_k, 0)^\top \qquad \text{on} \quad \Gamma_k, \tag{3.26}$$

respectively. With the above observations, for all cell membranes Γ_k, $k = 1, \ldots, J$, transmission conditions (2.16c) and (2.16d), may be written as

$$\boldsymbol{\gamma}^k u_k - \mathsf{X}_k \boldsymbol{\gamma}^{k,c} u_0 = \mathsf{X}_k \left(\boldsymbol{\gamma}^{k,c}\Phi_e + \mathcal{V}_k\right) \quad \text{on} \quad \Gamma_k, \tag{3.27}$$

wherein we have defined[3]

$$\mathsf{X}_k := \begin{pmatrix} \mathsf{I} & 0 \\ 0 & \frac{\sigma_0}{\sigma_k}\mathsf{I} \end{pmatrix} : \mathbf{V}_k \to \mathbf{V}_k. \tag{3.28}$$

Merging (3.21) together with (3.27) yields

$$\mathsf{A}_k \boldsymbol{\gamma}^k u_k - \frac{1}{2}\mathsf{X}_k \boldsymbol{\gamma}^{k,c} u_0 = \frac{1}{2}\mathsf{X}_k \left(\boldsymbol{\gamma}^{k,c}\Phi_e + \mathcal{V}_k\right) \quad \text{on} \quad \Gamma_k, \tag{3.29}$$

whereas (3.23) in (3.27) renders

$$-\mathsf{A}_k \boldsymbol{\gamma}^{k,c} u_0 + \sum_{\substack{j=1 \\ j\neq k}}^{J} \mathsf{T}_{k,j} \boldsymbol{\gamma}^{j,c} u_0 - \frac{1}{2}\mathsf{X}_k^{-1} \boldsymbol{\gamma}^k u_k = -\frac{1}{2}\left(\boldsymbol{\gamma}^{k,c}\Phi_e + \mathcal{V}_k\right) \quad \text{on} \quad \Gamma_k. \tag{3.30}$$

As shorthand, we denote the exterior and interior traces on a membrane Γ_j by $\boldsymbol{\lambda}_j^c := \boldsymbol{\gamma}^{j,c} u_0$ and $\boldsymbol{\lambda}_j := \boldsymbol{\gamma}^j u_j$, respectively. Moreover, since Neumann transmission conditions (2.16d) lead to ratios σ_j/σ_0, we introduce the notation:

$$\hat{\mathsf{A}}_j := \frac{\sigma_j}{\sigma_0}\mathsf{A}_j \quad \text{and} \quad \hat{\mathsf{X}}_j := \frac{\sigma_j}{\sigma_0}\mathsf{X}_j\ . \tag{3.31}$$

Define the block operator:

$$\mathsf{M}_j := \begin{pmatrix} \mathsf{A}_j & \frac{1}{2}\mathsf{X}_j^{-1} \\ -\frac{1}{2}\hat{\mathsf{X}}_j & \hat{\mathsf{A}}_j \end{pmatrix} : \mathbf{V}_j^{(2)} \to \mathbf{V}_j^{(2)}. \tag{3.32}$$

[3]Observe that this definition differs from that in [29, 30] as in this work Neumann traces are directed along the outward normal vector, and consequently, there is no minus sign (*cf.* Sect. 2.3).

Lemma 3.7. *The operator* M_j *is continuous in* $\mathbf{V}_j^{(2)}$*, injective and coercive, i.e. it satisfies the Gårding-type inequality:*

$$\left\langle \mathsf{M}_j \boldsymbol{\lambda}_j^{(2)}, \boldsymbol{\lambda}_j^{(2)} \right\rangle_{\times,j} + \left\langle \mathsf{T}_{\mathsf{M}_j} \boldsymbol{\lambda}_j^{(2)}, \boldsymbol{\lambda}_j^{(2)} \right\rangle_{\times,j} \geq \mu_{\mathsf{M}_j} \left\| \boldsymbol{\lambda}_j^{(2)} \right\|^2_{\mathbf{V}_j^{(2)}}, \quad \forall\, \boldsymbol{\lambda}_j^{(2)} \in \mathbf{V}_j^{(2)}, \tag{3.33}$$

and where $\mu_{\mathsf{M}_j} > 0$*, with duality products given as in* (2.8)*, and* $\mathsf{T}_{\mathsf{M}_j} : \mathbf{V}_j^{(2)} \to \mathbf{V}_j^{(2)}$ *is a compact operator.*

Proof. Conductivities σ_j, $j = 1, \ldots, J$ are positive, yielding quotients $\frac{\sigma_j}{\sigma_0}$ positive as well. Therefore, by Lemma 3.6, the operators A_j and $\hat{\mathsf{A}}_j$ are continuous and coercive with

$$\hat{\mathsf{T}}_{\mathsf{A}_j} := \frac{\sigma_j}{\sigma_0} \mathsf{T}_{\mathsf{A}_j} \quad \text{and} \quad \hat{\mu}_j := \mu_j \frac{\sigma_j}{\sigma_0}. \tag{3.34}$$

Coercivity of M_j follows as cross terms vanish yielding

$$\mathsf{T}_{\mathsf{M}_j} := \begin{pmatrix} \mathsf{T}_{\mathsf{A}_j} & 0 \\ 0 & \hat{\mathsf{T}}_{\mathsf{A}_j} \end{pmatrix} : \mathbf{V}_j^{(2)} \to \mathbf{V}_j^{(2)}, \quad \mu_{\mathsf{M}_j} := \mu_j \min\{1, \sigma_j/\sigma_0\}.$$

Injectivity follows verbatim from the proof of ([30], Thm. 4) but for the sake of completeness we include the proof. Let $\boldsymbol{\lambda} = (\boldsymbol{\lambda}_j^c, \boldsymbol{\lambda}_j)^\top \in \mathbf{V}_j^{(2)}$, where $\boldsymbol{\lambda}_j^c = (\lambda_{j,\mathrm{D}}^c, \lambda_{j,\mathrm{N}}^c)^\top \in \mathbf{V}_j$ and $\boldsymbol{\lambda}_j = (\lambda_{j,\mathrm{D}}, \lambda_{j,\mathrm{N}})^\top \in \mathbf{V}_j$, be the solution of $\mathsf{M}_j \boldsymbol{\lambda} = \mathbf{0}$. Then, one must conclude that $\boldsymbol{\lambda}_j \equiv 0$.

(i) First, we show that for $\boldsymbol{\lambda} = (\boldsymbol{\lambda}_j^c, \boldsymbol{\lambda}_j)^\top \in \mathbf{V}_j^{(2)}$ satisfying $\mathsf{M}_j \boldsymbol{\lambda} = \mathbf{0}$ one has

$$\left\langle \lambda_{j,\mathrm{N}}^c, 1 \right\rangle_j = 0 \quad \text{and} \quad \left\langle \lambda_{j,\mathrm{N}}, 1 \right\rangle_j = 0, \tag{3.35}$$

From $\mathsf{M}_j \boldsymbol{\lambda} = \mathbf{0}$, we conclude that it holds

$$\mathsf{W}_j\, \lambda_{j,\mathrm{D}}^c + \mathsf{K}_j'\, \lambda_{j,\mathrm{N}}^c + \frac{1}{2} \frac{\sigma_j}{\sigma_0} \lambda_{j,\mathrm{N}} = 0 \tag{3.36}$$

and

$$-\frac{1}{2} \lambda_{j,\mathrm{N}}^c + \frac{\sigma_j}{\sigma_0} \left(\mathsf{W}_j\, \lambda_{j,\mathrm{D}} + \mathsf{K}_j'\, \lambda_{j,\mathrm{N}} \right) = 0. \tag{3.37}$$

Taking means of (3.36) and (3.37) over Γ_j and considering that $\langle \mathsf{W}_j\, \lambda_{j,\mathrm{D}}, 1 \rangle_j = \left\langle \mathsf{W}_j\, \lambda_{j,\mathrm{D}}^c, 1 \right\rangle_j = 0$ together with $\mathsf{K}_j\, 1 = -\frac{1}{2}$, we obtain

$$-\left\langle \lambda_{j,\mathrm{N}}^c, 1 \right\rangle_j + \frac{\sigma_j}{\sigma_0} \left\langle \lambda_{j,\mathrm{N}}, 1 \right\rangle_j = 0, \tag{3.38a}$$

$$-\left\langle \lambda_{j,\mathrm{N}}^c, 1 \right\rangle_j - \frac{\sigma_j}{\sigma_0} \left\langle \lambda_{j,\mathrm{N}}, 1 \right\rangle_j = 0, \tag{3.38b}$$

implying that $\left\langle \lambda_{j,\mathrm{N}}^c, 1 \right\rangle_j = \left\langle \lambda_{j,\mathrm{N}}, 1 \right\rangle_j = 0$.

(ii) For $j = 1, \ldots, J$, recalling (3.10), we consider

$$\widetilde{u}_j := -\Psi_j\left(\boldsymbol{\lambda}_j\right) \quad \text{in} \quad \Omega_j \qquad \text{and} \qquad \widetilde{u}_j^c := \Psi_j\left(\boldsymbol{\lambda}_j^c\right) \quad \text{in} \quad \Omega_j^c. \tag{3.39}$$

Let us compute

$$\boldsymbol{\gamma}^j \widetilde{u}_j = \left(\frac{1}{2}\mathsf{I} + \mathsf{A}_j\right) \boldsymbol{\lambda}_j \quad \text{on} \quad \Gamma_j, \tag{3.40}$$

and

$$\boldsymbol{\gamma}^{j,c} \widetilde{u}_j^c = \left(\frac{1}{2}\mathsf{I} - \mathsf{A}_j\right) \boldsymbol{\lambda}_j^c \quad \text{on} \quad \Gamma_j, \tag{3.41}$$

for $j = 1, \ldots, J$. Recalling that $\mathsf{M}_j \boldsymbol{\lambda} = \mathbf{0}$, we have

$$\boldsymbol{\gamma}^j \widetilde{u}_j = \frac{1}{2}\left(\boldsymbol{\lambda}_j + \mathsf{X}_j \, \boldsymbol{\lambda}_j^c\right) \quad \text{and} \quad \boldsymbol{\gamma}^{j,c} \widetilde{u}_j^c = \frac{1}{2}\left(\boldsymbol{\lambda}_j^c + \mathsf{X}_j^{-1} \boldsymbol{\lambda}_j\right) \quad \text{on} \quad \Gamma_j. \tag{3.42}$$

We compute the jump

$$\boldsymbol{\gamma}^j \widetilde{u}_j - \mathsf{X}_j \boldsymbol{\gamma}^{j,c} \widetilde{u}_j^c = 0 \quad \text{on} \quad \Gamma_j. \tag{3.43}$$

Therefore, $\widetilde{u}_j$ and $\widetilde{u}_j^c$ are solutions of Problem 2.4 for a single domain, *i.e.* $J \equiv 1$. We remark that for $d = 2$ the condition at infinity (2.19e) is satisfied since as shown in item (i) we have $\left\langle \lambda_{j,\mathrm{N}}^c, 1 \right\rangle_j = \langle \lambda_{j,\mathrm{N}}, 1 \rangle_j = 0$. Hence, recalling Theorem 3.1 and Remark 3.2, one concludes that the behaviour at infinity of $\widetilde{u}_j$ and $\widetilde{u}_j^c$ is the one required in (2.19e). By Proposition 2.5, we conclude that $\widetilde{u}_j \equiv 0$ in Ω_j and $\widetilde{u}_j^c \equiv 0$ in Ω_j^c.

(iii) Let $j = 1, \ldots, J$ be arbitrary but fixed and define

$$\hat{u}_j := -\Psi_j\left(\boldsymbol{\lambda}_j^c\right) \quad \text{in} \quad \Omega_j \qquad \text{and} \qquad \hat{u}_j^c := -\Psi_j\left(\boldsymbol{\lambda}_j\right) \quad \text{in} \quad \Omega_j^c. \tag{3.44}$$

Taking interior and exterior traces, we obtain

$$\gamma^j \hat{u}_j = \left(\frac{1}{2}\mathsf{I} + \mathsf{A}_j\right) \boldsymbol{\lambda}_j^c \quad \text{on} \quad \Gamma_j, \tag{3.45}$$

and

$$\gamma^{j,c} \hat{u}_j^c = -\left(\frac{1}{2}\mathsf{I} - \mathsf{A}_j\right) \boldsymbol{\lambda}_j \quad \text{on} \quad \Gamma_j. \tag{3.46}$$

Recalling that it holds $\mathsf{M}_j \boldsymbol{\lambda} = \mathbf{0}$, we have

$$\gamma^j \hat{u}_j = \frac{1}{2}\boldsymbol{\lambda}_j^c - \frac{1}{2}\mathsf{X}_j^{-1} \boldsymbol{\lambda}_j \quad \text{and} \quad \gamma^{j,c} \hat{u}_j^c = -\frac{1}{2}\boldsymbol{\lambda}_j + \frac{1}{2}\mathsf{X}_j \boldsymbol{\lambda}_j^c \quad \text{on} \quad \Gamma_j. \tag{3.47}$$

We compute the jump

$$\boldsymbol{\gamma}^j \hat{u}_j - \mathsf{X}_j^{-1} \boldsymbol{\gamma}^{j,c} \hat{u}_j^c = 0. \tag{3.48}$$

Hence, $\hat{u}_j$ and $\hat{u}_j^c$ are also solutions of Problem 2.4 for a single domain. We remark that for $d = 2$ the condition at infinity (2.19e) is satisfied since, as shown in item (i), we have $\left\langle \lambda_{j,\mathrm{N}}^c, 1 \right\rangle_j = \langle \lambda_{j,\mathrm{N}}, 1 \rangle_j = 0$. Again, recalling Theorem 3.1 and Remark 3.2, one concludes that the behaviour at infinity of $\hat{u}_j$ and $\hat{u}_j^c$ is the one required in (2.19e). Thus, $\hat{u}_j \equiv 0$ in Ω_j and $\hat{u}_j^c \equiv 0$ in Ω_j^c.

(iv) From steps (ii) and (iii) we conclude that

$$\boldsymbol{\lambda}_j + \mathsf{X}_j \boldsymbol{\lambda}_j^c = 0 \quad \text{and} \quad \boldsymbol{\lambda}_j^c - \mathsf{X}_j^{-1} \boldsymbol{\lambda}_j = 0 \quad \text{on} \quad \Gamma_j, \tag{3.49}$$

respectively. Therefore, $\boldsymbol{\lambda}_j \equiv 0$ and $\boldsymbol{\lambda}_j^c \equiv 0$. □

Lemma 3.8. *For $j,k = 1,\dots,J$, with $j \neq k$, the operators $\mathsf{T}_{k,j} : \mathbf{V}_j^s \to \mathbf{V}_k^s$ are continuously bounded for $|s| \leq \frac{1}{2}$. Furthermore, they are compact as mappings from $\mathbf{V}_j$ to $\mathbf{V}_k$. If the Γ_j, $j = 1,\dots,J$, are $\mathcal{C}^\infty$-boundaries, the statement is valid for all $s \in \mathbb{R}$.*

Proof. Operators $\mathsf{T}_{k,j}$ for $j \neq k$ consist of four BIOs with continuous kernels as boundaries for integration and trace evaluation never coincide. Therefore, the maps $\mathsf{T}_{k,j} : \mathbf{V}_j^s \to \mathbf{V}_k^s$ are continuous for $|s| \leq \frac{1}{2}$ for Lipschitz domains, whereas for $\mathcal{C}^\infty$-boundaries, the statement holds for all $s \in \mathbb{R}$ (*cf.* Thm. 3.5). Compactness comes from the compact embedding $\mathbf{V}_k^s \hookrightarrow \mathbf{V}_k$, for $s > 0$, with $s \leq 1$ or $s \leq k$ for Lipschitz or $\mathcal{C}^k$-domains, respectively ([52], Thm 2.5.5). □

Lemma 3.9. *The $\times$-adjoint $\mathsf{T}_{k,j}^\dagger = \mathsf{T}_{j,k}$ for $j,k = 1,\dots,J$ and $j \neq k$.*

Proof. First, notice that $\mathcal{S}_j' = \gamma_{\mathrm{D}}^j \circ \mathcal{N}$ and $\mathcal{D}_j' = \gamma_{\mathrm{N}}^j \circ \mathcal{N}$, as $\mathcal{N}$ is self-adjoint. Then, by the definition of $\mathsf{T}_{j,k}$ (3.24) and using (2.5), we obtain

$$\mathsf{T}_{k,j}^\dagger = \begin{pmatrix} -\mathcal{S}_j' \circ \left(\gamma_{\mathrm{N}}^{k,c}\right)' & -\mathcal{S}_j' \circ \left(\gamma_{\mathrm{D}}^{k,c}\right)' \\ \mathcal{D}_j' \circ \left(\gamma_{\mathrm{N}}^{k,c}\right)' & \mathcal{D}_j' \circ \left(\gamma_{\mathrm{D}}^{k,c}\right)' \end{pmatrix} = \begin{pmatrix} -\gamma_{\mathrm{D}}^j \circ \mathcal{N} \circ \left(\gamma_{\mathrm{N}}^{k,c}\right)' & -\gamma_{\mathrm{D}}^j \circ \mathcal{N} \circ \left(\gamma_{\mathrm{D}}^{k,c}\right)' \\ \gamma_{\mathrm{N}}^j \circ \mathcal{N} \circ \left(\gamma_{\mathrm{N}}^{k,c}\right)' & \gamma_{\mathrm{N}}^j \circ \mathcal{N} \circ \left(\gamma_{\mathrm{D}}^{k,c}\right)' \end{pmatrix} \tag{3.50}$$

Observing that in this context $\gamma_{\mathrm{N}}^{\cdot,c} = -\gamma_{\mathrm{N}}^{\cdot}$ and that $\gamma_{\mathrm{D}}^{\cdot,c} = \gamma_{\mathrm{D}}^{\cdot}$, we conclude

$$\mathsf{T}_{k,j}^\dagger = = \begin{pmatrix} +\gamma_{\mathrm{D}}^{j,c} \circ \mathcal{N} \circ \left(\gamma_{\mathrm{N}}^k\right)' & -\gamma_{\mathrm{D}}^{j,c} \circ \mathcal{N} \circ \left(\gamma_{\mathrm{D}}^k\right)' \\ +\gamma_{\mathrm{N}}^{j,c} \circ \mathcal{N} \circ \left(\gamma_{\mathrm{N}}^k\right)' & -\gamma_{\mathrm{N}}^{j,c} \circ \mathcal{N} \circ \left(\gamma_{\mathrm{D}}^k\right)' \end{pmatrix} = \begin{pmatrix} \gamma_{\mathrm{D}}^{j,c} \circ \mathcal{D}_k & -\gamma_{\mathrm{D}}^{j,c} \circ \mathcal{S}_k \\ \gamma_{\mathrm{N}}^{j,c} \circ \mathcal{D}_k & -\gamma_{\mathrm{N}}^{j,c} \circ \mathcal{S}_k \end{pmatrix} = \mathsf{T}_{j,k} \tag{3.51}$$

as stated. □

Let us introduce the block operator:

$$\mathsf{Q}_{j,k} := \begin{pmatrix} -\mathsf{T}_{j,k} & 0 \\ 0 & 0 \end{pmatrix} : \mathbf{V}_k^{(2)} \to \mathbf{V}_j^{(2)}, \tag{3.52}$$

inheriting the same continuity and compactness properties of $\mathsf{T}_{j,k}$. Moreover, it also holds $\mathsf{Q}_{j,k}^\dagger = \mathsf{Q}_{k,j}$. Then, we can write down the boundary integral problem we seek to solve:

Problem 3.10 (MTF for J Mutually Disjoint Subdomains)**.** Find $\boldsymbol{\lambda} = (\boldsymbol{\lambda}_1^c, \boldsymbol{\lambda}_1, \dots, \boldsymbol{\lambda}_J^c, \boldsymbol{\lambda}_J)^\top \in \mathbb{V}_J$ such that the following variational problem:

$$\mathsf{m}_J(\boldsymbol{\lambda}, \boldsymbol{\varphi}) := \langle \mathbf{M}_J \boldsymbol{\lambda}, \boldsymbol{\varphi} \rangle_\times = \langle \mathbf{f}_J, \boldsymbol{\varphi} \rangle_\times, \quad \text{for all} \quad \boldsymbol{\varphi} \in \mathbb{V}_J, \tag{3.53}$$

is satisfied, with duality pairing set as sums of cross-pairings (2.4). The block operator on the left-hand side is defined using (3.32) and (3.52) as

$$\mathbf{M}_J := \begin{pmatrix} \mathsf{M}_1 & \mathsf{Q}_{1,2} & \cdots & \mathsf{Q}_{1,J} \\ \mathsf{Q}_{2,1} & \mathsf{M}_2 & \cdots & \mathsf{Q}_{2,J} \\ \vdots & \vdots & \ddots & \vdots \\ \mathsf{Q}_{J,1} & \mathsf{Q}_{J,2} & \cdots & \mathsf{M}_J \end{pmatrix} : \mathbb{V}_J \to \mathbb{V}_J, \tag{3.54}$$

with source term $\mathbf{f}_J$ given in terms of the following components:

$$\boldsymbol{\mathcal{V}} := (\mathcal{V}_1, \mathcal{V}_1, \ldots, \mathcal{V}_J, \mathcal{V}_J) \in \mathbb{V}_J, \tag{3.55}$$

$$\boldsymbol{\phi}_e := (\boldsymbol{\gamma}^{1,c}\Phi_e, \boldsymbol{\gamma}^{1,c}\Phi_e, \ldots, \boldsymbol{\gamma}^{J,c}\Phi_e, \boldsymbol{\gamma}^{J,c}\Phi_e) \in \mathbb{V}_J, \tag{3.56}$$

$$\mathsf{F}_j := \begin{pmatrix} \mathsf{I} & 0 \\ 0 & \hat{\mathsf{X}}_j \end{pmatrix} \in \mathbf{V}_j^{(2)} \to \mathbf{V}_j^{(2)}, \tag{3.57}$$

so that

$$\mathbf{f}_J(\mathcal{V}_1, \ldots, \mathcal{V}_J, \boldsymbol{\phi}_e) := \frac{1}{2}\mathrm{diag}\,(\mathsf{F}_1, \mathsf{F}_2, \ldots, \mathsf{F}_J)\,(\boldsymbol{\mathcal{V}} + \boldsymbol{\phi}_e) \in \mathbb{V}_J. \tag{3.58}$$

We now prove the well-posedness of Problem 3.10 as a consequence of the Fredholm alternative.

Proposition 3.11. *The operator $\mathbf{M}_J : \mathbb{V}_J \to \mathbb{V}_J$ is injective, namely Problem 3.10 admits at most one solution.*

Proof. We proceed as in the proof of Lemma 3.7. Let $\boldsymbol{\lambda} = (\boldsymbol{\lambda}_1^c, \boldsymbol{\lambda}_1, \ldots, \boldsymbol{\lambda}_J^c, \boldsymbol{\lambda}_J)^\top \in \mathbb{V}_J$, where $\boldsymbol{\lambda}_j^c = (\lambda_{j,\mathrm{D}}^c, \lambda_{j,\mathrm{N}}^c)^\top \in \mathbf{V}_j$ and $\boldsymbol{\lambda}_j = (\lambda_{j,\mathrm{D}}, \lambda_{j,\mathrm{N}})^\top \in \mathbf{V}_j$, be the solution of $\mathbf{M}_J\boldsymbol{\lambda} = \mathbf{0}$. Then one must show that $\boldsymbol{\lambda} \equiv 0$.

(i) First, we show that for $\boldsymbol{\lambda} \in \mathbb{V}_J$ satisfying $\mathbf{M}_J\boldsymbol{\lambda} = \mathbf{0}$ one has

$$\langle \lambda_{j,\mathrm{N}}^c, 1\rangle_j = 0 \quad \text{and} \quad \langle \lambda_{j,\mathrm{N}}, 1\rangle_j = 0, \quad j = 1, \ldots, J. \tag{3.59}$$

Since $\mathbf{M}_J\boldsymbol{\lambda} = \mathbf{0}$, we conclude that it holds

$$\mathsf{W}_j\,\lambda_{j,\mathrm{D}}^c + \mathsf{K}_j'\,\lambda_{j,\mathrm{N}}^c - \sum_{\substack{k=1 \\ k\neq j}}^{J} \left(\left(\gamma_{\mathrm{N}}^{j,c} \circ \mathcal{D}_k\right)\lambda_{k,\mathrm{D}}^c - \left(\gamma_{\mathrm{N}}^{j,c} \circ \mathcal{S}_k\right)\lambda_{k,\mathrm{N}}^c\right) + \frac{1}{2}\frac{\sigma_j}{\sigma_0}\lambda_{j,\mathrm{N}} = 0 \tag{3.60}$$

and

$$-\frac{1}{2}\lambda_{j,\mathrm{N}}^c + \frac{\sigma_j}{\sigma_0}\left(\mathsf{W}_j\,\lambda_{j,\mathrm{D}} + \mathsf{K}_j'\,\lambda_{j,\mathrm{N}}\right) = 0. \tag{3.61}$$

Testing (3.60) and (3.61) against one over Γ_j and considering that $\langle \mathsf{W}_j\,\lambda_{j,\mathrm{D}}, 1\rangle_j = \langle \mathsf{W}_j\,\lambda_{j,\mathrm{D}}^c, 1\rangle_j = 0$ and $\mathsf{K}_j\,1 = -\frac{1}{2}$, together with $\left\langle \left(\gamma_{\mathrm{N}}^{j,c} \circ \mathcal{D}_k\right)\lambda_{k,\mathrm{D}}^c, 1\right\rangle_j = \left\langle \left(\gamma_{\mathrm{N}}^{j,c} \circ \mathcal{S}_k\right)\lambda_{k,\mathrm{N}}^c, 1\right\rangle_j = 0$, for $j, k = 1, \ldots, J$, with $j \neq k$, we obtain

$$-\langle \lambda_{j,\mathrm{N}}^c, 1\rangle_j + \frac{\sigma_j}{\sigma_0}\langle \lambda_{j,\mathrm{N}}, 1\rangle_j = 0, \tag{3.62a}$$

$$-\langle \lambda_{j,\mathrm{N}}^c, 1\rangle_j - \frac{\sigma_j}{\sigma_0}\langle \lambda_{j,\mathrm{N}}, 1\rangle_j = 0, \tag{3.62b}$$

which in turn implies that $\left\langle \lambda^c_{j,\mathrm{N}}, 1\right\rangle_j = \langle \lambda_{j,\mathrm{N}}, 1\rangle_j = 0$.

(ii) Recalling (3.10), for $j = 1, \ldots, J$, we define

$$\widetilde{u}_j := -\Psi_j\left(\boldsymbol{\lambda}_j\right) \quad \text{in } \Omega_j \quad \text{and} \quad \widetilde{u}_0 := \sum_{\ell=1}^{J} \Psi_j\left(\boldsymbol{\lambda}^c_j\right) \quad \text{in } \Omega_0. \tag{3.63}$$

Let us compute

$$\boldsymbol{\gamma}^j \widetilde{u}_j = \left(\frac{1}{2}\mathsf{I} + \mathsf{A}_j\right)\boldsymbol{\lambda}_j \quad \text{on} \quad \Gamma_j, \tag{3.64}$$

for $j = 1, \ldots, J$, and

$$\boldsymbol{\gamma}^{j,c} \widetilde{u}_0 = \left(\frac{1}{2}\mathsf{I} - \mathsf{A}_j\right)\boldsymbol{\lambda}^c_j + \sum_{\substack{\ell=1 \\ \ell\neq j}}^{J} \mathsf{T}_{j,\ell}\boldsymbol{\lambda}^c_\ell \quad \text{on} \quad \Gamma_j, \tag{3.65}$$

for $j = 1, \ldots, J$. Recalling that $\mathbf{M}_J\boldsymbol{\lambda} = \mathbf{0}$, we have

$$\boldsymbol{\gamma}^j \widetilde{u}_j = \frac{1}{2}\left(\boldsymbol{\lambda}_j + \mathsf{X}_j\,\boldsymbol{\lambda}^c_j\right) \quad \text{and} \quad \boldsymbol{\gamma}^{j,c}\widetilde{u}_0 = \frac{1}{2}\left(\boldsymbol{\lambda}^c_j + \mathsf{X}_j^{-1}\boldsymbol{\lambda}_j\right) \quad \text{on} \quad \Gamma_j. \tag{3.66}$$

We compute the jump

$$\boldsymbol{\gamma}^j \widetilde{u}_j - \mathsf{X}_j\boldsymbol{\gamma}^{j,c}\widetilde{u}_0 = 0 \quad \text{on} \quad \Gamma_j. \tag{3.67}$$

By construction, $\widetilde{u}_j$ and $\widetilde{u}_0$ are solution of Problem 2.4. As in Lemma 3.7, we observe that for $d = 2$ the condition at infinity (2.19e) is satisfied, since as shown in item (i), we have that $\left\langle \lambda^c_{j,\mathrm{N}}, 1\right\rangle_j = \langle \lambda_{j,\mathrm{N}}, 1\rangle_j = 0$. Therefore, recalling Theorem 3.1 and Remark 3.2, one concludes that the behaviour at infinity of $\tilde{u}_j$ and $\tilde{u}_0$ is the one required in (2.19e), for $j = 1, \ldots, J$. Hence, from Proposition 2.5 we conclude that $\widetilde{u}_j \equiv 0$ in Ω_j and $\widetilde{u}_0 \equiv 0$ in Ω_0, for $j = 1, \ldots, J$.

(iii) Let us define

$$\hat{u}_j := -\sum_{\ell=1}^{J} \Psi_\ell\left(\boldsymbol{\lambda}^c_\ell\right) \quad \Omega_j \quad \text{and} \quad \hat{u}^c_j := -\Psi_j\left(\boldsymbol{\lambda}_j\right) \quad \text{in} \quad \Omega^c_j, \tag{3.68}$$

for $j = 1, \ldots, J$. Taking interior and exterior traces, we obtain

$$\gamma^j \hat{u}_j = \left(\frac{1}{2}\mathsf{I} + \mathsf{A}_j\right)\boldsymbol{\lambda}^c_j - \sum_{\substack{\ell=1 \\ \ell\neq j}}^{J} \widetilde{\mathsf{T}}_{j,\ell}\,\boldsymbol{\lambda}^c_\ell \quad \text{on} \quad \Gamma_j, \tag{3.69}$$

where

$$\widetilde{\mathsf{T}}_{j,\ell} := \begin{pmatrix} \gamma^j_{\mathrm{D}} \circ \mathcal{D}_\ell & -\gamma^j_{\mathrm{D}} \circ \mathcal{S}_\ell \\ \gamma^j_{\mathrm{N}} \circ \mathcal{D}_\ell & -\gamma^j_{\mathrm{N}} \circ \mathcal{S}_\ell \end{pmatrix} : \mathbf{V}_\ell \to \mathbf{V}_j. \tag{3.70}$$

and

$$\gamma^{j,c}\hat{u}_j^c = -\left(\frac{1}{2}\mathsf{I} - \mathsf{A}_j\right)\boldsymbol{\lambda}_j \quad \text{on} \quad \Gamma_j, \tag{3.71}$$

Note that $\widetilde{\mathsf{T}}_{j,\ell} = \mathsf{T}_{j,\ell}$, due to definitions (2.2) and (2.3). Recalling that it holds $\mathbf{M}_J\boldsymbol{\lambda} = \mathbf{0}$, we have

$$\gamma^j\hat{u}_j = \frac{1}{2}\boldsymbol{\lambda}_j^c - \frac{1}{2}\mathsf{X}_j^{-1}\boldsymbol{\lambda}_j \quad \text{and} \quad \gamma^{j,c}\hat{u}_j^c = -\frac{1}{2}\boldsymbol{\lambda}_j + \frac{1}{2}\mathsf{X}_j\boldsymbol{\lambda}_j^c \quad \text{on} \quad \Gamma_j. \tag{3.72}$$

We compute the jump

$$\boldsymbol{\gamma}^j\hat{u}_0 - \mathsf{X}_j^{-1}\boldsymbol{\gamma}^{j,c}\hat{u}_j^c = 0 \quad \text{on} \quad \Gamma_j. \tag{3.73}$$

Since the assumptions of Proposition 2.5 hold we can conclude that $\widetilde{u}_j \equiv 0$ in Ω_j and $\widetilde{u}_0 \equiv 0$ in Ω_0.

(iv) As in step (iv) of the proof for Lemma 3.7, from steps (ii) and (iii) we conclude that $\boldsymbol{\lambda}_j \equiv 0$ and $\boldsymbol{\lambda}_j^c \equiv 0$ for all $j = 1, \ldots, J$, so that $\boldsymbol{\lambda} \equiv 0$ as required.

□

Proposition 3.12. *Let $\Omega_j \in \mathbb{R}^d$, $d = 2, 3$, $j = 1, \ldots, J$, be Lipschitz domains. The bilinear form $\mathsf{m}_J : \mathbb{V}_J^s \times \mathbb{V}_J^s \to \mathbb{R}$ is continuously bounded for $|s| \leq \frac{1}{2}$, i.e. for a constant $\alpha_J(s) > 0$ there holds*

$$|\mathsf{m}_J(\boldsymbol{\lambda}, \boldsymbol{\varphi})| \leq \alpha_J(s)\,\|\boldsymbol{\lambda}\|_{\mathbb{V}_J^s}\,\|\boldsymbol{\varphi}\|_{\mathbb{V}_J^s}, \quad \forall\ \boldsymbol{\lambda}, \boldsymbol{\varphi} \in \mathbb{V}_J^s, \tag{3.74}$$

and it is $\mathbb{V}_J$-coercive, i.e. there exists another constant $\mu_{\mathsf{m}_J} > 0$ and $\mathbf{T}_J : \mathbb{V}_J \to \mathbb{V}_J$ compact such that

$$\mathsf{m}_J(\boldsymbol{\lambda}, \boldsymbol{\lambda}) + \langle \mathbf{T}_J\boldsymbol{\lambda}, \boldsymbol{\lambda}\rangle_\times \geq \mu_{\mathsf{m}_J}\,\|\boldsymbol{\varphi}\|_{\mathbb{V}_J}^2, \quad \forall\ \boldsymbol{\lambda} \in \mathbb{V}_J. \tag{3.75}$$

Proof. Splitting $\boldsymbol{\lambda}$ and $\boldsymbol{\varphi}$ into its J components in $\mathbf{V}_j^{(2)}$, for $j = 1, \ldots, J$, the bilinear form m_J can be cast as follows

$$\mathsf{m}_J(\boldsymbol{\lambda}, \boldsymbol{\varphi}) = \sum_{j=1}^{J} \left\langle \mathsf{M}_j\boldsymbol{\lambda}_j^{(2)}, \boldsymbol{\varphi}_j^{(2)} \right\rangle_{\times,j} + \sum_{j=1}^{J}\sum_{\substack{k=1 \\ k\neq j}}^{J} \left\langle \mathsf{Q}_{j,k}\boldsymbol{\lambda}_k^{(2)}, \boldsymbol{\varphi}_j^{(2)} \right\rangle_{\times,j}. \tag{3.76}$$

Continuity follows from Lemmae 3.7 and 3.8 whereas coercivity is derived by combining also Lemma 3.7 with the compactness of $\mathsf{Q}_{j,k}$. Specifically, the operator $\mathbf{T}_J$ is given by

$$\mathbf{T}_J := \begin{pmatrix} \mathsf{T}_{\mathsf{M}_1} & -\mathsf{Q}_{1,2} & \cdots & -\mathsf{Q}_{1,J} \\ -\mathsf{Q}_{2,1} & \mathsf{T}_{\mathsf{M}_2} & \ddots & -\mathsf{Q}_{2,J} \\ \vdots & \ddots & \ddots & \vdots \\ -\mathsf{Q}_{J,1} & -\mathsf{Q}_{J,2} & \cdots & \mathsf{T}_{\mathsf{M}_J} \end{pmatrix}. \tag{3.77}$$

Therefore,

$$\mathsf{m}_J(\boldsymbol{\lambda}, \boldsymbol{\lambda}) + \langle \mathbf{T}_J\boldsymbol{\lambda}\boldsymbol{\lambda}_\times\rangle \geq \min_{j=1,\ldots,J} \mu_{\mathsf{M}_j}\,\|\boldsymbol{\lambda}\|_{\mathbb{V}_J}^2, \tag{3.78}$$

with $\mu_{\mathsf{m}_J} := \min_{j=1,\ldots,J} \mu_{\mathsf{M}_j} > 0$. □

4. MTF for several biological cells

In what follows, we explain how the MTF given in Problem 3.10 relates to the transmembrane current in the HH model for many cells. Hence, from this point onwards all currents and potentials are time-dependent quantities. Yet, for the sake of brevity we forgo momentarily to write down such dependence. The transmembrane current across a cell boundary Γ_j can be expressed as contributions originated by the exterior potential Φ_e, ion currents $i_{\text{ion},j}$, and potential jumps v_j and v_k present at the surrounding $J-1$ cells. Explicitly, if we consider the unknown trace vector $\boldsymbol{\lambda} \in \mathbb{V}_J$ in (3.53), and recall the current equation (2.15), we deduce

$$-2i_j = \sigma_j \lambda_{j,\mathrm{N}} + \sigma_0 \lambda^c_{j,\mathrm{N}} + \sigma_0 \gamma^{j,c}_{\mathrm{N}} \Phi_e, \quad \text{on} \quad \Gamma_j, \quad \text{for } j = 1, \dots, J, \tag{4.1}$$

or, equivalently,

$$i_j = -\frac{1}{2} \begin{pmatrix} 0 & \sigma_0 & 0 & \sigma_j \end{pmatrix} \boldsymbol{\lambda}^{(2)}_j - \frac{1}{2} \sigma_0 \gamma^{j,c}_{\mathrm{N}} \Phi_e, \quad \text{on} \quad \Gamma_j, \quad \text{for } j = 1, \dots, J. \tag{4.2}$$

By linearity of Problem 3.10, we consider contributions for each term in (4.2) by switching on each component in $\mathbf{f}_J$ (3.58) while setting to zero all other sources. Recalling the definition of $\mathbf{f}_J$ (3.58), we can write the linear combination:

$$\mathbf{f}_J(\mathcal{V}_1, \dots \mathcal{V}_J, \boldsymbol{\phi}_e) = \sum_{j=1}^{J} \mathbf{f}^j_J(\boldsymbol{\phi}_e) + \sum_{j=1}^{J} \mathbf{f}^j_J(v_j) \in \mathbb{V}_J, \tag{4.3}$$

with components:

$$\mathbf{f}^j_J(\boldsymbol{\phi}_e) := \frac{1}{2} \left(\mathbf{0}, \dots, \mathbf{0}, \begin{pmatrix} \boldsymbol{\gamma}^{j,c} \Phi_e \\ \hat{\mathsf{X}}_j \boldsymbol{\gamma}^{j,c} \Phi_e \end{pmatrix}, \mathbf{0}, \dots, \mathbf{0} \right) \in \mathbb{V}_J, \tag{4.4}$$

$$\mathbf{f}^j_J(v_j) := \frac{1}{2} \left(\mathbf{0}, \dots, \mathbf{0}, \begin{pmatrix} \mathcal{V}_j \\ \hat{\mathsf{X}}_j \mathcal{V}_j \end{pmatrix}, \dots, \mathbf{0} \right) \in \mathbb{V}_J, \tag{4.5}$$

as v_j appears in the term $\mathcal{V}_j$. Each term leads to a corresponding solution of the MTF system given by the application of $\mathbf{M}_J^{-1}$ onto each right-hand side (4.4) and (4.5). From the statement of Problem 3.10, we can easily derive the jth block equation:

$$\boldsymbol{\lambda}^{(2)}_j = \frac{1}{2} \mathsf{M}_j^{-1} \mathbf{f}^j_J(\boldsymbol{\phi}_e) + \frac{1}{2} \mathsf{M}_j^{-1} \mathbf{f}^j_J(v_j) - \mathsf{M}_j^{-1} \sum_{\substack{k=1 \\ k \neq j}}^{J} \mathsf{Q}_{j,k} \boldsymbol{\lambda}^{(2)}_k \in \mathbf{V}^{(2)}_j. \tag{4.6}$$

Let us adopt the notation $\boldsymbol{\lambda}^{(2)}_j(v_k, \boldsymbol{\phi}_e)$ to explicitly show the dependence on a particular source, *e.g.*, $\boldsymbol{\lambda}^{(2)}_j(v_k, \mathbf{0})$ is the solution of the traces pair over the jth cell solely due to the transmembrane potential v_k. Plugging solutions (4.6) into (4.2) yields the electric current decomposition:

$$i_j = i_j(\boldsymbol{\phi}_e) + i_j(v_j) + \sum_{\substack{k=1 \\ k \neq j}}^{J} i_j(v_k) \quad \text{on} \quad \Gamma_j, \tag{4.7}$$

wherein

$$i_j(\boldsymbol{\phi}_e) := -\frac{1}{2}\sigma_0\gamma_{\mathrm{N}}^{j,c}\Phi_e - \frac{1}{2}\begin{pmatrix}0 & \sigma_0 & 0 & \sigma_j\end{pmatrix}\left[\frac{1}{2}\mathsf{M}_j^{-1}\begin{pmatrix}\boldsymbol{\gamma}^{j,c}\boldsymbol{\Phi}_e\\ \hat{\mathsf{X}}_j\boldsymbol{\gamma}^{j,c}\boldsymbol{\Phi}_e\end{pmatrix} - \mathsf{M}_j^{-1}\sum_{\substack{\ell=1\\ \ell\neq j}}^{J}\mathsf{Q}_{j,\ell}\boldsymbol{\lambda}_\ell^{(2)}(0,\boldsymbol{\phi}_e)\right], \tag{4.8}$$

$$i_j(v_j) := -\frac{1}{2}\begin{pmatrix}0 & \sigma_0 & 0 & \sigma_j\end{pmatrix}\left[\frac{1}{2}\mathsf{M}_j^{-1}\begin{pmatrix}\mathcal{V}_j\\ \hat{\mathsf{X}}_j\mathcal{V}_j\end{pmatrix} - \mathsf{M}_j^{-1}\sum_{\substack{\ell=1\\ \ell\neq j}}^{J}\mathsf{Q}_{j,\ell}\boldsymbol{\lambda}_\ell^{(2)}(v_j,\mathbf{0})\right], \tag{4.9}$$

$$i_j(v_k) := +\frac{1}{2}\begin{pmatrix}0 & \sigma_0 & 0 & \sigma_j\end{pmatrix}\mathsf{M}_j^{-1}\sum_{\substack{\ell=1\\ \ell\neq j}}^{J}\mathsf{Q}_{j,\ell}\boldsymbol{\lambda}_\ell^{(2)}(v_k,\mathbf{0}) \quad \text{for } j\neq k. \tag{4.10}$$

Recall that each term represents the electric current generated by a given source. We start by obtaining the contribution $i_j(v_j)$ due to one transmembrane potential v_j, or equivalently, set the external potential traces $\boldsymbol{\phi}_e$ as well as v_k, for all $k\neq j$, equal to zero. Defining the following maps:

$$\mathcal{J}_j(v_j) := \frac{1}{4\sigma_0}\begin{pmatrix}0 & \sigma_0 & 0 & \sigma_j\end{pmatrix}\mathsf{M}_j^{-1}\begin{pmatrix}\sigma_0\\ 0\\ \sigma_j\\ 0\end{pmatrix}v_j \;:\; H^{\frac{1}{2}}(\Gamma_j)\to H^{-\frac{1}{2}}(\Gamma_j), \tag{4.11}$$

$$\mathcal{J}_{j,k}(v_k) := \frac{1}{2}\begin{pmatrix}0 & \sigma_0 & 0 & \sigma_j\end{pmatrix}\mathsf{M}_j^{-1}\sum_{\substack{\ell=1\\ \ell\neq j}}^{J}\mathsf{Q}_{j,\ell}\boldsymbol{\lambda}_\ell^{(2)}(v_k,\mathbf{0}) \;: H^{\frac{1}{2}}(\Gamma_k)\to H^{-\frac{1}{2}}(\Gamma_j), \tag{4.12}$$

we can also write (4.9) as the sum of contributions:

$$i_j = i_j(\boldsymbol{\phi}_e) - \mathcal{J}_j(v_j) + \sum_{k=1}^{J}\mathcal{J}_{j,k}(v_k). \tag{4.13}$$

Lemma 4.1. *Let Γ_j be $\mathcal{C}^\infty$-boundaries of $\Omega_j\in\mathbb{R}^d$, $d=2,3$, for $j=1,\dots,J$. For $j=1,\dots,J$, the operators $\mathcal{J}_j : H^{\frac{1}{2}+s}(\Gamma_j)\to H^{-\frac{1}{2}+s}(\Gamma_j)$ defined in (4.11) are continuous for $s\in\mathbb{R}$. Moreover, they are $H^{\frac{1}{2}}(\Gamma_j)$-coercive, i.e. it holds*

$$\left\langle\left(\mathcal{J}_j+\mathsf{T}_{\mathcal{J}_j}\right)v, v\right\rangle_j \geq c_{\mathcal{J}_j}\left\|v\right\|^2_{H^{\frac{1}{2}}(\Gamma_j)}, \qquad \text{for all} \quad v\in H^{\frac{1}{2}}(\Gamma_j), \tag{4.14}$$

where $c_{\mathcal{J}_j}$ is a strictly positive constant and $\mathsf{T}_{\mathcal{J}_j} : H^{\frac{1}{2}+s}(\Gamma_j)\to H^{-\frac{1}{2}+s}(\Gamma_j)$ is compact. Besides, the operator $\mathcal{J}_j$ is self-adjoint.

For $k=1,\dots,J$ with $k\neq j$, the operators $\mathcal{J}_{j,k} : H^{\frac{1}{2}+s}(\Gamma_k)\to H^{-\frac{1}{2}+s}(\Gamma_j)$, are continuous for $s\in\mathbb{R}$ and, furthermore, compact.

Proof. Continuity of $\mathcal{J}_j$ and $\mathcal{J}_{j,k}$, for $k\neq j$, comes from the fact that both operators are by definition the composition of continuous operators (*cf.* Lems. 3.7 and 3.8). In particular, the operator $\mathcal{J}_{j,k}$ for $k\neq j$ is defined as the sum and composition of continuous and compact operators, therefore it is compact as well.

From Lemma 3.7, M_j is invertible. Let $\boldsymbol{\varphi}_j^{(2)} \in \mathbf{V}_j^{(2)}$, then it holds

$$\left\langle \mathsf{M}_j \boldsymbol{\varphi}_j^{(2)}, \boldsymbol{\varphi}_j^{(2)} \right\rangle_{\times,j} = \left\langle \mathsf{M}_j \left(\mathsf{M}_j^\dagger\right)^{-1} \mathsf{M}_j^\dagger \boldsymbol{\varphi}_j^{(2)}, \boldsymbol{\varphi}_j^{(2)} \right\rangle_{\times,j} = \left\langle \left(\mathsf{M}_j^\dagger\right)^{-1} \mathsf{M}_j^\dagger \boldsymbol{\varphi}_j^{(2)}, \mathsf{M}_j^\dagger \boldsymbol{\varphi}_j^{(2)} \right\rangle_{\times,j}. \tag{4.15}$$

By using (2.8) and (2.5), one can easily derive $\mathsf{M}_j^\dagger = -\mathsf{S}\mathsf{M}_j\mathsf{S}$, where

$$\mathsf{S} := \begin{pmatrix} \mathsf{D} & 0 \\ 0 & \mathsf{D} \end{pmatrix} \quad \text{and} \quad \mathsf{D} := \begin{pmatrix} \mathsf{I} & 0 \\ 0 & -\mathsf{I} \end{pmatrix}. \tag{4.16}$$

Notice that $\mathsf{S}^\dagger = -\mathsf{S}$ and $\mathsf{S}^{-1} = \mathsf{S}$. Then,

$$\left\langle \left(\mathsf{M}_j^\dagger\right)^{-1} \mathsf{M}_j^\dagger \boldsymbol{\varphi}_j^{(2)}, \mathsf{M}_j^\dagger \boldsymbol{\varphi}_j^{(2)} \right\rangle_{\times,j} = \left\langle \mathsf{M}_j^{-1} \mathsf{S}\, \mathsf{M}_j^\dagger \boldsymbol{\varphi}_j^{(2)}, \mathsf{S}\, \mathsf{M}_j^\dagger \boldsymbol{\varphi}_j^{(2)} \right\rangle_{\times,j}. \tag{4.17}$$

Defining $\boldsymbol{\lambda}_j^{(2)} = \mathsf{S}\, \mathsf{M}_j^\dagger \boldsymbol{\varphi}_j^{(2)} \in \mathbf{V}_j^{(2)}$ we have

$$\begin{aligned}
\left\langle (\mathsf{M}_j + \mathsf{T}_{\mathsf{M}_j}) \boldsymbol{\varphi}_j^{(2)}, \boldsymbol{\varphi}_j^{(2)} \right\rangle_{\times,j} &= \left\langle \mathsf{M}_j^{-1} \boldsymbol{\lambda}_j^{(2)}, \boldsymbol{\lambda}_j^{(2)} \right\rangle_{\times,j} + \left\langle \mathsf{T}_{\mathsf{M}_j} \left(\mathsf{M}_j^\dagger\right)^{-1} \mathsf{S}\, \boldsymbol{\lambda}_j^{(2)}, \left(\mathsf{M}_j^\dagger\right)^{-1} \mathsf{S}\, \boldsymbol{\lambda}_j^{(2)} \right\rangle_{\times,j} \\
&= \left\langle \mathsf{M}_j^{-1} \boldsymbol{\lambda}_j^{(2)}, \boldsymbol{\lambda}_j^{(2)} \right\rangle_{\times,j} - \left\langle \mathsf{M}_j^{-1} \mathsf{S}\, \mathsf{T}_{\mathsf{M}_j} \left(\mathsf{M}_j^\dagger\right)^{-1} \mathsf{S}\, \boldsymbol{\lambda}_j^{(2)}, \boldsymbol{\lambda}_j^{(2)} \right\rangle_{\times,j} \\
&= \left\langle \mathsf{M}_j^{-1} \boldsymbol{\lambda}_j^{(2)}, \boldsymbol{\lambda}_j^{(2)} \right\rangle_{\times,j} + \left\langle \mathsf{M}_j^{-1} \mathsf{S}\, \mathsf{T}_{\mathsf{M}_j} \mathsf{S} \mathsf{M}_j^{-1} \boldsymbol{\lambda}_j^{(2)}, \boldsymbol{\lambda}_j^{(2)} \right\rangle_{\times,j} \\
&\geq \mu_{\mathsf{M}_j} \left\| \boldsymbol{\varphi}_j^{(2)} \right\|^2_{\mathbf{V}_j^{(2)}} \\
&\geq \frac{\mu_{\mathsf{M}_j}}{\left\| \mathsf{M}_j^\dagger \right\|_{\mathcal{L}\left(\mathbf{V}_j^{(2)}, \mathbf{V}_j^{(2)}\right)}} \left\| \boldsymbol{\lambda}_j^{(2)} \right\|^2_{\mathbf{V}_j^{(2)}}
\end{aligned} \tag{4.18}$$

with μ_{M_j} given by Lemma 3.8. Therefore, if we define

$$\mu_{\mathsf{M}_j^{-1}} := \frac{\mu_{\mathsf{M}_j}}{\left\| \mathsf{M}_j^\dagger \right\|_{\mathcal{L}\left(\mathbf{V}_j^{(2)} \times \mathbf{V}_j^{(2)}\right)}} \quad \text{and} \quad \mathsf{T}_{\mathsf{M}_j^{-1}} := \mathsf{M}_j^{-1} \mathsf{S} \mathsf{T}_{\mathsf{M}_j} \mathsf{S}\, \mathsf{M}_j^{-1} : \mathbf{V}_j^{(2)} \to \mathbf{V}_j^{(2)}, \tag{4.19}$$

the operator M_j^{-1} satisfies

$$\left\langle \left(\mathsf{M}_j^{-1} + \mathsf{T}_{\mathsf{M}_j^{-1}}\right) \boldsymbol{\lambda}_j^{(2)}, \boldsymbol{\lambda}_j^{(2)} \right\rangle_{\times,j} \geq \mu_{\mathsf{M}_j^{-1}} \left\| \boldsymbol{\lambda}_j^{(2)} \right\|^2_{\mathbf{V}_j^{(2)}}, \quad \forall\, \boldsymbol{\lambda}_j^{(2)} \in \mathbf{V}_j^{(2)}. \tag{4.20}$$

Clearly, the operator $\mathsf{T}_{\mathsf{M}_j^{-1}}$ is compact being the composition of compact and continuous operators. For $v_j \in H^{\frac{1}{2}}(\Gamma_j)$, choose

$$\boldsymbol{\lambda}_j^{(2)} = (\sigma_0\ 0\ \sigma_j\ 0)^\top v_j \ \in \mathbf{V}_j^{(2)}. \tag{4.21}$$

It holds

$$\left\langle \begin{pmatrix} 0 & \sigma_0 & 0 & \sigma_j \end{pmatrix} \mathsf{M}_j^{-1} \begin{pmatrix} \sigma_0 \\ 0 \\ \sigma_j \\ 0 \end{pmatrix} v_j, v_j \right\rangle_j + \left\langle \begin{pmatrix} 0 & \sigma_0 & 0 & \sigma_j \end{pmatrix} \mathsf{T}_{\mathsf{M}_j^{-1}} \begin{pmatrix} \sigma_0 \\ 0 \\ \sigma_j \\ 0 \end{pmatrix} v_j, v_j \right\rangle_j \geq \mu_{\mathsf{M}_j^{-1}} \left\| \begin{pmatrix} \sigma_0 \\ 0 \\ \sigma_j \\ 0 \end{pmatrix} v_j \right\|^2_{\mathbf{V}_j^{(2)}}$$
$$\geq (\sigma_j^2 + \sigma_0^2) \mu_{\mathsf{M}_j^{-1}} \|v_j\|^2_{H^{\frac{1}{2}}(\Gamma_j)}. \tag{4.22}$$

Therefore, the operator $\mathcal{J}_j$ satisfies the following Gårding inequality:

$$\left\langle \left(\mathcal{J}_j + \mathsf{T}_{\mathcal{J}_j}\right) v_j, v_j \right\rangle_j \geq (\sigma_j^2 + \sigma_0^2) c_{\mathsf{M}_j^{-1}} \|v_j\|^2_{H^{\frac{1}{2}}(\Gamma_j)}, \quad \forall\, v_j \in H^{\frac{1}{2}}(\Gamma_j), \tag{4.23}$$

wherein

$$\mathsf{T}_{\mathcal{J}_j} := \begin{pmatrix} 0 & \sigma_0 & 0 & \sigma_j \end{pmatrix} \mathsf{T}_{\mathsf{M}_j^{-1}} \begin{pmatrix} \sigma_0 \\ 0 \\ \sigma_j \\ 0 \end{pmatrix} : \; H^{\frac{1}{2}}(\Gamma_j) \to H^{-\frac{1}{2}}(\Gamma_j) \tag{4.24}$$

is a compact operator. □

Define $\boldsymbol{v} = (v_1, \ldots, v_J)^\top$ and $\boldsymbol{g} = (g_1, \ldots, g_J)^\top$ and recall that all quantities are time-dependent. Let $\underline{\mathcal{J}} : \mathbb{H}_J^{\frac{1}{2}+s} \to \mathbb{H}_J^{-\frac{1}{2}+s}$, with $s \in \mathbb{R}$, be the operator defined as

$$\underline{\mathcal{J}} := \operatorname{diag}(\mathcal{J}_1, \mathcal{J}_2, \ldots, \mathcal{J}_J) - \begin{pmatrix} \mathcal{J}_{1,1} & \cdots & \mathcal{J}_{1,J} \\ \vdots & \ddots & \vdots \\ \mathcal{J}_{J,1} & \cdots & \mathcal{J}_{J,J} \end{pmatrix}. \tag{4.25}$$

Based on (4.8) and (2.13), we also set the following:

$$\boldsymbol{i}_{\phi_e} := \begin{pmatrix} i_1(\boldsymbol{\phi}_e) \\ \vdots \\ i_J(\boldsymbol{\phi}_e) \end{pmatrix} \quad \text{and} \quad \boldsymbol{i}_{\text{ion}}(\boldsymbol{v}, \boldsymbol{g}) := \begin{pmatrix} i_{\text{ion},1}(v_1, g_1) \\ \vdots \\ i_{\text{ion},J}(v_J, g_J) \end{pmatrix}. \tag{4.26}$$

For the HH model we define

$$\mathcal{HH}(\boldsymbol{v}, \boldsymbol{g}) := \begin{pmatrix} \mathcal{HH}_1(v_1, g_1) \\ \vdots \\ \mathcal{HH}_J(v_J, g_J) \end{pmatrix}, \tag{4.27}$$

where the $\mathcal{HH}_k$ are given as (2.14) and Remark 2.1 applies. With the above definitions we are now in position to set the continuous boundary problem we aim to solve.

Problem 4.2 (MTF for Packed Cells Problem)**.** Let $s > \frac{3}{2}$, initial given data $\boldsymbol{v}_0 \in \mathbb{H}_J^{\frac{1}{2}+s}$, $\boldsymbol{g}_0 \in \mathbb{H}_J^{-\frac{1}{2}+s}$ and $T \in \mathbb{R}_+$. We seek $\boldsymbol{v} \in \mathcal{C}^1\left([0,T]; \mathbb{H}_J^{-\frac{1}{2}+s}\right) \cap \mathcal{C}\left([0,T]; \mathbb{H}_J^{\frac{1}{2}+s}\right)$ and $\boldsymbol{g} \in \mathcal{C}^1\left([0,T]; \mathbb{H}_J^{-\frac{1}{2}+s}\right)$ such that, for all $t \in [0,T]$,

it holds on $\bigcup_{j=1}^{J}\Gamma_j$

$$c_m\partial_t\boldsymbol{v} = -\underline{\mathcal{J}}\boldsymbol{v} + \boldsymbol{i}_{\phi_e} - \boldsymbol{i}_{\text{ion}}(\boldsymbol{v},\boldsymbol{g}), \tag{4.28a}$$

$$\partial_t\boldsymbol{g} = \mathcal{H}\mathcal{H}(\boldsymbol{v},\boldsymbol{g}), \tag{4.28b}$$

where $\boldsymbol{i}_{\phi_e} \in \mathcal{C}\left([0,T];\mathbb{H}_J^{-\frac{1}{2}+s}\right)$ and with initial conditions

$$\boldsymbol{v}(0) = \boldsymbol{v}_0 \quad \text{and} \quad \boldsymbol{g}(0) = \boldsymbol{g}_0. \tag{4.29}$$

As a consequence of Lemma 4.1 we have the following result:

Lemma 4.3. *For $s \geq 0$, the operator $\underline{\mathcal{J}} : \mathbb{H}_J^{\frac{1}{2}+s} \to \mathbb{H}_J^{-\frac{1}{2}+s}$ is continuous and coercive, i.e. there exists a compact operator $\underline{\mathsf{T}}_{\underline{\mathcal{J}}} : \mathbb{H}_J^{\frac{1}{2}+s} \to \mathbb{H}_J^{-\frac{1}{2}+s}$ such that*

$$\left\langle (\underline{\mathcal{J}} + \underline{\mathsf{T}}_{\underline{\mathcal{J}}})\boldsymbol{v},\boldsymbol{v}\right\rangle_{\Gamma_0} \geq \mu \left\|\boldsymbol{v}\right\|^2_{\mathbb{H}_J^{\frac{1}{2}}}, \quad \textit{for all} \quad \boldsymbol{v} \in \mathbb{H}_J^{\frac{1}{2}}. \tag{4.30}$$

Furthermore, the operator $\underline{\mathcal{J}} : \mathbb{H}_J^{\frac{1}{2}} \to \mathbb{H}_J^{-\frac{1}{2}}$ is self-adjoint in the $\langle\cdot,\cdot\rangle_{\Gamma_0}$ duality product.

5. Existence and uniqueness of solutions for the multiple cell problem

We now aim to prove existence and uniqueness of the multiple cells problem, namely Problem 4.2. We follow the approach presented for the single cell problem in [43], which relies on the use of analytic semigroup theory [40].

5.1. Analytic semigroups

We present the required concepts on analytic semigroups to study the well-posedness of Problem 4.2. We refer to Chapter 2 from [40] for further details. Let X be a complex Banach space with norm $\|\cdot\|_X$ with dual X' and let $\mathcal{L}(X)$ be the space of linear endomorphisms on X.

Definition 5.1 ([40], Def. 2.0.1)**.** Let $\mathsf{A} : D(\mathsf{A}) \subset X \to X$ be a linear operator with domain $D(\mathsf{A})$. Recall the *resolvent set* $\rho(\mathsf{A}) := \{\lambda \in \mathbb{C} : \exists\, (\lambda\mathsf{I} - \mathsf{A})^{-1} \in \mathcal{L}(X)\}$ and *resolvent operator* $\mathsf{R}(\lambda,\mathsf{A}) := (\lambda I - \mathsf{A})^{-1}$ for $\lambda \in \rho(\mathsf{A})$. The operator A is said to be *sectorial* if there are constants $\omega \in \mathbb{R}$, $\theta \in (\pi/2,\pi)$ and $M > 0$ such that

(i) $S_{\theta,\omega} := \{\lambda \in \mathbb{C} :\ \lambda \neq \omega \ \wedge\ |\arg(\lambda-\omega)| < \theta\} \subset \rho(\mathsf{A})$,
(ii) $\|\mathsf{R}(\lambda,\mathsf{A})\|_{\mathcal{L}(X)} \leq \frac{M}{|\lambda-\omega|}$ for all $\lambda \in S_{\theta,\omega}$.

For $t > 0$, the properties stated in Definition 5.1 allow us to define a linear bounded operator $\exp(t\mathsf{A})$ in X by using the Dunford integral as follows:

$$\exp(t\mathsf{A}) = \frac{1}{2\pi\imath}\int_{\omega+\gamma_{r,\eta}} \exp(t\lambda)\mathsf{R}(\lambda,\mathsf{A})\mathrm{d}\lambda, \quad \forall\ t > 0, \tag{5.1}$$

where, for $r > 0$, $\eta \in (\pi/2,\theta)$, $\gamma_{r,\eta}$ is the curve $\{\lambda \in \mathbb{C} :\ |\arg\lambda| = \eta,\ |\lambda| \geq r\} \cup \{\lambda \in \mathbb{C} : |\arg\lambda| \leq \eta,\ |\lambda| = r\}$ oriented counterclockwise. Besides, we set

$$\exp(0\mathsf{A})x = x, \quad \forall\ x \in X. \tag{5.2}$$

Definition 5.2 ([40], Def. 2.0.2)**.** Let $\mathsf{A} : D(\mathsf{A}) \subset X \to X$ be a sectorial operator. The family $\{\exp(t\mathsf{A}) : t > 0\}$ defined by (5.1) and (5.2) is said to be the *analytic semigroup generated by* A *in* X.

The following proposition states sufficient conditions for an operator to be sectorial.

Proposition 5.3 ([40], Prop. 2.1.11)**.** *Let* $\mathsf{A} : D(\mathsf{A}) \subset X \to X$ *be a linear operator such that* $\rho(\mathsf{A})$ *contains a half plane* $\{\lambda \in \mathbb{C} : \mathfrak{Re}\lambda \geq \omega\}$*, and*

$$\|\lambda \mathsf{R}(\lambda, \mathsf{A})\|_{\mathcal{L}(X)} \leq M, \quad \mathfrak{Re}\ \lambda \geq \omega, \tag{5.3}$$

with $\omega \in \mathbb{R}$*,* $M > 0$*. Then, the operator* A *is sectorial.*

Let us now consider the following abstract evolution problem.

Problem 5.4 (Evolution problem)**.** Find u in X such that for all $t > 0$, it holds

$$u'(t) = \mathsf{A}u(t) + f(t, u(t)), \quad u(0) = u_0 \ \in X, \tag{5.4}$$

where $\mathsf{A} : D(\mathsf{A}) \subset X \to X$ is a linear sectorial operator, f is a continuous function defined in $[0, T] \times X$ with values in X.

One may define the different solution categories for the abstract evolution problem (5.4) as follows.

Definition 5.5 ([40], Defs 7.0.1 and 7.0.2)**.** We distinguish the following solution classes for Problem 5.4:

(i) A continuous function $u : (0, T] \to X$ such that $u(t) \in X$ for every $t \in (0, T]$ and $f(\cdot, u(\cdot)) \in L^1([0, T]; X)$, is said to be a *mild solution* in the interval $[0, T]$ if u satisfies

$$u(t) = \exp(t\mathsf{A})u_0 + \int_0^t \exp\left[(t - s)\mathsf{A}\right] f(s, u(s))\mathrm{d}s, \quad t \in [0, T]. \tag{5.5}$$

(ii) A function $u \in \mathcal{C}^1((0, T]; X) \cap \mathcal{C}((0, T]; D(\mathsf{A})) \cap \mathcal{C}([0, T]; X)$ such that $u(t) \in X$ for all $t \in [0, T]$ is said to be a *classical solution* in the interval $[0, T]$ if (5.4) is satisfied for each $t \in (0, T]$.

(iii) A function $u \in \mathcal{C}^1([0, T]; X) \cap \mathcal{C}([0, T]; D(\mathsf{A}))$ such that $u(t) \in X$ for all $t \in [0, T]$ is said to be a *strict solution* in the interval $[0, T]$ if (5.4) is satisfied for each $t \in [0, T]$.

Existence and uniqueness results together with conditions on the initial data u_0 and the nonlinear function f have been established for mild, classical and strict solutions ([40], Thm 7.1.2 and Prop. 7.1.10).

5.2. Existence and uniqueness of the multiple cells boundary problem

Using the previous definitions and results, we first prove that the operator $-\underline{\mathcal{J}}$, defined in (4.25), is actually sectorial, thus generating an analytic semigroup $\exp(-t\underline{\mathcal{J}})$ in $\mathbb{H}_J^{-\frac{1}{2}+s}$, for $s \geq \frac{1}{2}$. Throughout this section, we work with complex-valued Sobolev spaces, denoted also by $\mathbb{H}_J^s$, to fit in the framework for analytic semigroups presented previously. This impacts directly coercivity estimates in Lemma 4.3. For complex valued Sobolev spaces we should take the real part on the left hand side of the coercivity estimates. However, since the fundamental solution to the Laplace operator (3.1) is real valued, it holds

$$\mathfrak{Re}\left\{\left\langle \left(\underline{\mathcal{J}} + \underline{\mathsf{T}}_{\underline{\mathcal{J}}}\right)\boldsymbol{v}, \overline{\boldsymbol{v}}\right\rangle_{\Gamma_0}\right\} = \left\langle \left(\underline{\mathcal{J}} + \underline{\mathsf{T}}_{\underline{\mathcal{J}}}\right)\boldsymbol{v}, \overline{\boldsymbol{v}}\right\rangle_{\Gamma_0} \geq \mu \|\boldsymbol{v}\|^2_{\mathbb{H}_J^{\frac{1}{2}}}, \quad \text{for all} \quad \boldsymbol{v} \in \mathbb{H}_J^{\frac{1}{2}}. \tag{5.6}$$

Proposition 5.6. *Let $s \geq 0$ and $\boldsymbol{f} \in \mathbb{H}_J^{-\frac{1}{2}+s}$ as in (2.10). Then, there exists a unique $\boldsymbol{v} \in \mathbb{H}_J^{\frac{1}{2}+s}$ satisfying*

$$\left(\underline{\mathcal{J}} + \underline{\mathsf{T}}_{\underline{\mathcal{J}}}\right) \boldsymbol{v} = \boldsymbol{f}, \tag{5.7}$$

where $\underline{\mathsf{T}}_{\underline{\mathcal{J}}}$ is the same as in Lemma 4.3.

Proof. By the Lax–Milgram lemma ([55], Thm 3.4) and Lemma 4.3, the assertion holds for $s = 0$. The result for $s > 0$ follows from the regularity properties of the boundary integral equations and mapping properties of the BIOs in smooth boundaries ([52], Thm 3.2.2) and Theorem 3.5, respectively. □

Lemma 5.7. *For $s \geq \frac{1}{2}$, the operator $\underline{\mathcal{J}} : \mathbb{H}_J^{\frac{1}{2}+s} \to \mathbb{H}_J^{-\frac{1}{2}+s}$ generates an analytic semigroup $\exp(-t\underline{\mathcal{J}})$ on $\mathbb{H}_J^{-\frac{1}{2}+s}$.*

Proof. We take our cue from ([47], Thm 7.2.7). Set $\underline{\mathcal{R}} := -(\underline{\mathcal{J}} + \underline{\mathsf{T}}_{\mathcal{J}})$. According to Proposition 5.6, for $s = \frac{1}{2}$, the operator $\underline{\mathcal{R}}$ has the following mapping property $\underline{\mathcal{R}} : \mathbb{H}_J^1 \subset \mathbb{L}_J^2 \to \mathbb{L}_J^2$ with domain $D(\underline{\mathcal{R}}) = \mathbb{H}_J^1$. We define the set $S(\underline{\mathcal{R}})$ as

$$S(\underline{\mathcal{R}}) := \left\{ \langle \underline{\mathcal{R}}\boldsymbol{u}, \overline{\boldsymbol{u}} \rangle_{\Gamma_0} : \ \boldsymbol{u} \in \mathbb{H}_J^1, \text{ such that } \|\boldsymbol{u}\|_{\mathbb{L}_J^2} = 1 \right\}. \tag{5.8}$$

By Lemma 4.3, one can conclude that

$$S(\underline{\mathcal{R}}) \subset S := \{\lambda \in \mathbb{R} : \ \lambda < 0\} \subset \mathbb{C}. \tag{5.9}$$

Indeed, for $\boldsymbol{u} \in \mathbb{H}_J^1$, it holds

$$-\langle \underline{\mathcal{R}}\boldsymbol{u}, \overline{\boldsymbol{u}} \rangle_{\Gamma_0} \geq \mu \|\boldsymbol{u}\|^2_{\mathbb{H}_J^{\frac{1}{2}}} \geq \mu \|\boldsymbol{u}\|^2_{\mathbb{L}_J^2}, \tag{5.10}$$

and therefore

$$\frac{\langle \underline{\mathcal{R}}\boldsymbol{u}, \overline{\boldsymbol{u}} \rangle_{\Gamma_0}}{\|\boldsymbol{u}\|^2_{\mathbb{L}_J^2}} \leq -\mu < 0. \tag{5.11}$$

On the other hand, one has

$$\rho(\underline{\mathcal{R}}) \supset \Sigma := \{\lambda \in \mathbb{C} : \ \mathfrak{Re}\{\lambda\} \geq 0\}. \tag{5.12}$$

Also, we have that

$$\begin{aligned} \mathfrak{Re}\left\{ \langle (\lambda \mathsf{I} - \underline{\mathcal{R}})\, \boldsymbol{v}, \overline{\boldsymbol{v}} \rangle_{\Gamma_0} \right\} &= \mathfrak{Re}\left\{ \left\langle \left(\lambda \mathsf{I} + \underline{\mathcal{J}} + \underline{\mathsf{T}}_{\underline{\mathcal{J}}}\right) \boldsymbol{v}, \overline{\boldsymbol{v}} \right\rangle_{\Gamma_0} \right\} = \left\langle (\underline{\mathcal{J}} + \underline{\mathsf{T}}_{\underline{\mathcal{J}}})\boldsymbol{v}, \overline{\boldsymbol{v}} \right\rangle_{\Gamma_0} + \mathfrak{Re}\{\lambda\} \langle \boldsymbol{v}, \overline{\boldsymbol{v}} \rangle_{\Gamma_0} \\ &\geq \mu \|\boldsymbol{v}\|^2_{\mathbb{H}_J^{\frac{1}{2}}} + \mathfrak{Re}\{\lambda\} \|\boldsymbol{v}\|^2_{\mathbb{L}_J^2} \geq \mu \|\boldsymbol{v}\|^2_{\mathbb{H}_J^{\frac{1}{2}}} \end{aligned}$$

holds for all $\boldsymbol{v} \in \mathbb{H}_J^{\frac{1}{2}}$ if $\lambda \in \Sigma$. In this case, the complex version of Lax–Milgram lemma ([55], Thm 3.4) ensures that $\lambda \mathsf{I} - \underline{\mathcal{R}}$ has a bounded inverse for $\lambda \in \Sigma$. One may conclude that

$$\mathrm{d}(\lambda, \overline{S}) = |\lambda|, \quad \text{for} \quad \lambda \in \Sigma, \tag{5.13}$$

where $\mathrm{d}(\lambda, \overline{S})$ is the distance between λ and the closure of S. Moreover, for $\lambda \in \Sigma$ and $\boldsymbol{u} \in \mathbb{H}^1_J$ such that $\|\boldsymbol{u}\|_{\mathbb{L}^2_J} = 1$, we have

$$\mathrm{d}(\lambda, \overline{S}) \leq \left|\lambda - \langle \underline{\mathcal{R}}\boldsymbol{u}, \overline{\boldsymbol{u}}\rangle_{\Gamma_0}\right| \leq \left|\langle(\lambda \mathsf{I} - \underline{\mathcal{R}})\boldsymbol{u}, \overline{\boldsymbol{u}}\rangle_{\Gamma_0}\right| \leq \|(\lambda \mathsf{I} - \underline{\mathcal{R}})\boldsymbol{u}\|_{\mathbb{L}^2_J}. \tag{5.14}$$

Therefore, we have

$$\left\|\mathsf{R}(\lambda, -(\underline{\mathcal{J}} + \underline{\mathsf{T}}_{\mathcal{J}})\right\|_{\mathcal{L}(\mathbb{L}^2_J, \mathbb{L}^2_J)} = \|\mathsf{R}(\lambda, \underline{\mathcal{R}})\|_{\mathcal{L}(\mathbb{L}^2_J, \mathbb{L}^2_J)} \leq \frac{1}{|\lambda|}, \quad \lambda \in \Sigma. \tag{5.15}$$

By Proposition 5.3, $\underline{\mathcal{R}}$ is a sectorial operator and generates an analytic semigroup of bounded linear operators in $\mathbb{L}^2_J$. Being $\mathbb{H}^1_J$ dense in $\mathbb{L}^2_J$ and $\underline{\mathsf{T}}_{\mathcal{J}} : \mathbb{H}^1_J \to \mathbb{L}^2_J$ a compact operator, from Proposition 2.4.3 in [40] we conclude that $-\underline{\mathcal{J}}$ itself is sectorial and also generates an analytic semigroup in $\mathbb{L}^2_J$. Finally, the mapping properties of the operator $\underline{\mathcal{J}}$ (*cf.* Lem. 4.3) guarantee the existence of an analytic semigroup in $\mathbb{H}^{-\frac{1}{2}+s}_J$, for $s \geq \frac{1}{2}$. □

We now recall the following result regarding the smoothness of the mappings $\mathcal{HH}(\boldsymbol{v}, \boldsymbol{g})$ and $\boldsymbol{i}_{\mathrm{ion}}(\boldsymbol{v}, \boldsymbol{g})$.

Lemma 5.8 ([43], Lem. 5.4)**.** *Let $R > 0$ and $s > \frac{3}{2}$, then for all $\boldsymbol{v} \in \mathbb{H}^{-\frac{1}{2}+s}_J$ and $\boldsymbol{g} \in \mathbb{H}^{-\frac{1}{2}+s}_J$ such that $\|\boldsymbol{v}\|_{\mathbb{H}^{-\frac{1}{2}+s}_J} \leq R$ and $\|\boldsymbol{g}\|_{\mathbb{H}^{-\frac{1}{2}+s}_J} \leq R$, there exist constants C_0, depending on $\mathcal{HH}$ and $\boldsymbol{i}_{\mathrm{ion}}$, and C_1, depending on R and the derivatives of $\mathcal{HH}$ and $\boldsymbol{i}_{\mathrm{ion}}$, such that*

$$\|\mathcal{HH}(\boldsymbol{v}, \boldsymbol{g})\|_{\mathbb{H}^{-\frac{1}{2}+s}_J} + \|\boldsymbol{i}_{\mathrm{ion}}(\boldsymbol{v}, \boldsymbol{g})\|_{\mathbb{H}^{-\frac{1}{2}+s}_J} \leq C_0 + C_1(R)\left(\|\boldsymbol{v}\|_{\mathbb{H}^{-\frac{1}{2}+s}_J} + \|\boldsymbol{g}\|_{\mathbb{H}^{-\frac{1}{2}+s}_J}\right). \tag{5.16}$$

Besides, for $\boldsymbol{v}, \boldsymbol{v}', \boldsymbol{g}, \boldsymbol{g}' \in \mathbb{H}^{-\frac{1}{2}+s}_J$ such that $\|\boldsymbol{v}\|_{\mathbb{H}^{-\frac{1}{2}+s}_J}, \|\boldsymbol{v}'\|_{\mathbb{H}^{-\frac{1}{2}+s}_J}, \|\boldsymbol{g}\|_{\mathbb{H}^{-\frac{1}{2}+s}_J}, \|\boldsymbol{g}'\|_{\mathbb{H}^{-\frac{1}{2}+s}_J} \leq R$, there exists a constant $C_2(R)$, depending on R and the derivatives of $\mathcal{HH}$ and $\boldsymbol{i}_{\mathrm{ion}}$, such that

$$\|\mathcal{HH}(\boldsymbol{v}, \boldsymbol{g}) - \mathcal{HH}(\boldsymbol{v}', \boldsymbol{g}')\|_{\mathbb{H}^{-\frac{1}{2}+s}_J} + \|\boldsymbol{i}_{\mathrm{ion}}(\boldsymbol{v}, \boldsymbol{g}) - \mathcal{HH}(\boldsymbol{v}', \boldsymbol{g}')\|_{\mathbb{H}^{-\frac{1}{2}+s}_J} \tag{5.17}$$

$$\leq C_2(R)\left(\|\boldsymbol{v} - \boldsymbol{v}'\|_{\mathbb{H}^{-\frac{1}{2}+s}_J} + \|\boldsymbol{g} - \boldsymbol{g}'\|_{\mathbb{H}^{-\frac{1}{2}+s}_J}\right). \tag{5.18}$$

We are now in position to enunciate the local existence and uniqueness results for Problem 4.2.

Theorem 5.9 (Local Existence and Uniqueness of Problem 4.2)**.** *For $s > \frac{3}{2}$, let $\boldsymbol{v}_0 \in \mathbb{H}^{-\frac{1}{2}+s}_J$ and $\boldsymbol{g}_0 \in \mathbb{H}^{-\frac{1}{2}+s}_J$ be initial conditions of Problem 4.2. Then, Problem 4.2 admits a unique mild solution $\boldsymbol{v}, \boldsymbol{g} \in \mathcal{C}([0, T], \mathbb{H}^{-\frac{1}{2}+s}_J)$ depending continuously on the initial data. Besides, Problem 4.2 also admits a unique classical solution which coincides with the mild solution. Finally, if $\boldsymbol{v}_0 \in \mathbb{H}^{\frac{1}{2}+s}_J$ then the solution is strict.*

Proof. For $s \geq \frac{1}{2}$, let us consider the augmented operator defined as

$$\mathcal{G} := \begin{pmatrix} \underline{\mathcal{J}} \\ \mathbf{0} \end{pmatrix} : \mathbb{H}^{\frac{1}{2}+s}_J \times \mathbb{H}^{-\frac{1}{2}+s}_J \to \mathbb{H}^{-\frac{1}{2}+s}_J \times \mathbb{H}^{-\frac{1}{2}+s}_J \tag{5.19}$$

with domain $D(\mathcal{G}) = \mathbb{H}^{\frac{1}{2}+s}_J \times \mathbb{H}^{-\frac{1}{2}+s}_J$. Being $\underline{\mathcal{J}}$ sectorial, we have that $\mathcal{G}$ is sectorial as well, therefore generating an analytic semigroup in $\mathbb{H}^{-\frac{1}{2}+s}_J \times \mathbb{H}^{-\frac{1}{2}+s}_J$. The claim on mild, classical and strict solutions is a consequence of the analyticity of the semigroup generated by $\mathcal{G}$ ([40], Chap. 7). The condition $s > \frac{3}{2}$ comes from Lemma 5.8, which provides the required smoothness for $\mathcal{HH}(\boldsymbol{v}, \boldsymbol{g})$ and $\boldsymbol{i}_{\mathrm{ion}}(\boldsymbol{v}, \boldsymbol{g})$ to lie in the right Sobolev spaces. □

Finally, for $\boldsymbol{u}, \boldsymbol{v} \in \mathbb{H}_J^{\frac{1}{2}}$, we define the following bilinear form:

$$\mathsf{J}(\boldsymbol{u}, \boldsymbol{v}) := \langle \underline{\mathcal{J}} \boldsymbol{u}, \boldsymbol{v} \rangle_{\Gamma_0} : \mathbb{H}_J^{\frac{1}{2}} \times \mathbb{H}_J^{\frac{1}{2}} \to \mathbb{R}. \tag{5.20}$$

6. Numerical discretization

Though Problem 4.2 is valid in two and three dimensions, in what follows we present an efficient two-dimensional discretization scheme proved to be stable and convergent. Our numerical scheme relies on two key elements. On one hand, we take advantage of the smoothness inherent to biological cells by using Fourier polynomials for space discretization, which yields exponential convergence rates. On the other hand, we use a semi-implicit strategy in time to deal with the nonlinearities arising in the terms $\boldsymbol{i}_{\text{ion}}(\boldsymbol{v}, \boldsymbol{g})$ and $\mathcal{HH}(\boldsymbol{v}, \boldsymbol{g})$.

6.1. Fourier expansion

We recall some useful results of Fourier analysis and refer to ([36], Chap. 8) and ([7], Sect. 6.5) for more details. Define the equivalence class of square integrable complex-valued functions as

$$L^2[0, 2\pi] := \left\{ \varphi : [0, 2\pi] \to \mathbb{C} \quad \text{such that } \int_0^{2\pi} |f(\theta)|^2 \, \mathrm{d}\theta < \infty \right\}. \tag{6.1}$$

As usual, the $L^2[0, 2\pi]$-norm is induced by the inner product:

$$(\varphi, \psi)_{L^2[0,2\pi]} = \int_0^{2\pi} \varphi(\theta) \overline{\psi(\theta)} \mathrm{d}\theta. \tag{6.2}$$

The Fourier series of $\varphi \in L^2[0, 2\pi]$ is

$$\varphi(\theta) = \sum_{k \in \mathbb{Z}} a_k \exp(\imath k \theta). \tag{6.3}$$

Let us define the Fourier polynomials $\varphi_k := \exp(\imath k \theta)$, for $k \in \mathbb{Z}$. Then, Fourier coefficients a_k in (6.3) are given by

$$a_k := \frac{1}{2\pi} (\varphi, \varphi_k)_{L^2[0,2\pi]} = \frac{1}{2\pi} \int_0^{2\pi} \varphi(\theta) \exp(-\imath k \theta) \mathrm{d}\theta, \tag{6.4}$$

and Parseval's equality holds, *i.e.*

$$\|\varphi\|^2_{L^2[0,2\pi]} = 2\pi \sum_{k \in \mathbb{Z}} |a_k|^2 . \tag{6.5}$$

Definition 6.1 ([36], Def. 8.1)**.** Let $0 \leq p < \infty$. By $H^p[0, 2\pi]$ we denote the space of all complex-valued functions $\varphi \in L^2[0, 2\pi]$ with the property

$$\sum_{k \in \mathbb{Z}} (1 + k^2)^p \, |a_k|^2 < \infty, \tag{6.6}$$

for the Fourier coefficients a_k of φ. Notice that $H^0[0, 2\pi]$ can be identified with $L^2[0, 2\pi]$.

Theorem 6.2 ([36], Thm. 8.2)**.** *The Sobolev space $H^p[0,2\pi]$ is a Hilbert space with scalar product defined by*

$$(\varphi,\psi)_{H^p[0,2\pi]} = \sum_{k\in\mathbb{Z}} (1+k^2)^p a_k \overline{b_k}, \tag{6.7}$$

for $\varphi,\psi \in H^p[0,2\pi]$ with Fourier coefficients a_k and b_k, respectively. We can also define a semi-norm in $H^p[0,2\pi]$ as follows

$$|\varphi|^2_{H^p[0,2\pi]} = \sum_{k\in\mathbb{Z}} |k|^{2p} |a_k|^2 . \tag{6.8}$$

Finally, the set of Fourier polynomials is dense in $H^p[0,2\pi]$.

Set $\mathcal{S}_K := \operatorname{span}\{\varphi_k : \ k = -K,\dots,K\}$ as the finite dimensional space of Fourier polynomials up to degree K. We define the *partial Fourier summation* up to order K as follows

$$(\mathsf{P}_K\varphi)(\theta) := \sum_{|k|\le K} a_k \exp(\imath k\theta) \in \mathcal{S}_K. \tag{6.9}$$

Lemma 6.3 ([12], Sect. 5.1.1)**.** *Let $0 \le s \le p$. For $\varphi \in H^p[0,2\pi]$ there exists a constant $c(s,p)$ such that*

$$\|\varphi - \mathsf{P}_K\varphi\|_{H^s[0,2\pi]} \le c(s,p) K^{-(p-s)} |\varphi|_{H^p[0,2\pi]} . \tag{6.10}$$

Exponential convergence rates can be achieved when assuming analyticity as the next result shows [56] or ([12], Sect. 5.1).

Lemma 6.4. *If φ is 2π-periodic analytic, with analyticity strip of width $2\eta_0$, i.e. for $|\mathrm{Im}(z)| \le \eta_0$, $\varphi(z)$ admits the absolutely convergent expansion:*

$$\varphi(z) = \sum_{k\in\mathbb{Z}} \varphi_k \exp(\imath k z).$$

Then, for any η, $0 < \eta < \eta_0$, it holds

$$\|\varphi - \mathsf{P}_K\varphi\|_{H^s[0,2\pi]} \le c(s,\eta) K^s \exp(-\eta K), \tag{6.11}$$

with c and η independent of K.

Assume that Γ is the boundary of a simply connected bounded $\mathcal{C}^k$-domain, $k \in \mathbb{N}$ and that $\boldsymbol{\chi}(\theta)$ for $\theta \in [0,2\pi)$ is a k-times regular and continuously differentiable 2π-periodic parametric representation of Γ. Then, for $0 \le p \le k$, we have the following characterization of the Sobolev space $H^p(\Gamma)$:

$$H^p(\Gamma) := \left\{\varphi \in L^2(\Gamma) : \ \tau_{\boldsymbol{\chi}}\varphi \in H^p[0,2\pi]\right\}, \tag{6.12}$$

where $\tau_{\boldsymbol{\chi}} : H^p(\Gamma) \to H^p[0,2\pi]$ is defined as $\tau_{\boldsymbol{\chi}}\varphi := \varphi \circ \boldsymbol{\chi}$ for $\varphi \in H^p(\Gamma)$, for $p \ge 0$, with inner product:

$$(\varphi,\psi)_{H^p(\Gamma)} := (\tau_{\boldsymbol{\chi}}\varphi, \tau_{\boldsymbol{\chi}}\psi)_{H^p[0,2\pi]}, \quad \forall\ \varphi,\psi \in H^p(\Gamma). \tag{6.13}$$

In particular, it holds

$$\|\varphi\|_{H^p(\Gamma)} = \|\tau_{\boldsymbol{\chi}}\varphi\|_{H^p[0,2\pi]}, \quad \forall\ \varphi \in H^p(\Gamma), \quad 0 \le p \le k. \tag{6.14}$$

Moreover, the definition of Sobolev spaces $H^p(\Gamma)$ is independent of the chosen parametric representation of the boundary Γ ([36], Thm. 8.14). For $s<0$, $H^p(\Gamma)$ are defined as the dual spaces of $H^{-s}(\Gamma)$ ([36], Def. 8.9).

6.2. Semi-implicit time stepping scheme

Define $\Upsilon_N := \{t_n\}_{n=0}^N$ as the uniform partition of the time interval $[0,T]$, for $T\in\mathbb{R}_+$ and $N\in\mathbb{N}$, where $t_n := n\tau$ and $\tau := T/N$ is the time step. Let

$$t_{n+\frac{1}{2}} := t_n + \frac{\tau}{2}, \qquad n=0,\dots,N-1, \tag{6.15}$$

be a midstep between t_n and t_{n+1}. For a time dependent quantity $\phi(t)$, we denote $\phi^n := \phi(t_n)$ and, for $n=1,\dots,N-1$, we consider the following quantities:

$$\bar\partial\phi^n := \frac{\phi^{n+1}-\phi^n}{\tau}, \qquad \phi^{n+\frac{1}{2}} := \phi\left(t_{n+\frac{1}{2}}\right), \tag{6.16}$$

$$\bar\phi^{n+\frac{1}{2}} := \frac{\phi^{n+1}+\phi^n}{2}, \qquad \widehat\phi^{n+\frac{1}{2}} := \frac{3\phi^n-\phi^{n-1}}{2}. \tag{6.17}$$

With these definitions one may derive the following time-local estimates:

Lemma 6.5 ([29], Lem. 7)**.** *Let $\varphi\in\mathcal{C}^2([0,T];L^2[0,2\pi])$, then it holds*

$$\left\|\bar\varphi^{n+\frac{1}{2}}-\varphi^{n+\frac{1}{2}}\right\|_{L^2[0,2\pi]} \le \frac{1}{4}\tau^2 \max_{t\in[t_n,t_{n+1}]}\left\|\partial_t^2\varphi(t)\right\|_{L^2[0,2\pi]}, \tag{6.18}$$

$$\left\|\hat\varphi^{n+\frac{1}{2}}-\varphi^{n+\frac{1}{2}}\right\|_{L^2[0,2\pi]} \le \frac{5}{16}\tau^2 \max_{t\in[t_{n-1},t_{n+1}]}\left\|\partial_t^2\varphi(t)\right\|_{L^2[0,2\pi]}. \tag{6.19}$$

Furthermore, if $\varphi\in\mathcal{C}^3([0,T];L^2[0,2\pi])$,

$$\left\|\bar\partial\varphi^n-\partial_t\varphi^{n+\frac{1}{2}}\right\|_{L^2[0,2\pi]} \le \frac{\tau^2}{48} \max_{t\in[t_n,t_{n+1}]}\left\|\partial_t^2\varphi(t)\right\|_{L^2[0,2\pi]}. \tag{6.20}$$

6.3. Fully discrete scheme

In what follows, we assume that each subdomain boundary Γ_j, for $j=1,\dots,J$ admits a 2π-periodic $\mathcal{C}^\infty$-parametric representation denoted by $\boldsymbol{\chi}_j$. Given $K\in\mathbb{N}$, on each boundary we define the subspaces $\mathcal{S}_K(\Gamma_j) := \tau_{\boldsymbol{\chi}_j}^{-1}\circ\mathcal{S}_K$, for $j=1,\dots,J$ and

$$\mathbb{S}_{J,K} := \mathcal{S}_K(\Gamma_1)\times\cdots\times\mathcal{S}_K(\Gamma_J).$$

At each time step $t_n\in\Upsilon_N$, we seek sets of functions $\boldsymbol{v}_K^n$ and $\boldsymbol{g}_K^n\in\mathbb{S}_{J,K}$. Each one of them is an approximation at times t_n of the vector of continuous membrane potentials membrane potential $\boldsymbol{v}$ and gate variables $\boldsymbol{g}$, respectively. With these elements, we state the semi-implicit time-space numerical discretization of Problem 4.2.

Problem 6.6 (Fully Discrete Boundary Integral Problem)**.** Let $\boldsymbol{v}_K^0$, $\boldsymbol{v}_K^1$, $\boldsymbol{g}_K^0$ and $\boldsymbol{g}_K^1$, belonging to $\mathbb{S}_{J,K}$, be given. Then, for time steps $n=1,\dots,N-1$ we seek $\boldsymbol{v}_K^n$, $\boldsymbol{g}_K^n$ in $\mathbb{S}_{J,K}$ solutions of

$$\left\langle c_m\bar\partial\boldsymbol{v}_K^n,\boldsymbol{\varphi}_K\right\rangle_{\Gamma_0} + \mathsf{J}\left(\bar{\boldsymbol{v}}_K^{n+\frac{1}{2}},\boldsymbol{\varphi}_K\right) = \left\langle \boldsymbol{i}_{\Phi_e}^{n+\frac{1}{2}},\boldsymbol{\varphi}_K\right\rangle_{\Gamma_0} - \left\langle \boldsymbol{i}_{\text{ion}}\left(\hat{\boldsymbol{v}}_K^{n+\frac{1}{2}},\hat{\boldsymbol{g}}_K^{n+\frac{1}{2}}\right),\boldsymbol{\varphi}_K\right\rangle_{\Gamma_0}, \tag{6.21a}$$

$$\left\langle\bar\partial\boldsymbol{g}_K^n,\boldsymbol{\varphi}_K\right\rangle_{\Gamma_0} = \left\langle \mathcal{HH}\left(\hat{\boldsymbol{v}}_K^{n+\frac{1}{2}},\hat{\boldsymbol{g}}_K^{n+\frac{1}{2}}\right),\boldsymbol{\varphi}_K\right\rangle_{\Gamma_0}, \tag{6.21b}$$

for all $\boldsymbol{\varphi}_K \in \mathbb{S}_{J,K}$, where the bilinear form J is defined in (5.20).

To properly solve Problem 6.6 values for $\boldsymbol{v}_K^0$, $\boldsymbol{v}_K^1$, $\boldsymbol{g}_K^0$ and $\boldsymbol{g}_K^1$ must be provided. A straightforward choice for $\boldsymbol{v}_K^0$ and $\boldsymbol{g}_K^0$ comes from initial conditions $\boldsymbol{v}_0$ and $\boldsymbol{g}_0$. For instance, one may choose $\boldsymbol{v}_K^0 := \underline{\hat{\mathsf{P}}}_K \boldsymbol{v}_0$ and $\boldsymbol{g}_K^0 := \underline{\hat{\mathsf{P}}}_K \boldsymbol{g}^0$, where $\underline{\hat{\mathsf{P}}}_K : \mathbb{H}_J^p \to \mathbb{S}_{J,K}$ is defined as $\underline{\hat{\mathsf{P}}}_K := (\hat{\mathsf{P}}_{K,1}, \cdots, \hat{\mathsf{P}}_{K,J})$ and $\hat{\mathsf{P}}_{K,j} := \tau_{\boldsymbol{\chi}_j}^{-1} \circ \mathsf{P}_K \circ \tau_{\boldsymbol{\chi}_j}$, for $j = 1, \ldots, J$ and $p \geq 0$.

Values for $\boldsymbol{v}_K^1$ and $\boldsymbol{g}_K^1$ are estimated by solving the following *predictor–corrector algorithm* summarized in Algorithm 6.7 (*cf.* Chap. 13 from [58], and [26]), as it has been done in [29] for the single biological cell case:

Algorithm 6.7 (Predictor–Corrector method)**.** Set $\boldsymbol{w}_K^0 := \boldsymbol{v}_K^0$ and $\boldsymbol{r}_K^0 := \boldsymbol{g}_K^0$, then we proceed as follows:

(I) *Predictor.* We first construct predictions $\boldsymbol{w}_K^1$ and $\boldsymbol{r}_K^1$, for $\boldsymbol{v}_K^1$ and $\boldsymbol{g}_K^1$, respectively, by solving the linear system:

$$\begin{aligned} \left\langle c_m \bar{\partial} \boldsymbol{w}_K^0, \boldsymbol{\varphi}_K \right\rangle_{\Gamma_0} + \mathsf{J}\left(\bar{\boldsymbol{w}}_K^{\frac{1}{2}}, \boldsymbol{\varphi}_K\right) &= \left\langle \boldsymbol{i}_{\Phi_e}^{\frac{1}{2}}, \boldsymbol{\varphi}_K \right\rangle_{\Gamma_0} - \left\langle \boldsymbol{i}_{\text{ion}}\left(\boldsymbol{v}_K^0, \boldsymbol{g}_K^0\right), \boldsymbol{\varphi}_K \right\rangle_{\Gamma_0}, \\ \left\langle \bar{\partial} \boldsymbol{r}_K^0, \boldsymbol{\varphi}_K \right\rangle_{\Gamma_0} &= \left\langle \mathcal{HH}\left(\boldsymbol{w}_K^0, \boldsymbol{r}_K^0\right), \boldsymbol{\varphi}_K \right\rangle_{\Gamma_0}, \end{aligned}$$

for all $\boldsymbol{\varphi}_K \in \mathbb{S}_{J,K}$. Notice that both $\boldsymbol{w}_K^1$ and $\boldsymbol{r}_K^1$ appear through the definitions given in Section 6.2.

(II) *Corrector.* We now correct $\boldsymbol{w}_K^1$ and $\boldsymbol{r}_K^1$, to obtain final values for $\boldsymbol{v}_K^1$ and $\boldsymbol{g}_K^1$ through

$$\begin{aligned} \left\langle c_m \bar{\partial} \boldsymbol{v}_K^0, \boldsymbol{\varphi}_K \right\rangle_{\Gamma_0} + \mathsf{J}\left(\bar{\boldsymbol{v}}_K^{\frac{1}{2}}, \boldsymbol{\varphi}_K\right) &= \left\langle \boldsymbol{i}_{\Phi_e}^{\frac{1}{2}}, \boldsymbol{\varphi}_K \right\rangle_{\Gamma_0} - \left\langle \boldsymbol{i}_{\text{ion}}\left(\bar{\boldsymbol{w}}_K^{\frac{1}{2}}, \bar{\boldsymbol{r}}_K^{\frac{1}{2}}\right), \boldsymbol{\varphi}_K \right\rangle_{\Gamma_0}, \\ \left\langle \bar{\partial} \boldsymbol{g}_K^0, \boldsymbol{\varphi}_k \right\rangle_{\Gamma_0} &= \left\langle \mathcal{HH}\left(\bar{\boldsymbol{w}}_K^{\frac{1}{2}}, \bar{\boldsymbol{r}}_K^{\frac{1}{2}}\right), \boldsymbol{\varphi}_K \right\rangle_{\Gamma_0}, \end{aligned}$$

for all $\boldsymbol{\varphi}_K \in \mathbb{S}_{J,K}$. Again, both $\boldsymbol{v}_K^1$ and $\boldsymbol{g}_K^1$ are implicit in the previous equations through the quantities defined in Section 6.2.

6.4. Convergence analysis

We seek to prove bounds for the total approximation error for the transmembrane potential and gate variables. In particular, we are interested in measuring the errors $\boldsymbol{v}(t_n) - \boldsymbol{v}^n$ and $\boldsymbol{g}(t_n) - \boldsymbol{g}^n$ in the $\mathbb{L}_J^2$-norm for all $t_n \in \Upsilon_N$.

For $\boldsymbol{v} \in \mathcal{C}^1([0,T], \mathbb{H}_J^{\frac{1}{2}})$ and $\zeta \in \mathbb{R}_+$, let us define $\boldsymbol{v}_\zeta := \exp(-\zeta t)\boldsymbol{v}$, for $t \in [0,T]$. Then

$$\partial_t \boldsymbol{v} = \zeta \exp(\zeta t)\boldsymbol{v}_\zeta + \exp(\zeta t)\partial_t \boldsymbol{v}_\zeta. \tag{6.22}$$

Consequently, one can rewrite Problem 4.2 in terms $\boldsymbol{v}_\zeta$ as presented in Problem 6.8.

Problem 6.8. Let $s > \frac{3}{2}$ and $\zeta > 0$, $\boldsymbol{v}_0 \in \mathbb{H}_J^{\frac{1}{2}+s}$, $\boldsymbol{g}_0 \in \mathbb{H}_J^{-\frac{1}{2}+s}$ and $T \in \mathbb{R}_+$. We seek $\boldsymbol{v} \in \mathcal{C}^1([0,T], \mathbb{H}_J^{-\frac{1}{2}+s}) \cap \mathcal{C}([0,T], \mathbb{H}_J^{\frac{1}{2}+s})$ and $\boldsymbol{g} \in \mathcal{C}^1([0,T], \mathbb{H}_J^{-\frac{1}{2}+s})$ such that for all $t \in [0,T]$ it holds

$$c_m \partial_t \boldsymbol{v}_\zeta = -\underline{\mathcal{J}}_\zeta \boldsymbol{v}_\zeta + \exp(-\zeta t)\left(\boldsymbol{i}(t) - \boldsymbol{i}_{\text{ion}}\left(\exp(\zeta t)\boldsymbol{v}_\zeta, \boldsymbol{g}\right)\right), \tag{6.23a}$$

$$\partial_t \boldsymbol{g} = \mathcal{HH}\left(\exp(\zeta t)\boldsymbol{v}_\zeta, \boldsymbol{g}\right), \tag{6.23b}$$

where $\boldsymbol{i} \in \mathcal{C}\left([0,T]; \mathbb{H}_J^{-\frac{1}{2}+s}\right)$ and $\underline{\mathcal{J}}_\zeta := c_m \zeta \,\mathsf{I} + \underline{\mathcal{J}}$ and which induces the bilinear form $\mathsf{J}_\zeta(\cdot,\cdot)$.

Remark 6.9. We can choose ζ large so that $\underline{\mathcal{J}}_\zeta$ becomes elliptic. In fact, it is enough to pick

$$\zeta \geq \zeta_{\min} := \frac{\left\| \underline{\mathsf{T}}_{\underline{\mathcal{J}}} \right\|_{\mathcal{L}\left(\mathbb{H}_J^{\frac{1}{2}}, \mathbb{L}_J^2\right)}}{c_m}. \tag{6.24}$$

Indeed, we have

$$\begin{aligned} \left\langle \underline{\mathcal{J}}_\zeta \boldsymbol{v}, \boldsymbol{v} \right\rangle_{\Gamma_0} &= \left\langle (\underline{\mathcal{J}} + c_m \zeta \, \mathsf{I} + \underline{\mathsf{T}}_{\underline{\mathcal{J}}} - \underline{\mathsf{T}}_{\underline{\mathcal{J}}}) \boldsymbol{v}, \boldsymbol{v} \right\rangle_{\Gamma_0} \\ &\geq \mu \left\| \boldsymbol{v} \right\|^2_{\mathbb{H}_J^{\frac{1}{2}}} + \underbrace{\left(c_m \zeta - \left\| \underline{\mathsf{T}}_{\underline{\mathcal{J}}} \right\|_{\mathcal{L}\left(\mathbb{H}_J^{\frac{1}{2}}, \mathbb{L}_J^2\right)} \right)}_{\geq 0} \left\| \boldsymbol{v} \right\|^2_{\mathbb{L}_J^2} \geq \mu \left\| \boldsymbol{v} \right\|^2_{\mathbb{H}_J^{\frac{1}{2}}}, \end{aligned} \tag{6.25}$$

with μ coming from (5.6), and where the boundedness of the map $\underline{\mathsf{T}}_{\underline{\mathcal{J}}} : \mathbb{H}_J^{\frac{1}{2}} \to \mathbb{L}_J^2$ is a consequence of the smoothing properties of the BIOs (*cf.* [55], Sect. 6.1 and [52], Thm. 3.5.5).

The use of the $\mathbb{H}_J^{\frac{1}{2}}$-ellipticity of $\underline{\mathcal{J}}_\zeta$, for ζ large enough, requires first to compute the error in the $\mathbb{L}_J^2$-norm of $\boldsymbol{v}_\zeta(t_n) - \boldsymbol{v}_\zeta^n$ and $\boldsymbol{g}_\zeta(t_n) - \boldsymbol{g}_\zeta^n$ for $t_n \in \Upsilon_N$. Indeed, it holds

$$\left\| \boldsymbol{v}(t_n) - \boldsymbol{v}^n \right\|_{\mathbb{L}_J^2} = \exp(\zeta t_n) \left\| \boldsymbol{v}_\zeta(t_n) - \boldsymbol{v}_\zeta^n \right\|_{\mathbb{L}_J^2} \quad \text{and} \tag{6.26a}$$

$$\left\| \boldsymbol{g}(t_n) - \boldsymbol{g}^n \right\|_{\mathbb{L}_J^2} = \exp(\zeta t_n) \left\| \boldsymbol{g}_\zeta(t_n) - \boldsymbol{g}_\zeta^n \right\|_{\mathbb{L}_J^2}. \tag{6.26b}$$

We drop momentarily the explicit time-dependence in n, reintroducing the corresponding superscript in Section 6.5. The forthcoming error analysis relies on the one presented in ([29], Sect. 6) hinging on the so-called *elliptic projection* $\boldsymbol{w}_\zeta$, defined as the solution of the following variational problem:

$$\mathsf{J}_\zeta(\boldsymbol{v}_\zeta - \boldsymbol{w}_\zeta, \boldsymbol{\varphi}) = 0, \quad \text{for all} \quad \boldsymbol{\varphi} \in \mathbb{H}_J^{\frac{1}{2}}. \tag{6.27}$$

One may similarly define the *discrete elliptic projection* $\boldsymbol{w}_{\zeta,K}$, unique solution of

$$\mathsf{J}_\zeta(\boldsymbol{v}_\zeta - \boldsymbol{w}_{\zeta,K}, \boldsymbol{\varphi}_K) = 0, \quad \text{for all} \quad \boldsymbol{\varphi}_K \in \mathbb{S}_{J,K}. \tag{6.28}$$

In particular, we notice that if $\boldsymbol{v}_\zeta \in \mathbb{S}_{J,K}$, then $\boldsymbol{v}_\zeta \equiv \boldsymbol{w}_{\zeta,K}$. We decompose the error between the exact solution $\boldsymbol{v}_\zeta$ and the discrete approximation $\boldsymbol{v}_{\zeta,K} \in \mathbb{S}_{J,K}$ into

$$\boldsymbol{v}_\zeta - \boldsymbol{v}_{\zeta,K} = (\boldsymbol{v}_\zeta - \boldsymbol{w}_{\zeta,K}) + (\boldsymbol{w}_{\zeta,K} - \boldsymbol{v}_{\zeta,K}) \tag{6.29}$$

and study each contribution independently.

6.4.1. Properties of the elliptic projector J_ζ.

Let us consider the following auxiliary problem:

Problem 6.10. For a given $\boldsymbol{f} \in \mathbb{H}_J^{-\frac{1}{2}}$, find $\boldsymbol{w}_\zeta \in \mathbb{H}_J^{\frac{1}{2}}$ such that

$$\mathsf{J}_\zeta(\boldsymbol{w}_\zeta, \boldsymbol{\varphi}) = \langle \boldsymbol{f}, \boldsymbol{\varphi} \rangle_{\Gamma_0}, \quad \text{for all} \quad \boldsymbol{\varphi} \in \mathbb{H}_J^{\frac{1}{2}}. \tag{6.30}$$

For a parameter $\zeta \in \mathbb{R}_+$ large as in Remark 6.9, continuity and ellipticity of J_ζ are ensured by Lemma 4.3. Consequently, the Lax–Milgram lemma ([55], Thm. 3.4) guarantees existence and uniqueness for Problem 6.10. It also holds

$$\|\boldsymbol{w}_\zeta\|_{\mathbb{H}_J^{\frac{1}{2}}} \leq \frac{1}{\mu} \|\boldsymbol{f}\|_{\mathbb{H}_J^{-\frac{1}{2}}}, \tag{6.31}$$

where μ is the ellipticiy constant of J_ζ in (6.25). Cea's lemma ([55], Thm. 8.1) allows us to extend those properties to the discrete setting in $\mathbb{S}_{J,K}$. It provides as well the best approximation error estimate:

$$\|\boldsymbol{w}_\zeta - \boldsymbol{w}_{\zeta,K}\|_{\mathbb{H}_J^{\frac{1}{2}}} \leq \frac{\alpha_\zeta}{\mu} \inf_{\boldsymbol{\varphi}_K \in \mathbb{S}_{J,K}} \|\boldsymbol{w}_\zeta - \boldsymbol{\varphi}_K\|_{\mathbb{H}_J^{\frac{1}{2}}}, \tag{6.32}$$

where $\alpha_\zeta := c_m \zeta + \|\underline{\mathcal{J}}\|_{\mathcal{L}\left(\mathbb{H}_J^{\frac{1}{2}}, \mathbb{H}_J^{-\frac{1}{2}}\right)}$ is the continuity constant of J_ζ.

Lemma 6.11. *Assume $\boldsymbol{f} \in \mathbb{H}_J^{-\frac{1}{2}+s}$ and boundaries Γ_j to be of class $\mathcal{C}^\infty$, for $j = 1, \ldots, J$. Then, for $s > 0$, the solution $\boldsymbol{w}_\zeta$ of Problem 6.10 belongs to $\mathbb{H}_J^{-\frac{1}{2}+s}$ and the following* a priori *estimate is valid*

$$\|\boldsymbol{w}_\zeta\|_{\mathbb{H}_J^{\frac{1}{2}+s}} \leq c(s) \left(\|\boldsymbol{w}_\zeta\|_{\mathbb{H}_J^{\frac{1}{2}}} + \|\boldsymbol{f}\|_{\mathbb{H}_J^{-\frac{1}{2}+s}} \right), \tag{6.33}$$

where $c(s)$ is a positive constant depending on s.

Proof. Follows directly from BIOs regularity properties for smooth domains (*cf.* [52], Thm. 3.2.2). □

6.4.2. Elliptic projection – error estimates

The triangle inequality yields

$$\|\boldsymbol{v}_\zeta - \boldsymbol{w}_{\zeta,K}\|_{\mathbb{H}_J^{\frac{1}{2}}} \leq \|\boldsymbol{v}_\zeta - \boldsymbol{w}_\zeta\|_{\mathbb{H}_J^{\frac{1}{2}}} + \|\boldsymbol{w}_\zeta - \boldsymbol{w}_{\zeta,K}\|_{\mathbb{H}_J^{\frac{1}{2}}}. \tag{6.34}$$

However, from the definition of elliptic projection, namely (6.27), and the ellipticity of the bilinear form $\mathsf{J}_\zeta(\cdot,\cdot)$, we have $\|\boldsymbol{v}_\zeta - \boldsymbol{w}_\zeta\|_{\mathbb{H}_J^{\frac{1}{2}}} = 0$. Therefore, it holds

$$\|\boldsymbol{v}_\zeta - \boldsymbol{w}_{\zeta,K}\|_{\mathbb{H}_J^{\frac{1}{2}}} \leq \|\boldsymbol{w}_\zeta - \boldsymbol{w}_{\zeta,K}\|_{\mathbb{H}_J^{\frac{1}{2}}}. \tag{6.35}$$

Using estimates (6.35) and (6.32) we obtain

$$\|\boldsymbol{v}_\zeta - \boldsymbol{w}_{\zeta,K}\|_{\mathbb{H}_J^{\frac{1}{2}}} \leq \|\boldsymbol{w}_\zeta - \boldsymbol{w}_{\zeta,K}\|_{\mathbb{H}_J^{\frac{1}{2}}} \leq \frac{\alpha_\zeta}{\mu} \inf_{\boldsymbol{\varphi}_K \in \mathbb{S}_{J,K}} \|\boldsymbol{w}_\zeta - \boldsymbol{\varphi}_K\|_{\mathbb{H}_J^{\frac{1}{2}}}. \tag{6.36}$$

Recall that $\boldsymbol{\chi}_j$ is the 2π-periodic parametric representation of the boundary Γ_j, for $j = 1, \ldots, J$. Expanding the total error bound (6.36) into its components over each boundary Γ_j and invoking (6.14), we have

$$\|\boldsymbol{v}_\zeta - \boldsymbol{w}_{\zeta,K}\|_{\mathbb{H}_J^{\frac{1}{2}}} \leq \frac{\alpha_\zeta}{\mu} \sum_{j=1}^{J} \inf_{\varphi_{j,K} \in \mathcal{S}_K(\Gamma_j)} \left\| \tau_{\boldsymbol{\chi}_j} w_j^\zeta - \tau_{\boldsymbol{\chi}_j} \varphi_{j,K} \right\|_{H^{\frac{1}{2}}[0,2\pi]}, \tag{6.37}$$

TABLE 1. Simulation parameters.

Parameters	Symbol	Value	Units
Extracellular conductivity	σ_e	20	mS/cm
Intracellular conductivity	σ_i	5	mS/cm
Membrane capacitance	c_m	1	μF/cm^2
Cell radius	R	7.5×10^{-4}	cm

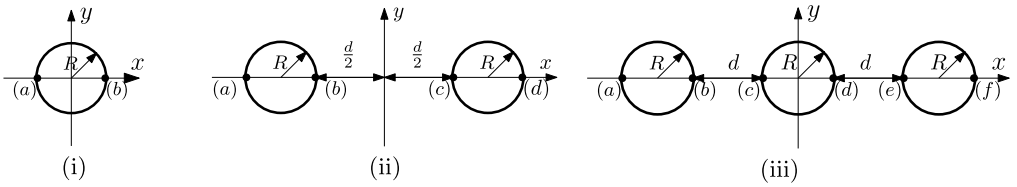

FIGURE 1. Configurations used in the convergence analysis. We consider the three following settings wherein all cells are of radius R. The distance d between cells will be specified later. (i) A single cell centered at the origin of the coordinate system; (ii) two cells separated by a distance d to be specified later; and, (iii) three cells separated by a distance d to be specified later. In the three scenarios we assume that the electric field $\mathbf{E}$ is constant in space and time.

where $\boldsymbol{w}_\zeta = (w_1^\zeta, \dots, w_J^\zeta)$ with elements $w_j^\zeta \in H^{\frac{1}{2}}[0, 2\pi]$, $\boldsymbol{w}_{\zeta,K} = (w_{1,K}^\zeta, \dots, w_{J,K}^\zeta)$ and $\boldsymbol{\varphi}_K = (\varphi_{1,K}, \dots, \varphi_{J,K})$ are such that $w_{j,K}^\zeta$, $\varphi_{j,K} \in \mathcal{S}_K(\Gamma_j)$, for $j = 1, \dots, J$. By Lemma 6.11, we can employ the Aubin-Nitsche trick ([52], Sect. 4.2.5) to shift the error norm from $\mathbb{H}_J^{\frac{1}{2}}$ to $\mathbb{L}_J^2$. Then, by Lemma 6.3, we obtain the following error estimate:

$$\|\boldsymbol{v}_\zeta - \boldsymbol{w}_{\zeta,K}\|_{\mathbb{L}_J^2} \leq \frac{\alpha_\zeta}{\mu} c(p) J K^{-p} \sum_{j=1}^{J} \left| v_j^\zeta \right|_{H^p[0,2\pi]}, \tag{6.38}$$

by acknowledging that $\boldsymbol{v}_\zeta = \boldsymbol{w}_\zeta$. Furthermore, if the solution is 2π-periodic and analytic, we can use Lemma 6.4 to derive the following bound:

$$\|\boldsymbol{v}_\zeta - \boldsymbol{w}_{\zeta,K}\|_{\mathbb{L}_J^2} \leq \frac{\alpha_\zeta}{\mu} J \Theta \exp(-\eta K), \tag{6.39}$$

where Θ and η are positive constants independent of K and the number of cells J. Finally, using (6.26a), (6.26b) to retrieve $\boldsymbol{v}_\zeta$ from $\boldsymbol{v}$, we can state the following theorem:

Theorem 6.12. *Let $\boldsymbol{v}$ be the solution of Problem 4.2 and assume that it satisfies the analyticity conditions of Lemma 6.4. Then, for all times $t \in [0, T]$, the following error estimate holds*

$$\|\boldsymbol{v} - \boldsymbol{w}_K\|_{\mathbb{L}_J^2} \leq \frac{\alpha_\zeta}{\mu} J \Theta \exp(\zeta T) \exp(-\eta K), \tag{6.40}$$

where Θ and η are positive constants independent of K and the number of cells J.

TABLE 2. Convergence results for a single axon setting $\varepsilon = 0.25$ and $\delta = 0.75$ and $\Phi_e^{(1)}$ as external source. The rates of exponential convergence are 2.057, 1.051 and 0.774 for the single, two and three cell cases, respectively.

K	τ	Error single cell	Error two cells	Error three cells
1	1.648721×10^{-3}	$4.614530 \times 10^{+1}$	$8.217310 \times 10^{+1}$	$1.024221 \times 10^{+2}$
2	1.284025×10^{-3}	$1.289820 \times 10^{+0}$	$6.872140 \times 10^{+0}$	$4.231990 \times 10^{+1}$
3	1.000000×10^{-3}	1.903200×10^{-2}	$2.961200 \times 10^{+0}$	$1.194092 \times 10^{+1}$
4	7.788008×10^{-4}	3.359740×10^{-3}	9.206260×10^{-1}	$7.724340 \times 10^{+0}$
5	6.065307×10^{-4}	5.495460×10^{-4}	2.992460×10^{-1}	$2.080491 \times 10^{+0}$
6	4.723666×10^{-4}	1.055950×10^{-4}	9.794200×10^{-2}	$1.693611 \times 10^{+0}$
7	3.678794×10^{-4}	2.145180×10^{-5}	3.243720×10^{-2}	5.353650×10^{-1}
8	2.865048×10^{-4}	3.701340×10^{-6}	1.150910×10^{-2}	4.547880×10^{-1}
9	2.231302×10^{-4}	5.856280×10^{-7}	4.870160×10^{-3}	1.573761×10^{-1}
10	1.737739×10^{-4}	1.228320×10^{-7}	2.578580×10^{-3}	1.411557×10^{-1}

TABLE 3. Convergence results for a single axon setting $\varepsilon = 0.5$ and $\delta = 1.0$ and $\Phi_e^{(1)}$ as external source. The rates of exponential convergence are 1.853, 1.051 and 0.749 for the single, two and three cell cases, respectively.

K	τ	Error single cell	Error two cells	Error three cells
1	1.648721×10^{-3}	$3.584630 \times 10^{+1}$	$6.432560e \times 10^{+1}$	$5.851500 \times 10^{+1}$
2	1.000000×10^{-3}	9.673760×10^{-1}	$4.304700e \times 10^{+0}$	$2.588640 \times 10^{+1}$
3	6.065307×10^{-4}	3.079990×10^{-2}	$1.928888 \times 10^{+0}$	$6.519960 \times 10^{+0}$
4	3.678794×10^{-4}	6.512100×10^{-3}	5.907100×10^{-1}	$4.784040 \times 10^{+0}$
5	2.231302×10^{-4}	1.209490×10^{-3}	1.958070×10^{-1}	$1.245723 \times 10^{+0}$
6	1.353353×10^{-4}	2.821550×10^{-4}	6.648340×10^{-2}	$1.009443 \times 10^{+0}$
7	8.208500×10^{-5}	6.493960×10^{-5}	2.386200×10^{-2}	3.125430×10^{-1}
8	4.978707×10^{-5}	1.226060×10^{-5}	1.006122×10^{-2}	2.617374×10^{-1}
9	4.978707×10^{-5}	2.540470×10^{-6}	5.285280×10^{-3}	9.018660×10^{-2}
10	1.831564×10^{-5}	5.752190×10^{-7}	3.053620×10^{-3}	7.857030×10^{-2}

6.5. Convergence estimates

We now return our attention to the time discretization. At a time $t_n \in \Upsilon_N$, we split the full error $\boldsymbol{v}^n - \boldsymbol{v}_K^n$ as follows

$$\boldsymbol{v}^n - \boldsymbol{v}_K^n = \underbrace{(\boldsymbol{v}^n - \boldsymbol{w}_K^n)}_{=:\boldsymbol{\rho}^n} + \underbrace{(\boldsymbol{w}_K^n - \boldsymbol{v}_K^n)}_{=:\boldsymbol{\theta}^n}, \tag{6.41}$$

where $\boldsymbol{w}_K^n$ is defined as in (6.28) for each time step t_n, $n = 0, \ldots, N$. Due to Lemma 6.4, one concludes that $\boldsymbol{\rho}^n$ is bounded in the $\mathbb{L}^2_J$-norm by Theorem 6.12. Following the error analysis presented ([29], Sect. 6.3), one can derive the next result for $\boldsymbol{\theta}^n$, for $n = 0, \ldots, N$.

Lemma 6.13. *Let $\boldsymbol{v}$ and $\boldsymbol{g}$ be the solution of Problem 4.2 for initial data $\boldsymbol{v}_0$ and $\boldsymbol{g}_0$. Besides, let $\boldsymbol{v}_K^n$ and $\boldsymbol{g}_K^n$ be the solution of Problem 6.6 for initial boundary data $\boldsymbol{v}_K^0$, $\boldsymbol{v}_K^1$, $\boldsymbol{g}_K^0$ and $\boldsymbol{g}_K^1$ in $\mathbb{S}_{J,K}$, for $n = 1, \ldots, N-1$. Then,*

TABLE 4. Convergence results for a single axon setting $\varepsilon = 0.25$ and $\delta = 0.75$ and $\Phi_e^{(2)}$ as external source. The rates of exponential convergence are 2.138, 1.061 and 0.673 for the single, two and three cell cases, respectively.

K	τ	Error single cell	Error two cells	Error three cells
1	1.648721×10^{-3}	$1.985580\times10^{+0}$	$4.326700\times10^{+0}$	$8.099550\times10^{+0}$
2	1.284025×10^{-3}	2.689180×10^{-2}	2.165740×10^{-1}	6.036660×10^{-1}
3	1.000000×10^{-3}	2.401830×10^{-2}	5.510000×10^{-2}	2.174205×10^{-1}
4	7.788008×10^{-4}	1.722150×10^{-4}	1.310898×10^{-3}	7.859420×10^{-2}
5	6.065307×10^{-4}	1.721510×10^{-4}	9.184340×10^{-4}	6.394830×10^{-2}
6	4.723666×10^{-4}	3.037490×10^{-6}	4.069820×10^{-4}	3.217640×10^{-2}
7	3.678794×10^{-4}	3.037250×10^{-6}	3.313340×10^{-4}	2.720043×10^{-2}
8	2.865048×10^{-4}	7.669300×10^{-8}	2.556620×10^{-4}	1.313981×10^{-2}
9	2.231302×10^{-4}	7.663710×10^{-8}	1.852766×10^{-4}	1.135493×10^{-2}
10	1.737739×10^{-4}	2.605920×10^{-9}	1.281980×10^{-4}	5.607000×10^{-3}

it holds:

$$\left\|\boldsymbol{\theta}^{n+1}\right\|_{\mathbb{L}^2_J}^2 \leq c_1 \left(\left\|\boldsymbol{\theta}^1\right\|_{\mathbb{L}^2_J}^2 + \tau \left\|\boldsymbol{\theta}^0\right\|_{\mathbb{L}^2_J}^2 + \tau \sum_{j=1}^{n} (1+\delta_1\tau)^{-(j+1)} \left\| \hat{\boldsymbol{g}}_K^{j+\frac{1}{2}} - \underline{\hat{\mathrm{P}}}_K \boldsymbol{g}^{j+\frac{1}{2}} \right\|_{\mathbb{L}^2_J}^2 + \left(\exp(-\eta K) + \tau^2\right)^2 \right),$$

and

$$\left\|\boldsymbol{g}^{n+1} - \boldsymbol{g}_K^{n+1}\right\|_{\mathbb{L}^2_J} \leq c_2 \left(\left\|\boldsymbol{g}^1 - \boldsymbol{g}_K^1\right\|_{\mathbb{L}^2_J} + \tau \left\|\boldsymbol{g}^0 - \boldsymbol{g}_K^0\right\|_{\mathbb{L}^2_J} + \tau \sum_{j=1}^{n} (1+\delta_2\tau)^{-(j+1)} \left\| \hat{\boldsymbol{v}}_K^{j+\frac{1}{2}} - \underline{\hat{\mathrm{P}}}_K \boldsymbol{v}^{j+\frac{1}{2}} \right\|_{\mathbb{L}^2_J} + \tau^2 \right),$$

where c_1, c_2, δ_1 and δ_2 are positive constants independent of τ and K and depending on α_ζ, μ, J and Θ from Theorem 6.12.

With this last result, we can now state the main convergence result of our numerical scheme:

Theorem 6.14. *Under the same hypotheses of Lemma 6.13, if $\boldsymbol{v}_K^1$ and $\boldsymbol{g}_K^1$ are chosen according to Algorithm 6.7, the following error estimates hold*

$$\|\boldsymbol{v}^n - \boldsymbol{v}_K^n\|_{\mathbb{L}^2_J} \leq c_C \left(\left\|\boldsymbol{v}_K^0 - \boldsymbol{v}_0\right\|_{\mathbb{L}^2_J} + \left\|\boldsymbol{g}_0 - \boldsymbol{g}_K^0\right\|_{\mathbb{L}^2_J} + \exp(-\eta K) + \tau^2 \right),$$
$$\|\boldsymbol{g}^n - \boldsymbol{g}_K^n\|_{\mathbb{L}^2_J} \leq c_C \left(\left\|\boldsymbol{v}_K^0 - \boldsymbol{v}_0\right\|_{\mathbb{L}^2_J} + \left\|\boldsymbol{g}_0 - \boldsymbol{g}_K^0\right\|_{\mathbb{L}^2_J} + \exp(-\eta K) + \tau^2 \right),$$

for $n = 2, \ldots, N$, with c_C and η are positive constants independent of τ and K and depending on the constants α_ζ, μ, J and Θ from Theorem 6.12.

Proof. The proof is a direct consequence of Lemma 6.13 together with approximation properties of $\boldsymbol{v}_K^1$ and $\boldsymbol{g}_K^1$ given in Algorithm 6.7. For details, we refer to ([58], Thm. 13.5) and ([29], Thm. 4). □

6.6. Stability analysis

We now provide stability conditions for the numerical scheme given in Problem 6.6. As shown in ([29], Sect. 5), two time-dependent systems are coupled: one describing the evolution of HH gate variables (6.21b), while the

TABLE 5. Convergence results for a single axon setting $\varepsilon = 0.5$ and $\delta = 1.0$ and $\Phi_e^{(2)}$ as external source. The rates of exponential convergence are 2.132, 1.060 and 0.671 for the single, two and three cell cases, respectively.

K	τ	Error single cell	Error two cells	Error three cells
1	1.648721×10^{-3}	$1.985580\times10^{+0}$	$4.326700\times10^{+0}$	$8.099550\times10^{+0}$
2	1.000000×10^{-3}	2.401830×10^{-2}	2.100040×10^{-1}	5.749320×10^{-1}
3	6.065307×10^{-4}	2.323540×10^{-2}	5.509560×10^{-2}	2.169405×10^{-1}
4	3.678794×10^{-4}	1.721810×10^{-4}	1.310730×10^{-3}	7.858980×10^{-2}
5	2.231302×10^{-4}	1.722310×10^{-4}	9.183680×10^{-4}	6.399840×10^{-2}
6	1.353353×10^{-4}	3.040350×10^{-6}	4.022760×10^{-4}	3.218520×10^{-2}
7	8.208500×10^{-5}	3.042640×10^{-6}	3.293040×10^{-4}	2.720861×10^{-2}
8	4.978707×10^{-5}	7.662220×10^{-8}	2.549920×10^{-4}	1.313952×10^{-2}
9	4.978707×10^{-5}	7.663600×10^{-8}	1.851376×10^{-4}	1.135508×10^{-2}
10	1.831564×10^{-5}	2.605780×10^{-9}	1.281256×10^{-4}	5.607240×10^{-3}

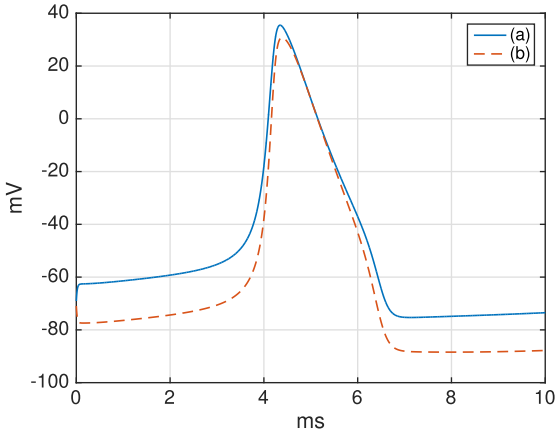

FIGURE 2. Transmembrane potential of the single biological cell setting at points (a) and (b) as defined in Figure 1(i). The electric field used in this computation is $\mathbf{E} = (5000, 0, 0)^\top$ mV/cm.

second model depicts the transmembrane voltage and current (6.21a). We establish bounds for the time-spacing τ in both cases and define a global criterion to be later used in numerical simulations.

In the HH model, the system of gating variables (6.21b) can be arranged as follows [21]:

$$\partial_t g_j = -\frac{g_j - g_j^\infty(v_j)}{\tau_j(v_j)}, \qquad g_j(0) = g_{j,0},$$

where g_j represents the gate variable related to the cellular membrane Γ_j, $j = 1, \ldots, J$, with

$$g_j^\infty(v_j) = \frac{\alpha_j(v_j)}{\alpha_j(v_j) + \beta_j(v_j)} \quad \text{and} \quad \tau_j(v_j) = \frac{1}{\alpha_j(v_j) + \beta_j(v_j)},$$

for a given transmembrane potential v_j. Moreover, assume that the ionic current $i_{\text{ion},j}$ can be written as the product of a function depending solely on g_j and v_j, *i.e.*

$$i_{\text{ion},j}(v_j, g_j) = \mathcal{H}_j(g_j)\, v_j. \tag{6.42}$$

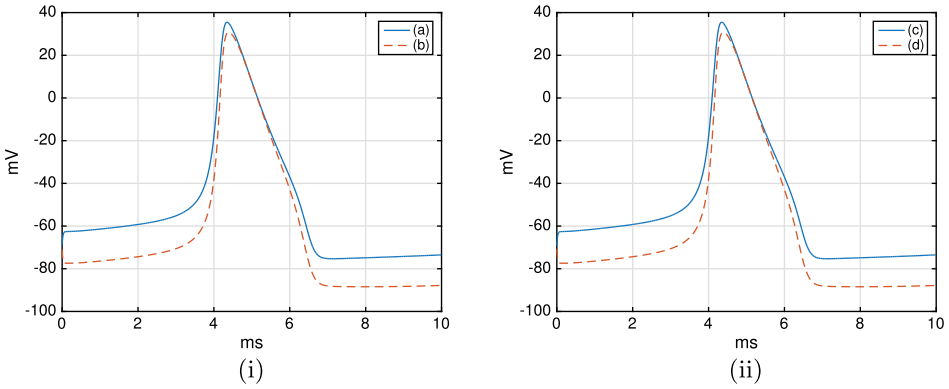

FIGURE 3. Transmembrane potential of the two biological cells setting. The electric field is this computation is $\mathbf{E} = (5000, 0, 0)^\top$ mV/cm and the distance between cells is $d = 5R$. Figure 6(i) depicts the transmembrane voltage at points (a) and (b) and Figure 6(ii) at points (c) and (d), as defined in Figure 1(ii).

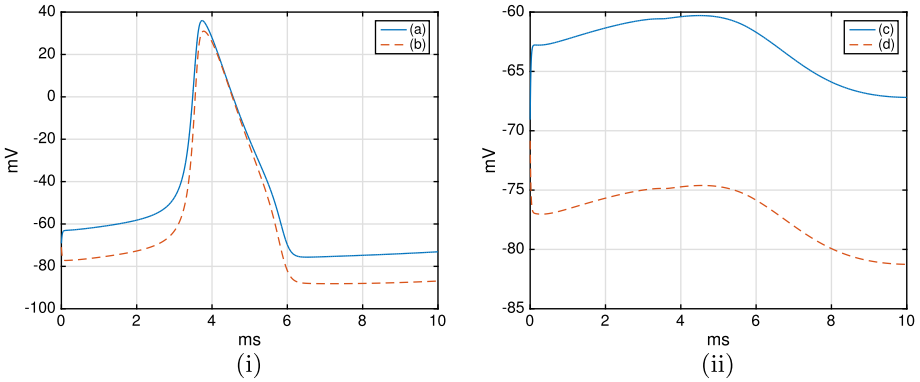

FIGURE 4. Transmembrane potential of the two biological cells setting. The electric field used int this computation is $\mathbf{E} = (5000, 0, 0)^\top$ mV/cm and the distance between cells is $d = 0.1R$. Figure 6(i) portrays the transmembrane voltage at points (a) and (b) and Figure 6(ii) at points (c) and (d), as defined in Figure 1(ii).

Based on this assumption, we can state the following result regarding the stability of Problem 6.6 (*cf.* [29], Thm. 3).

Theorem 6.15. *Let $\boldsymbol{v}_K^n$, $\boldsymbol{g}_K^n$ for $n = 2, \ldots, N-1$, denote solutions of the fully discrete Problem 6.6 at times $t_n \in \Upsilon_N$. If $v_{\max} > 0$ denotes the bounded maximum value for the transmembrane potential for all biological cells, the numerical scheme proposed is stable for all positive time-spacings τ such that*

$$\tau < \min\left\{ \frac{c_m}{\mathcal{H}_{1,\max}}, \cdots, \frac{c_m}{\mathcal{H}_{J,\max}}, \frac{2}{3} \min_{|v_1| \le v_{\max}} \frac{1}{\alpha_1(v_1) + \beta_1(v_1)}, \ldots, \frac{2}{3} \min_{|v_J| \le v_{\max}} \frac{1}{\alpha_J(v_J) + \beta_J(v_J)} \right\}$$

where α_j, β_j, $j = 1, \ldots, J$, denote the v_j-dependent gate model variables and $\mathcal{H}_{j,\max}$ is the maximum value for $\mathcal{H}_j$.

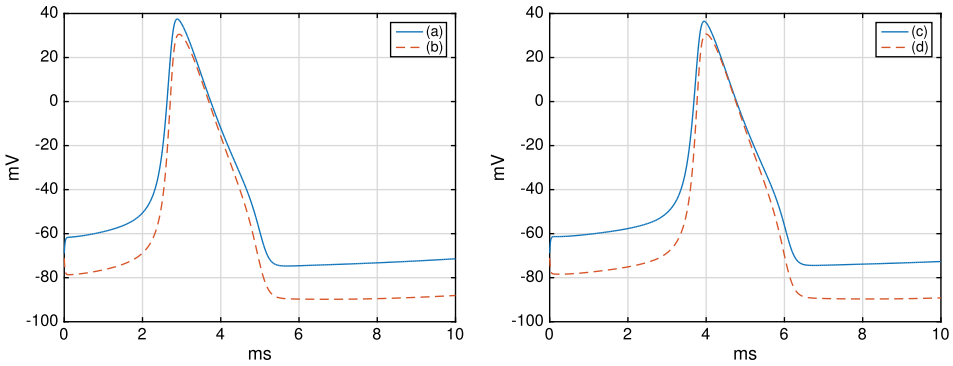

FIGURE 5. Transmembrane potential of the two biological cells setting. The electric field is this computation is $\mathbf{E} = (6000, 0, 0)^\top$ mV/cm and the distance between cells is $d = 0.1R$. Figure 6(i) shows the transmembrane voltage at points (a) and (b) and Figure 6(ii) at points (c) and (d), as defined in Figure 1(ii).

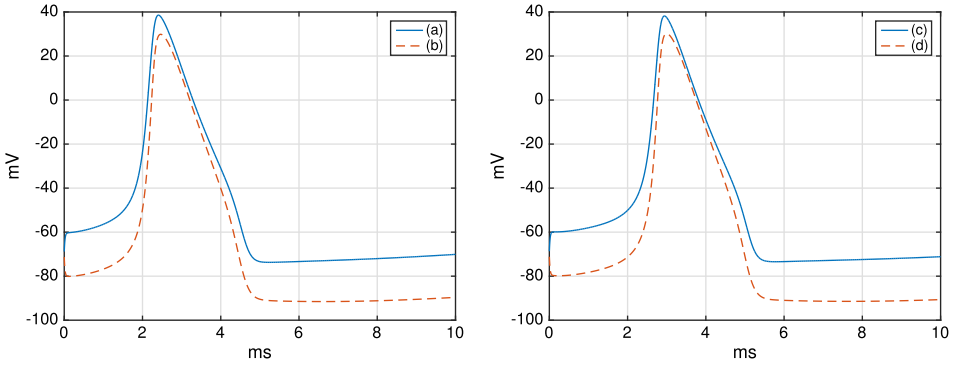

FIGURE 6. Transmembrane potential of the two biological cells setting. The electric field is this computation is $\mathbf{E} = (7500, 0, 0)^\top$ mV/cm and the distance between cells is $d = 0.1R$. Figure 6(i) displays the transmembrane voltage at points (a) and (b) and Figure 6(ii) at points (c) and (d), as defined in Figure 1(ii).

7. NUMERICAL RESULTS

The numerical scheme presented in Section 6 was implemented in C++ with basic linear algebra routines coming from Lapack [5]. Simulations where run on a AMD FX-8350 Eight-Core processor at 2.8 GHz. In all the simulations the biological cells are assumed to be circles of equal radius. Table 1 contains a list of parameters employed in the computations presented here.

Simulations are carried out assuming a membrane behavior given by the HH model (*cf.* Appendix A or [21, 31]). We consider the following external sources:

$$\Phi_e^{(1)}(\boldsymbol{x}) := -\mathbf{E} \cdot \boldsymbol{x}, \tag{7.1}$$

$$\Phi_e^{(2)}(\boldsymbol{x}) := -\|\mathbf{E}\| \left(\exp(\omega x) + \exp(-\omega x)\right) \cos(\omega y), \tag{7.2}$$

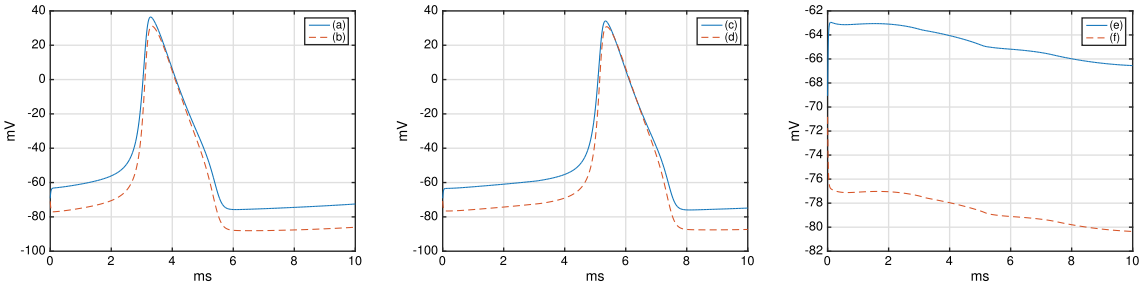

FIGURE 7. Transmembrane potential of the three biological cells setting. The electric field is this computation is $\mathbf{E} = (5000, 0, 0)^\top$ mV/cm and the distance between cells is $d = 0.1R$. (i) The transmembrane voltage at points (a) and (b); (ii) at points (c) and (d); and (iii) at points (e) and (f), as defined in Figure 1(iii).

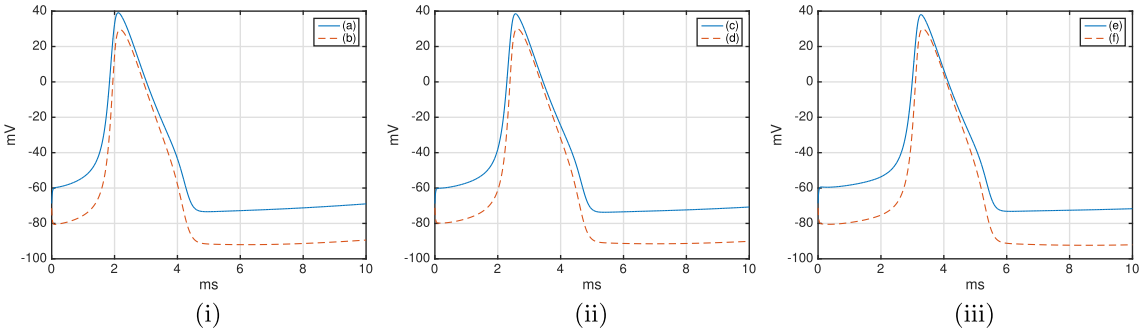

FIGURE 8. Transmembrane potential of the three biological cells setting. The electric field is this computation is $\mathbf{E} = (7500, 0, 0)^\top$ mV/cm and the distance between cells is $d = 0.1R$. (i) The transmembrane voltage at points (a) and (b); (ii) at points (c) and (d); and (iii) at points (e) and (f), as defined in Figure 1(iii).

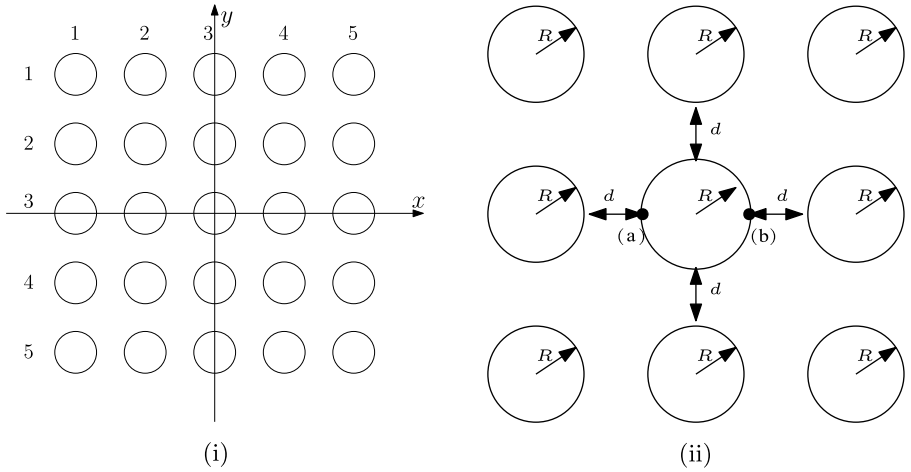

FIGURE 9. Configuration of 25 interacting biological cells. The cells are rranged in a grid of size 5×5 as depicted in (i). The distance between cells is $d = 0.2R$ and transmembrane voltage is measured at points and (a) and (b), as depicted in (ii).

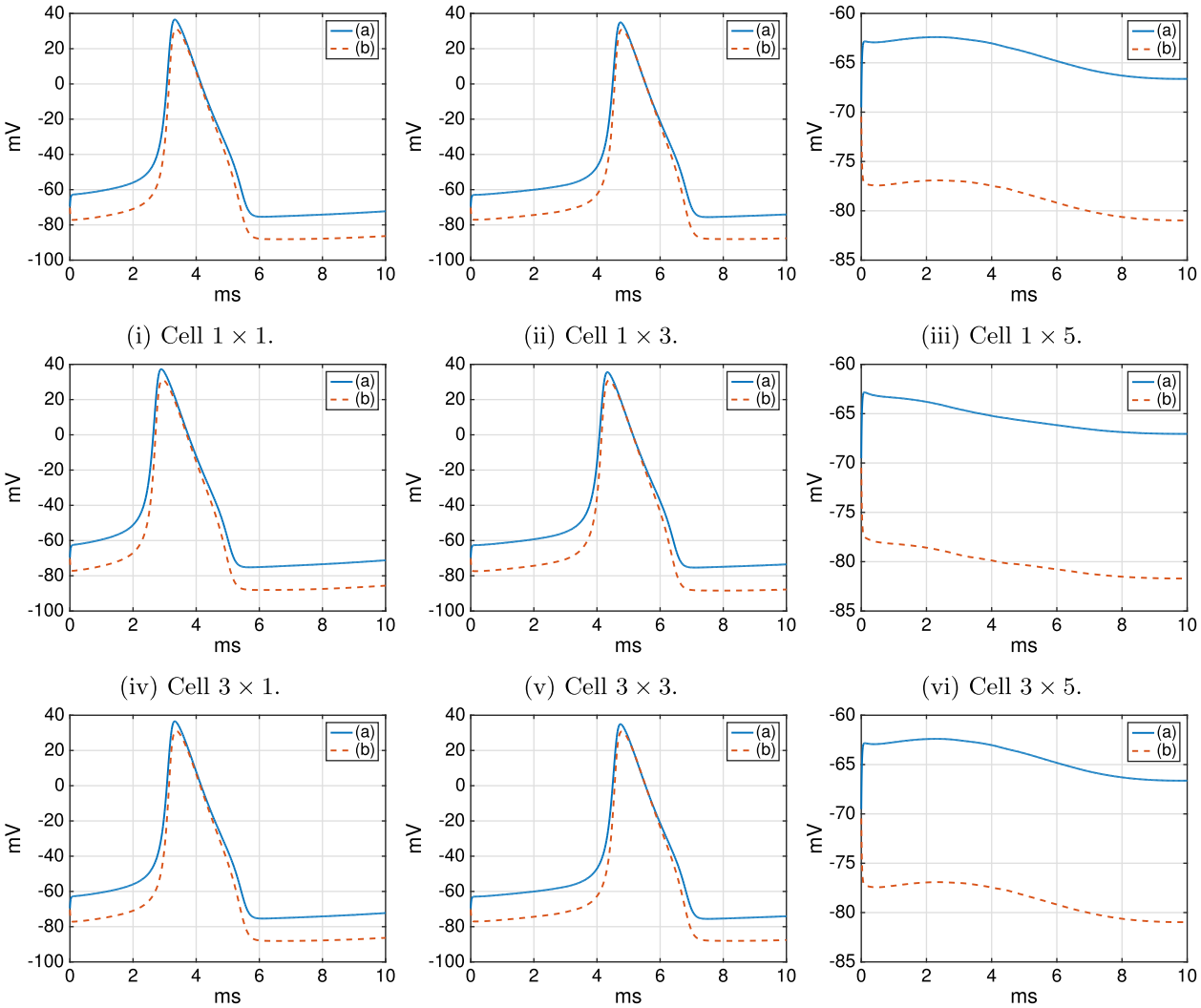

(i) Cell 1×1. (ii) Cell 1×3. (iii) Cell 1×5.

(iv) Cell 3×1. (v) Cell 3×3. (vi) Cell 3×5.

(vii) Cell 5×1. (viii) Cell 5×3. (ix) Cell 5×5.

FIGURE 10. Transmembrane potential in the 5×5 biological cells configuration shown Figure 9. The electric field is this computation is $\mathbf{E} = (7500, 0, 0)^\top$ mV/cm. We show the transmembrane potential at points (a) and (b) as described in Figure 9(ii), *i.e.* the left- and right-most points on the cell boundary. We show results for 9 of the 25 biological cells, following the numbering described in Figure 9(i).

where $\boldsymbol{x} = (x, y)$ and we select $\omega = 5$. The electric field $\mathbf{E}$ is assumed to be constant in space and time. The error is measured in the following norm:

$$\|\boldsymbol{u}\|_{L^\infty(\Upsilon_N, \mathbb{L}^2_J)} := \max_{t_n \in \Upsilon_N} \|\boldsymbol{u}(t_n)\|_{\mathbb{L}^2_J} . \tag{7.3}$$

7.1. Convergence results

We present convergence results of the numerical scheme presented in Section 6. We consider three different configurations, as depicted in Figure 1. Figure 1(i)–(iii) shows one, two and three biological cell configurations, respectively. Convergence analysis is performed with a number of Fourier modes K ranging from 1 up to 10 and time steps are chosen such that $\tau = 0.001\exp(-\varepsilon K + \delta)$ ms, with ε and δ to be chosen, and for the simulation time window $[0, 1]$ ms.

Tables 2–5 show convergence results for the configurations described in Figure 1(i–iii) assuming $d = 0.1R$ and $\mathbf{E} = (5000, 0, 0)^\top$ mV/cm. The first column in Tables 2 and 3 is the number of Fourier modes K, the second column corresponds to the time step τ, which has been chosen according to the rule $\tau = 0.001\exp(-\varepsilon K + \delta)$. Finally, the third, fourth and fifth columns present the error measured in the $\|\cdot\|_{L^\infty(\Upsilon_N, \mathbb{L}^2_J)}$-norm as defined in (7.3), with $J = 1, 2, 3$, for the single, two and three biological cells configurations presented in Figure 1, respectively.

7.2. Transmembrane voltage

Transmembrane voltages at different points over biological cells for the three configurations described in Figure 1 are provided using $\Phi_e^{(1)}$ defined by (7.2) as external source. Figure 2 shows the transmembrane voltage for the single biological cell configuration at points (a) and (b) defined in Figure 1(i). The electric field employed in this computation is $\mathbf{E} = (5000, 0, 0)^\top$ mV/cm. Figures 3–6 shown results for the two cells scenario. In Figure 3 the distance between cells is $d = 5R$ and the electric field is $\mathbf{E} = (5000, 0, 0)^\top$ mV/cm. In Figure 4 the electric field remains the same, however the distance between cells is reduced to $d = 0.1R$. In Figures 5 and 6 the distance between cells is still $d = 0.1R$, nevertheless the electric field is increased to $\mathbf{E} = (6000, 0, 0)^\top$ mV/cm and $\mathbf{E} = (7500, 0, 0)^\top$ mV/cm, respectively. Figures 7 and 8 portray the results for the three biological configuration, presented in Figure 1(iii). In both figures, the distance between biological cells is $d = 0.1R$ however in the Figure 7 the electric field is $\mathbf{E} = (5000, 0, 0)^\top$ mV/cm, while in Figure 8 it is set to $\mathbf{E} = (7500, 0, 0)^\top$ mV/cm.

Consider now electrical interactions among 25 biological cells distributed in a homogeneous lattice of size 5×5, as shown in Figure 9. Cells are numbered following the scheme presented in Figure 9(i). As in previous computations, all the cells are of equal radius R with a distance between them is $d = 0.2R$, as portrayed in Figure 9(ii). Figure for 9 out the 25 biological cells we have considered in the computation. The transmembrane potential at the left and rightmost points, respectively points (a) and (b) as described in Figure 9(ii), are plotted. Figure 10(i–iii) show results for the biological cells in positions 1×1, 1×3 and 1×5. Figure 10(iv–vi) show results for the biological cells in positions 3×1, 3×3 and 3×5. Figure 10(vii–ix) show results for the biological cells in positions 5×1, 5×3 and 5×5.

7.3. Discussion

The results validate the expected exponential convergence rates when taking $\tau \propto \exp(-\varepsilon K + \delta)$, for $\varepsilon > 0$ and $\delta > 0$, for the nonlinear membrane dynamics. Based on this observation, we calibrate our quadrature scheme for the nonlinear terms using the same spatial nodes. Indeed, higher order quadratures would not improve convergence rates though perhaps proportionality constants. In terms of computational effort, we observe a rapid increase in computational times as expected as no acceleration routines were implemented. Interestingly, we observed that as cells came closer to each other exponential rates decreased. This can be explained by a loss of analyticity in the solutions, which disappears once cells touch each other.

From a biological perspective, our numerical results support the claim for membrane potentials depending on both axon geometry and position with respect to external electrical excitations. Such interrelations are extremely relevant when analyzing and modeling closely packed cells and their interactions [46]. For instance, cells lying between the excitation and a given target cell can delay or even block the stimulation.

8. Conclusions and future work

We have presented a novel numerical method to compute the temporal evolution of cellular membrane potentials under electrical excitation. Key to the scheme's success is the boundary reduction *via* the MTF along with the coupling of the HH model for transmembrane voltages. The resulting problem is proven to be well posed. In time-domain, the proposed semi-implicit method was shown to possess a time-step stability condition independent of spatial discretization, relying solely on problem parameters. Moreover, for analytic solutions exponential convergence rates were found for suitable chosen time and space steps, which was validated numerically for two-dimensional cells. Simulations are found to agree with experimental observations. In particular, our numerical results depict the blocking effect that surrounding axons can yield onto a particular one as well as the change of excitation phase due to the multiple cellular interactions. Future work includes the extension to 3D simulations as well as further acceleration for cross interactions including the use of iterative solvers by implementing preconditioners based on Calderón identities or mass matrices. Also, further research should include the case of touching cells as well as the comparison of other single or multiple trace formulations.

Appendix A. Hodgkin–Huxley model

We provide details on the HH model. More precisely, the explicit expression of $\mathcal{HH}_k$ and $i_{\text{ion,k}}$ considered in the model – *cf.* (2.14) and (2.13), respectively – and in our computations. The content presented here comes from ([21], Chap. 2). In the following, we drop the index k, which denotes the biological cell on which $\mathcal{HH}_k$ and $i_{\text{ion,k}}$ are defined. We adopt the same convention for the transmembrane potential v_k.

In the HH formalism ionic channels are characterized by the so-called *gate variables* to regulate the transport of ionic species across the cellular membrane. As pointed out in Remark 2.1, the HH model makes use of three gate variables to account for the nonlinear nature of the electrophysiological dynamics taking place over the membrane of a biological cell. These gate variables, from now on denoted by m, n and h, are dimensionless quantities taking values between zero and one and they can be understood as the probability of the corresponding gates to be open. Two main ionic species are considered: sodium (Na^+) and potassium (K^+). The gate variables m and h are used to describe the flow of the sodium ions, while only the gate variable n is employed to describe the movement of potassium. Let $\mathbf{g} := (m, n, h)^\top$ be the vector containing the aforementioned gate variables and v the transmembrane voltage. The HH model states that the total current produced by the transport of ionic species across the cellular membrane can be described as follows:

$$i_{\text{ion}}(v, \mathbf{g}) = \overline{g}_{\text{Na}^+} m^3 h (v - v_{\text{Na}^+}) + \overline{g}_{\text{K}^+} n^4 (v - v_{\text{K}^+}) + \overline{g}_{\text{L}} (v - v_{\text{L}}), \tag{A.1}$$

where the constants $\overline{g}_{\text{Na}^+}$ and $\overline{g}_{\text{K}^+}$ are called the *maximum conductance* of Na^+ and K^+ channels, respectively, and the voltages v_{Na^+} and v_{K^+} are known as the *Nernst potentials* or *equilibrium potentials* for each ion. When the transmembrane potential v reaches these values, the total flux of an specific ion vanishes. At this point, the flow of ionic species due to concentration gradients matches the flow produced by the potential difference across the cellular membrane. The term $\overline{g}_{\text{L}}(v - v_{\text{L}})$ in (A.1) models a residual current produced by the flow of ionic species other than sodium and potassium. Table A.1 provides numerical values for the parameters introduced in (A.1).

The system of ODEs describing the dynamics of the gate variables $\mathbf{g}$:

$$\partial_t \mathbf{g} = \mathcal{HH}(v, \mathbf{g}) \tag{A.2}$$

contains three equations, one per each gate variable in the HH model (*cf.* Rem. 2.1). These ordinary differential equation (A.2) can expanded in the following way:

$$\partial_t m = \alpha_m(v)(1 - m) - \beta_m(v) m, \tag{A.3}$$

$$\partial_t n = \alpha_n(v)(1 - n) - \beta_n(v) n, \tag{A.4}$$

TABLE A.1. Parameters of the Hodgkin–Huxley model.

Parameter	Mean	Range	Standard	Units
$\overline{g}_{\mathrm{Na}^+}$	0.91	0.8–1.5	1.0	$[\mathrm{mS/cm}^2]$
$\overline{g}_{\mathrm{K}^+}$	34	26–49	36	$[\mathrm{mS/cm}^2]$
$\overline{g}_{\mathrm{L}}$	0.26	0.13–0.5	0.3	$[\mathrm{mS/cm}^2]$
v_{Na^+}	109	95–119	115	[mV]
v_{K^+}	−11	9–14	-12	[mV]
v_{L}	11	4–22	10.6	[mV]

$$\partial_t h = \alpha_h(v)(1-h) - \beta_h(v)h, \tag{A.5}$$

where

$$\alpha_m(v) = \frac{0.1(25-v)}{\exp(2.5-0.1v)-1}, \qquad \beta_m(v) = 4\exp(-v/18), \tag{A.6}$$

$$\alpha_n(v) = \frac{0.01(10-v)}{\exp(1-0.1v)-1}, \qquad \beta_n(v) = 0.125\exp(-v/80), \tag{A.7}$$

$$\alpha_h(v) = 0.07\exp(-v/20), \qquad \beta_h(v) = \frac{1}{\exp(3-0.1v)+1}. \tag{A.8}$$

REFERENCES

[1] M. Amar, D. Andreucci, P. Bisegna and R. Gianni, A hierarchy of models for the electrical conduction in biological tissues via two-scale convergence: the nonlinear case. *Differ. Integral Equ.* **26** (2013) 885–912.

[2] M. Amar, D. Andreucci and R. Gianni, Asymptotic decay under nonlinear and noncoercive dissipative effects for electrical conduction in biological tissues. *Nonlinear Differ. Equ. Appl.* **23** (2016) 48.

[3] H. Ammari, L. Giovangigli, H. Kwon, J.K. Seo and T. Wintz, Spectroscopic conductivity imaging of a cell culture. *Asymptotic Anal.* **100** (2016) 87–109.

[4] H. Ammari, T. Widlak and W. Zhang, Towards monitoring critical microscopic parameters for electropermeabilization. *Quart. Appl. Math.* **75** (2017) 1–17.

[5] E. Anderson, Z. Bai, C. Bischof, S. Blackford, J. Dongarra, J. Du Croz, A. Greenbaum, S. Hammerling, A. McKenney and D. Sorenson, LAPACK Users' Guide. Vol. 9. SIAM (1999).

[6] X. Antoine, C. Chniti and K. Ramdani, On the numerical approximation of high-frequency acoustic multiple scattering problems by circular cylinders. *J. Comput. Phys.* **227** (2008) 1754–1771.

[7] K. Atkinson and W. Han, Theoretical Numerical Analysis. Vol. 39. Springer (2005).

[8] M. Balabane, Boundary decomposition for Helmoltz and Maxwell equations I. Disjoint subscatterers. *Asymptotic Anal.* **38** (2004) 1–10.

[9] P. J. Basser and B. J. Roth, New currents in electrical stimulation of excitable tissues. *Ann. Rev. Biomed. Eng.* **2** (2000) 377–397.

[10] C. Bollini and F. Cacheiro, Peripheral nerve stimulation. *Tech. Reg. Anesth. Pain Manag.* **10** (2006) 79–88.

[11] C. Canuto and A. Quarteroni, Approximation results for orthogonal polynomials in Sobolev spaces. *Math. Comput.* **38** (1982) 67–86.

[12] C. Canuto, M. Y. Hussaini, A. Quarteroni and T. A. Zang, Spectral Methods. Scientific Computation. Springer-Verlag, Berlin (2006).

[13] Y. Chang and R. Harrington, A surface formulation or characteristic modes of material bodies. *IEEE Trans. Antennas. Propag.* **25** (1977) 789–795.

[14] D. Chapelle, A. Collin and J.-F. Gerbeau, A surface-based electrophysiology model relying on asymptotic analysis and motivated by cardiac atria modeling. *Math. Models Meth. Appl. Sci.* **23** (2013) 2749–2776.

[15] S. O. Choi, Y. Kim, J. W. Lee, J. H. Park, M. R. Prausnitz and M. G. Allen, Intracellular protein delivery and gene transfection by electroporation using a microneedle electrode array. *Small* **10** (2012) 1081–1091.

[16] X. Claeys, R. Hiptmair and C. Jerez-Hanckes, Multitrace boundary integral equations, in Direct and Inverse Problems in Wave Propagation and Applications. Vol. 14 of *Radon Series on Computational and Applied Mathematics*. De Gruyter, Berlin (2013) 51–100.

[17] X. Claeys, R. Hiptmair, C. Jerez-Hanckes and S. Pintarelli, Novel Multi-Trace Boundary Integral Equations for Transmission Boundary Value Problems, in *Unified Transform for Boundary Value Problems: Applications and Advances*, edited by A.S. Fokas and B. Pelloni. SIAM (2015) 227–258.
[18] M. Costabel, Boundary integral operators on Lipschitz domains: elementary results. *SIAM J. Math. Anal.* **19** (1988) 613–626.
[19] M. Costabel and E. Stephan, A direct boundary integral equation method for transmission problems. *J. Math. Anal. Appl.* **106** (1985) 367–413.
[20] Y. Coudiere, J. Henry and S. Labarthe, An asymptotic two-layer monodomain model of cardiac electrophysiology in the atria: derivation and convergence. *SIAM J. Appl. Math.* **77** (2017) 409–429.
[21] S. Doi, J. Inoue., Z. Pan and K. Tsumoto, Computational electrophysiology. Vol. 2 of *Springer Series, A First Course in On Silico Medicine*, Tokyo, Japan (2010).
[22] I. Dotsinskya, B. Nikolova, E. Peychevab and I. Tsonevaa, New modality for electrochemotherapy of surface tumors. *Biotechnol. Biotechnol. Equip.* **26** (2012) 3402–3406.
[23] M. Ganesh and S. Hawkins, Simulation of acoustic scattering by multiple obstacles in three dimensions. *ANZIAM J.* **50** (2008) 31–45.
[24] M. Ganesh and S. C. Hawkins, A high-order algorithm for multiple electromagnetic scattering in three dimensions. *Numer. Algor.* **50** (2009) 469–510.
[25] M. Ganesh and S. Hawkins, An efficient $\mathcal{O}(n)$ algorithm for computing $\mathcal{O}(n^2)$ acoustic wave interactions in large N-obstacle three dimensional configurations. *BIT Numer. Math.* **55** (2015) 117–139.
[26] M. Ganesh and K. Mustapha, A fully discrete H^1-Galerkin method with quadrature for nonlinear advection–diffusion–reaction equations. *Numer. Algorithms* **43** (2006) 355–383.
[27] D. Gottlieb and S. Orszag, Numerical analysis of spectral methods: theory and applications. *Soc. Ind. Appl. Math.* (1983).
[28] A. Guittet, C. Poignard and F. Gibou, A Voronoi Interface approach to cell aggregate electropermeabilization. *J. Comput. Phys.* **332** (2017) 143–159.
[29] F. Henríquez, C. Jerez-Hanckes and F. Altermatt, Boundary integral formulation and semi-implicit scheme coupling for modeling cells under electrical stimulation. *Numer. Math.* **136** (2016) 101–145.
[30] R. Hiptmair and C. Jerez-Hanckes, Multiple traces boundary integral formulation for Helmholtz transmission problems. *Adv. Comput. Math.* **37** (2012) 39–91.
[31] A. Hodgkin and A. Huxley, A quantitative description of membrane current and its application to conduction and excitation in nerve. *J. Physiol.* **117** (1952) 500–544.
[32] S. Joucla and B. Yvert, Modeling extracellular electrical neural stimulation: from basic understanding to MEA-based applications. *J. Physiol. Paris* **106** (2012) 146–158.
[33] S. Joucla, A. Glière and B. Yvert, Current approaches to model extracellular electrical neural microstimulation. *Front. Comput. Neurosci.* **8** (2014) 13.
[34] O. Kavian, M. Leguèbe, C. Poignard and L. Weynans, "Classical" electropermeabilization modeling at the cell scale. *J. Math. Biol.* **68** (2014) 235–265.
[35] J. Keener and J. Sneyd, Mathematical Physiology I: Cellular Physiology. Springer-Verlag, New York (1998).
[36] R. Kress, Linear Integral Equations. Vol. 82 Springer (1989).
[37] R. Kress and I. H. Sloan, On the numerical solution of a logarithmic integral equation of the first kind for the Helmholtz equation. *Numer. Math.* **66** (1993) 199–214.
[38] M. Leguèbe, C. Poignard and L. Weynans, A second-order Cartesian method for the simulation of electropermeabilization cell models. *J. Comput. Phys.* **292** (2015) 114–140.
[39] K. Lindsay, From Maxwell's equations to the cable equation and beyond. *Prog. Biophys. Mol. Biol.* **85** (2004) 71–116.
[40] A. Lunardi, Analytic Semigroups and Optimal Regularity in Parabolic Problems. Springer Science & Business Media (2012).
[41] P. K. Maini, Making sense of complex phenomena in biology. *Novartis Found. Symp.* **247** (2002) 53–59; discussion 60–65, 84–90, 244–252.
[42] P. Martin, Multiple Scattering: Interaction of Time-Harmonic Waves with N Obstacles. Cambridge University Press (2006).
[43] H. Matano and Y. Mori, Global existence and uniqueness of a three-dimensional model of cellular electrophysiology. *Discrete Contin. Dyn. Syst.* **29** (2011) 1573–1636.
[44] W. McLean, Strongly Elliptic Systems and Boundary Integral Equations. Cambridge University Press, Cambridge (2000).
[45] L. M. Mir, M. F. Bureau, J. Gehl, R. Rangara, D. Rouy, J. M. Caillaud, P. Delacre, D. Branellec, B. Schwartz and D. Scherman High-efficiency gene transfer into skeletal muscle mediated by electric pulses. *Proc. Nat. Acad. Sci. USA* **96** (1999) 4262–4267.
[46] M. Pavlin, N. Pavselj and D. Miklavcic, Dependence of induced transmembrane potential on cell density, arrangement and cell position inside a cell system. *IEEE Trans. Biomed. Eng.* **40** (2002) 605–612.
[47] A. Pazy, Semigroups of Linear Operators and Applications to Partial Differential Equations. Vol. 44. Springer Science & Business Media (2012).
[48] C. Pham-Dang, O. Kick, T. Collet, F. Gouin and M. Pinaud, Continuous peripheral nerve blocks with stimulating catheters. *Reg. Anesth. Pain Med.* **28** (2003) 83–88.
[49] A. Poggio and E. Miller, Integral equation solution of three-dimensional scattering problems, in Computer Techniques for Electromagnetics, Chap. 4, edited by R. Mittra. Pergamon, New York (1973) 159–263.
[50] T. Runst and W. Sickel. Sobolev Spaces of Fractional Order, Nemytskij Operators, and Nonlinear Partial Differential Equations. Vol. 3. Walter de Gruyter (1996).

[51] J. Saranen and G. Vainikko, Periodic Integral and Pseudodifferential Equations With Numerical Approximation. Springer Science & Business Media (2013).
[52] S. Sauter and C. Schwab. Boundary Element Methods. Springer-Verlag, Berlin, Heidelberg (2011).
[53] G. Sersa, T. Cufer, M. Cemazar, M. Rebersek and R. Zvonimir, Electrochemotherapy with bleomycin in the treatment of hypernephroma metastasis: case repeat and literature review. *Tumori* **86** (2000) 163–165.
[54] N. Sepulveda, J. Wikswo and D. Echt, Finite element analysis of cardiac defibrillation current distributions. *IEEE Trans. Biomed. Eng.* **37** (1997) 354–365.
[55] O. Steinbach, Numerical Approximation Methods for Elliptic Boundary Value Problems. Springer-Verlag, New York (2008).
[56] E. Tadmor, The exponential accuracy of Fourier and Chebyshev differencing methods. *SIAM J. Numer. Anal.* **23** (1986) 1–10.
[57] J. Teissié, N. Eynard, B. Gabriel and M. Rols, Electropermeabilization of cell membranes. *Adv. Drug Deliv. Rev.* **35** (1999) 3–19.
[58] V. Thomée. Galerkin finite element methods for parabolic problems, in *Springer Series in Computational Mathematics* (2006).
[59] N. Trayanova, J. Constantino, T. Ashihara and G. Plank, Modeling defibrillation of the heart: approaches and insights. *IEEE Rev. Biomed. Eng.* **4** (2012) 89–102.
[60] U. van Rienen, U. Schreiber, S. Schulze, U. Gimsa, W. Baumann, D. Weiss, J. Gimsa, R. Benecke and H.W. Pau, Electro-quasistatic simulations in bio-systems engineering and medical engineering. *Adv. Radio Sci.* **3** (2005) 39–49.
[61] P. Waterman, Matrix formulation of electromagnetic scattering. *Proc. of IEEE* **53** (1965) 805–812.
[62] T.-K. Wu and L. L. Tsai, Scattering from arbitrarily-shaped lossy dielectric bodies of revolution. *Radio Sci.* **12** (1977) 709–718.